AK DGGS
33447000035836

PROPERTY OF ALASKA STATE
GEOLOGICAL SURVEY LIBRARY

MIRL Report Number 74

Geology of a Subarctic, Tin-Bearing Batholith Circle Hot Springs, Alaska

By

Katy Wilkinson

MINERAL INDUSTRY RESEARCH LABORATORY
School of Mineral Engineering
University of Alaska-Fairbanks
Fairbanks, Alaska 99775-1180

TN
24
A4
A65
no.74
c.3

State of Alaska / DNR
Division of Geological &
Geophysical Surveys
3354 College Road
Fairbanks, AK 99709-3707
ADGGS Library

33447000035836

To my dear parents,
Jesse William and Helen Louise McKerney

State of Alaska / DNR
Division of Geological &
Geophysical Surveys
3354 College Road
Fairbanks, AK 99709-3707
ADGGS Library

ABSTRACT

A small batholith (56 mi^2) outcrops approximately 94 miles northeast of Fairbanks. It occurs in a historically rich area for placer gold. Additionally, placer tin has been recorded in the creeks that flow through or adjacent to the batholith.

As determined from macrocrystalline textures, modal analysis, mineralogy and potassium-argon age dates, the batholith was formed from two separate intrusives, which are referred to as the Circle Hot Springs and the Two-bit plutons, 57 and 70 m.y. old respectively. Evidence suggests that the diversity of rocks seen within each pluton could be a result of fractional crystallization from two parent magmas that originated from closely associated sources. In the Circle Hot Springs pluton, tin mineralization was found in greisen and less altered intrusive rock hosted within the biotite syenogranite.

ACKNOWLEDGMENTS

I am very grateful to Dr. Ernest Wolff for my first job at the Mineral Industry Research Laboratory (MIRL) of the University of Alaska-Fairbanks which lead to receiving a one year research assistantship. This assistantship was funded from September 1982 through August 1983 by the Fairbanks North Star Borough via a grant award to MIRL. I would also like to thank the University of Alaska Geology and Geophysics Department for directing scholarship monies to me from Arco in the amount of $474.71 to pay for trace-element analyses.

One of the less enjoyable aspects of a study like this one is the amount of time spent sawing; crushing, pulverizing, rolling, shattering, grinding, staining, dissolving, heating, titrating and fusing rock material as preparation for analysis. I am indebted to Namok Veach (Chemist, Alaska Geologic Survey (ADGGS)), Maria Polly (Laboratory Technician - ADGGS) and Robin Cottrell (Lab Manager for the Alaska Cooperative Geochronology Laboratory) for their cheerful and efficient assistance in obtaining reliable and accurate data.

Given the mosquitoes, terrain and area of the study, I am deeply thankful to my geologist comrades, Steve Masterman and Bruce Campbell for their hearty assistance in sample collection and late night aerial photo séances to determine the following days' traverses in search of the elusive intrusive contact.

Several people have, in one aspect or many, helped me to achieve the goals outlined in this study. Their useful advice and friendship are an integral part of the success of completing this research. They are as follows:

Mary Albanese - Alaska Geologic Survey Geologist
Patrick and Barbara Amberg
Dirk Bodnar - Geologist
Tina Balog - Geologist
Richard Calamari - President, Oxford Assaying and Refining, Fairbanks
Tina Denton - Professional Civil Engineer
Kathleen Goff - Geologist
Mark Hall - Geologist
Dr. Mary Keskinen - Assistant Professor of Geology, University of Alaska
Linda Reinink-Smith - Geologist
Dr. T.E. Smith - Senior Minerals Geologist, Alaska Geologic Survey
Dr. Samuel E. Swanson - Associate Professor of Geology and Department Head of Geology and Geophysics, University of Alaska-Fairbanks
Dr. Florence Weber - Geologist, U.S. Geological Survey

I wish to express my gratitude to Dr. Rainer Newberry (Associate Professor of Geology, University of Alaska-Fairbanks) for his willingness to discuss geologic questions that I had throughout the study. He has often provided invaluable insight and excellent ideas on how to proceed. Dr. Daniel Hawkins (Professor of Geology, University of Alaska-Fairbanks) has been extremely helpful and enthusiastic whenever I have needed his assistance. I especially thank him for his geochemical, statistical and editorial expertise.

The environment at MIRL is one of progressive, innovative research which is created and nurtured by the people who work there. I would like to express heartfelt thanks to Daniel Walsh (Instructor, MIRL) for his statistical and editorial critiques of this manuscript and to Cathy Farmer (Word Processing Specialist, MIRL) for her competence and speed in preparation of this report for publication.

Alaska is unwieldy at best in size, extent and terrain. The logistics and cost alone of field work can present insurmountable obstacles for the student or research scientist. Space to store boxes of collected samples and room to work can and often is a continual problem. Backed by my desire, I attribute the success and completion of this research to two people; Dr. P. Dharma Rao (Professor of Coal Technology and Associate Director, MIRL) and my dear husband, Richard H. Wilkinson. Over the five year span of this study, Dr. Rao has graciously helped to eliminate many obstacles by providing office and lab space, employment in the coal lab and never ending encouragement. Jane Smith (MIRL laboratory assistant) has come to my aid in all aspects of lab work. I completely credit the high quality of photographs in this report to Jane's expertise. She was a tremendous help in pinpointing the tin mineralization and this study was greatly improved by her input.

During a geologic traverse on the ridges around Deadwood Creek, a fierce lightning storm moved in from the south and forced me to leave the hills and move to lower elevations. It was at that time that I met a heavy equipment operator, Richard, who was to become my husband and the financial backer of this research. I am indebted to him for his continual encouragement and stoic willingness to periodically share our small Alaskan quarters with over 300 sacks of rocks.

TABLE OF CONTENTS

ABSTRACT iv

ACKNOWLEDGMENTS iv

TABLE OF CONTENTS v

LIST OF PLATES viii

LIST OF FIGURES x

I. INTRODUCTION 1
- Regional Setting 1
- Location and Local Geology 1
- Physiographic Features 1
- Location of the Circle Mining District 1
- Previous Studies 1
  - Gold Mineralization 1
  - Tin and Tungsten Mineralization 1
- Previous Geologic Mapping 8

II. SAMPLE COLLECTION 8
- Accessibility and Sample Location 8

III. METHODS OF ANALYSIS 8
- Macrocrystalline Textural Variation Analysis 8
- Modal Analysis 10
  - Statistical Reliability Study Summary 11
- Geochemical Analysis 11
  - Whole-rock 11
  - Trace-element 11
- Geochronology 11

IV. ANALYSIS OF MACROCRYSTALLINE TEXTURES 11
- Textural Terms: Redefined for the Circle Intrusive Complex 12
  - Porphyritic versus Mediophyric and Megaphyric 12
- The Importance of the Volume Percentage of the Large Feldspars 15
- Groundmass: Fine-grained, Medium-grained and Coarse-grained 17
- Groundmass: Equigranular Versus Subequigranular 17
- Large Quartz Crystals: Phenocryst Versus Groundmass 18
- Summary 18

TABLE OF CONTENTS (Continued)

V. GEOCHRONOLOGY 18

VI. ROCK TYPES 18
- The Circle Intrusive Complex 18
- Circle Hot Springs Pluton 21
  - Medium-grained to Slightly Mediophyric to Mediophyric Biotite Syenogranite 24
  - Greisen 24
  - Slightly Mediophyric to Mediophyric Biotite Monzogranite 25
  - Mediophyric Quartz Monzonite 26
  - Slightly Mediophyric Granodiorite 26
  - Aplite-Pegmatite Dikes 26
  - Mafic Dikes 26
- Two-Bit Pluton 26
  - Megaphyric Biotite Monzogranite 26
  - Megaphyric Granodiorite 27
  - Megaphyric Quartz Syenite 27
  - Aplite-Pegmatite Dikes 27
  - Mafic Dikes 27
  - Enclaves 27
  - Discussion and Summary 27

VII. MODAL ANALYSIS 33
- Crystallization and Bowen's Reaction Series 33
- Magmatic Differentiation 36
- Discussion and Summary 37

VIII. DISCRIMINANT ANALYSIS 37

IX. MINERALOGY 40
- Circle Hot Springs Pluton 40
  - Major Mineral 40
  - Mafic Minerals 40
  - White Mica 43
  - Accessory Minerals 43
- Two-bit Pluton 43
  - Major Minerals 43
  - Mafic Minerals 43
  - White Mica 43
  - Accessory Minerals 43
- Discussion and Summary 44

TABLE OF CONTENTS (Continued)

X. CHEMICAL ANALYSIS 44
Major Oxides 44
Harker Variation Diagrams 44
AFM and Ca-Na-K Triangular Diagrams 48
Discussion and Summary 48
Trace Elements 50
CIPW Norm and the Differentiation Index 51
Seward Tin Granites Versus the Circle Intrusive Complex 51
Summary and Conclusions 51

APPENDIX A
A-1 Location of sample sites in the Bedrock Creek area 57
A-2 Location of sample sites in the Deadwood Creek area 58
A-3 Location of sample sites in the Portage Creek area 59
A-4 Location of sample sites in the Half Dollar Creek area 60
A-5 Location of sample sites in the Buckley Bar area 61

APPENDIX B - Grain Size Analysis of Rocks from the Circle Intrusive Complex 62

APPENDIX C - A Method of Point-counting Medium-grained, Porphyritic Rocks for Modal Analysis 65

APPENDIX D - Whole-rock Analytical Data and CIPW Norms 66

APPENDIX E
E-1 Trace-element Analyses of 18 Samples from the Circle Intrusive Complex 67
E-2 Trace-element Analyses of 14 Samples from the Circle Intrusive Complex 68
Detection Limits in the Trace-element Analysis of 14 Samples from the Circle Intrusive Complex 68

REFERENCES 69

LIST OF PLATES

Plate I A. Looking northeast from the headwaters of Deadwood Creek 4

B. Intrusive (i) contact with schist (s) just south of the Portage Creek headwaters 4

Plate II A. Placer gold mined on Deadwood Creek in 1984 5

B. Placer mining operation on Deadwood Creek (Photos by R.H. Wilkinson) 5

Plate III A. A polished section containing Deadwood Creek placer tin (1.25 inch Ring Form) 8

B. A single grain of Deadwood Creek placer tin. Photo taken in normal incident light, width of field 1750 microns 8

Plate IV A. A Boulder Creek intrusive spire. Boulder Creek is toward the west, located in the lower right of the photograph 9

B. Intrusive spires are located just west of the confluence of Half Dollar and Bottom Dollar Creeks on the north side of the road 9

Plate V A. A 57 m.y. old syenogranite (see p.21 for plutonic rock classification) 13

B. and C. 70 m.y. old monzogranites 13

Plate VI Representative rock types of the Circle Hot Springs pluton 23
A - SM319, syenogranite B - BC68, quartz monzonite
C - KM147, syenogranite D - SM88, quartz monzonite
E - 1933, granodiorite F - KM139, monzogranite

Plate VII A. Sample taken from Boulder Creek intrusive spire (Plate IV-A). KM74, enclave in syenogranite 24

B. Sample CH61, interstitial tourmaline in syenogranite. Photomicrograph taken in plain light, width of field 1330 microns 24

Plate VIII A. CH58A, magnetite. Photo taken in normal incident light, width of field 440 microns 25

B. CH58A, a polished section containing cassiterite and magnetite in greisen (1.5 inch Ring Form) 25

Plate IX A. and B. SM230A, cassiterite. Photo taken in normal incident light, width of field 440 microns 25

C. SM230A, small veinlets in sample containing cassiterite (1.5 inch Ring Form) 25

Plate X A. PM73, mafic dike. Photomicrograph taken under crossed nichols, width of field, 3400 microns 27

B. PM73, hornblende. Photomicrograph taken in plain light, width of field 1330 microns 27

LIST OF PLATES (Continued)

Plate XI A. and B. Aplite-pegmatite dikes crosscutting intrusive spires located a short distance west of the confluence of Half Dollar Creek and Bottom Dollar Creek (Plate IV-B) 29

Plate XII A. and B. Located near KM122 (Figure 16, p. 22), mafic dikes crosscutting megaphyric biotite monzogranite 30

Plate XIII A. KM122, megaphyric biotite monzogranite contact with mafic dike 31

B. KM122, mafic dike with increasing grain size away from the contact. Photomicrograph taken in plain light, width of field 3400 microns 31

Plate XIV A. KM147, metamict zircons enclosed by biotite in a slightly mediophyric, biotite syenogranite. Photomicrograph taken in plain light, width of field 3400 microns 32

B. PM75, zoned zircon enclosed by chlorite in greisen. Photomicrograph taken in plain light, width of field 520 microns 32

Plate XV Sample 1933, albite (a) and pericline (p) twin lamellae in a plagioclase feldspar. Photomicrograph taken under crossed nichols, width of field 3400 microns 41

Plate XVI Sample 1933, a zoned plagioclase feldspar in a granodiorite. Photomicrograph taken under crossed nichols, width of field 1330 microns 41

Plate XVII A. PM280, micrographic texture in biotite syenogranite. Photomicrograph taken under crossed nichols, width of field 3400 microns 42

B. PM281, granophyric texture in a biotite syenogranite. Photomicrograph taken under crossed nichols, width of field 3400 microns 42

Plate XVIII A. KM66, myrmekitic (m) and graphic (g) textures in a pegmatite vein 44

B. KM66, myrmekitic texture. Quartz labeled (Q) and plagioclase (P). Photomicrograph taken under crossed nichols, width of field 1300 microns 44

C. KM66, graphic texture. Two quartz blebs are enclosed by perthitic alkali feldspar. Photomicrograph taken under crossed nichols, width of field 3,400 microns 44

Plate XIX A. and B. KM114, sphene crystals in a megaphyric granodiorite. Photomicrographs taken in plain light, width of field 1330 microns 45

Plate XX A. CH54, zoned plagioclase feldspars with albite twinning in a Two-bit pluton monzogranite. Photomicrograph taken under crossed nichols, width of field 3400 microns 46

B. PM280, a typical unzoned plagioclase feldspar with albite twinning in a Circle Hot Springs syenogranite. Photomicrograph taken under crossed nichols, width of field 3400 microns 46

LIST OF PLATES (Continued)

Plate XXI A. CH56A, perthitic microcline with Carlsbad twinning in a Two-bit pluton granodiorite. Photomicrograph taken under crossed nichols, width of field 3400 microns 47

B. CH60, a perthitic orthoclase with Carlsbad twinning in a Circle Hot Springs syenogranite. Photomicrograph taken under crossed nichols, width of field 3400 microns 47

LIST OF FIGURES

Figure 1 - Location of the Yukon-Tanana Upland (modified from Foster and others, 1973) 2

Figure 2 - Location of the Circle intrusive complex. The complex is composed of the Circle Hot Springs and Two-bit plutons 3

Figure 3 - Location of the Circle mining district 6

Figure 4 - Generalized locations of reported occurrences of tin and tungsten in the area of the Circle intrusive complex (see Table 1 for summaries and references of these occurrences) 6

Figure 5 - Study area showing locations of enlarged maps. (See Appendix A-1 through A-5, p. 57) 10

Figure 6 - Textural variation of 104 rocks from the Circle intrusive complex. For each sample, the size of the largest feldspar and the size of the largest crystal in the groundmass was plotted. Each of the four groups represents rock samples that share textural similarities. The division between Groups C and D is based on field observations 14

Figure 7 - Geographic locations of four distinct textures that compose the Circle intrusive complex 14

Figure 8 - Shown above is the location of samples used for modal analysis in the Circle Hot Springs and Two-bit plutons. Also shown (left) is a variation diagram with each sample's modal composition plotted. The modal analyses indicates that the northern lobe of the batholith is generally higher in potassium than the southern lobe 15

Figure 9 - The maps show the location of samples with their corresponding rubidium, differentiation index and tin values plotted. The range of values suggest that the batholith is composed of two compositionally different intrusives 16

Figure 10 - Map shows geographic distribution of the large feldspars 17

LIST OF FIGURES (Continued)

Figure 11 - This drawing shows the textural relationship between the large potassium feldspar crystals, interstitial plagioclase and biotite, and the large, subhedral quartz crystals 19

Figure 12 - Map shows geographic distribution of the large quartz crystals 19

Figure 13 - Analytical data for potassium-argon ages of the Circle intrusive complex. Map shows sample locations 20

Figure 14 - Classification of plutonic rocks based on their actual mineral composition (adapted from Figure 1, Geotimes, October, 1973, p. 26). Q-Quartz, A-Alkali feldspar, P-Plagioclase, F-Feldspathoid (abr. foid) 21

Figure 15 - Shown above is a composition map of the Circle intrusive complex that is based on modal analysis data. The compositions have been determined by using the modified Streckeisen's classification previously discussed (p. 18) 22

Figure 16 - Location of samples that were examined in thin section. Also shown is the distribution of enclaves and aplite, pegmatite and mafic dikes 22

Figure 17 - Four structural cross sections of a portion of the Circle Hot Springs pluton showing topography and mineralized areas 34

Figure 18 - Variation diagrams showing modal compositions of the Two-bit pluton (A), Circle Hot Springs pluton (B), and both plutons (C) 35

Figure 19 - Bowen's igneous reaction series (adapted from Williams and others, 1982) 36

Figure 20 - Quartz-total feldspar-mafic variation diagrams of the Two-bit pluton (A), Circle Hot Springs pluton (B), and both plutons (C) 38

Figure 21 - BMDP-7M classification of samples from Two-bit and Circle Hot Springs pluton using plagioclase as the discriminant variable. Map shows location of misclassified cases 39

Figure 22 - BMDP-7M classification of samples from Two-bit and Circle Hot Springs pluton using potassium feldspar as the discriminant variable. Map shows location of misclassified cases 40

Figure 23 - Harker variation diagrams. Map shows location of samples 49

Figure 24 - (a) AFM and (b) CaO-Na_2O-K_2O diagrams for rocks from the Circle intrusive complex in weight percent. A, Na_2O+K_2O; F, FeO_{total}; M, MgO. (See fig. 23 for sample locations) 50

Figure 25 - Tin and fluorine versus rubidium plots of 18 samples from the Circle intrusive complex 52

Figure 26 - Lithium, beryllium, tungsten and boron versus rubidium plots of 18 samples from the Circle intrusive complex. (See fig. 25 for explanation of symbols) 53

LIST OF FIGURES (Continued)

Figure 27 - Rubidium, tin, fluorine, lithium, beryllium, tungsten and boron versus differentiation index of 9 samples from the Circle intrusive complex 54

Figure 28 - Location of Seward Peninsula and distribution of plutons (circles, exposed; squares, inferred at depth) in the tin-granite belt, northwest Alaska. Plutons include those at Cape Mountain (1), Potato Mountain (2), Brooks Mountain (3), Lost River (4), Tin Creek (5), Black Mountain (6), Ear Mountain (7), Kougarok Mountain (8), and the Oonatut Granite Complex (9) (from Hudson and Arth, 1983) 55

Figure 29 - Comparison plot of Seward tin-granite normative mineral ratios versus Circle intrusive complex normative mineral ratios 55

Figure 30 - Location of sample sites in the Bedrock Creek area 57

Figure 31 - Location of sample sites in the Deadwood Creek area 58

Figure 32 - Location of sample sites in the Portage Creek area 59

Figure 33 - Location of sample sites in the Half Dollar Creek area 60

Figure 34 - Location of sample sites in the Buckley Bar area 61

I. INTRODUCTION

Regional Setting

In east-central Alaska the Yukon-Tanana Upland extends from the Yukon to the Tanana River. Large-scale structural features mark the northern and southern upland edges and are known respectively as the Tintina and Denali right lateral fault systems (Aleinikoff and others, 1981).

The upland consists largely of Precambrian completely deformed low- to high-grade metamorphic terrane that has been intruded by Mesozoic and Tertiary plutons (Aleinikoff and others, 1981), (Fig. 1). This study focuses on the geology of two upland plutons.

In previous literature these two plutons have been referred to as a single, undifferentiated intrusion which has been called the Ketchem Dome, Circle or Circle Hot Springs pluton. In this report, these two plutons will be collectively referred to as the Circle intrusive complex which is composed of the Circle Hot Springs (CHS) and the "Two-bit" plutons (named after Two-bit Creek) (Fig. 2). Additionally, reference will be made to "3165 Knob" which is a prominent hill in the western portion of the Two-bit pluton (Fig. 2).

Location and Local Geology

The Circle intrusive complex outcrops approximately 94 miles northeast of Fairbanks near mile 114 on the Steese Highway (Fig. 2). The intrusive bodies form an irregular, elliptical shape and lie (NW-SE direction) along and parallel to the Tintina fault zone (Fig. 1). The total exposed area of the complex is 56 square miles. Intrusive contacts to the east, west and south are against metamorphic rocks. In years past the metamorphic sequence in the area has been called the Birch Creek Schist (Mertie, 1937). The country rocks adjacent to the intrusive bodies are mostly composed of grey, mica quartzites, quartz-mica schists, feldspathic quartzites and quartzo-feldspathic schists with minor hornfels present near intrusive contacts in a few areas. Chloritic schist, garnetiferous chlorite schist and calcareous schist also occur. Mafic dikes, aplite and pegmatite dikes predominately occur in the intrusive complex but are occasionally found nearby in the schist.

Physiographic Features

The elevation around the Circle intrusive complex ranges from 1,000 feet to 4,000 feet above sea level. With an average annual precipitation of 8-12 inches in addition to the long, dark, cold winters (35 to -60 degrees Fahrenheit) and the short, relatively warm (60 to 80 degrees Fahrenheit) summers, the area is equivalent to subarctic desert (Wahrhaftig, 1965). The region is thought to have been glaciated (Florence Weber, pers. comm.) but due to uplift and erosion the streams and low lying areas lack a mantle of deep, glacial overburden. Discontinuous permafrost underlies most of the region. Glaciation, (Florence Weber, pers. comm.) in addition to the combined erosional effects of solifluction, snow-patch erosion and altiplanation have resulted in smooth, flat ridges with adjoining elongated spurs (Mertie, 1930) (Plate I).

Location of the Circle Mining District

The Circle intrusive complex lies within the Circle mining district. The term "circle" originated from the areas' close proximity to the Arctic Circle. Mertie and other early workers referred to the Circle district, the Birch Creek district, the Eagle-Circle district, the Circle mining district, and the Birch Creek mining district. The new frontier terms were loosely used to describe areas that had not been legally defined (Ransome and Kerns, 1954). Consequently, it is easy to become confused as to what was meant in terms of specific boundaries or when various names were used synonymously for the same area.

For this report, based on the composite work of J.B. Mertie (1930, 1937) and Ransome and Kerns (1954), the area of the Circle mining district will be defined as that which is bounded on the east, west and south by Birch Creek and on the north by Porcupine and Crooked Creeks (Fig. 3).

Previous Studies

Gold Mineralization

The first discovery of placer gold in the area was made by two Russians, Pitka and Sorresco, in 1893 on Birch Creek (Mertie, 1937). Gold was discovered on many of the creeks in the Birch Creek drainage net the following year (Mertie, 1937). Many of the gold producing creeks cut through or flow in close proximity to the Circle intrusive complex. According to Mertie, "the gold ores have originated as a phase of granitic intrusion; and that therefore where bodies of granitic rocks are found the conditions in general are favorable for the occurrence of gold", (Mertie, 1930). It was his belief that some or all of the intrusives exposed in the Yukon-Tanana Upland if followed down to great depth would connect into one large body (Mertie, 1930). Current workers are exploring new theories as to the origin of the gold. Plate II shows some of the larger gold nuggets that have been mined on Deadwood Creek along with the placer mining operation.

Tin and Tungsten Mineralization

In 1908, wolframite (a manganese-iron tungstate) was first identified in the gold placer concentrates of Deadwood Creek (Johnson, 1910). Figure 4 is a generalized compilation of occurrences of tin and tungsten in or near the Circle intrusive complex. Table I is a summary of these occurrences with references. This compilation of tin and tungsten occurrences suggests that mineralization is more prevalent near the contact areas. Plate III shows a polished section of

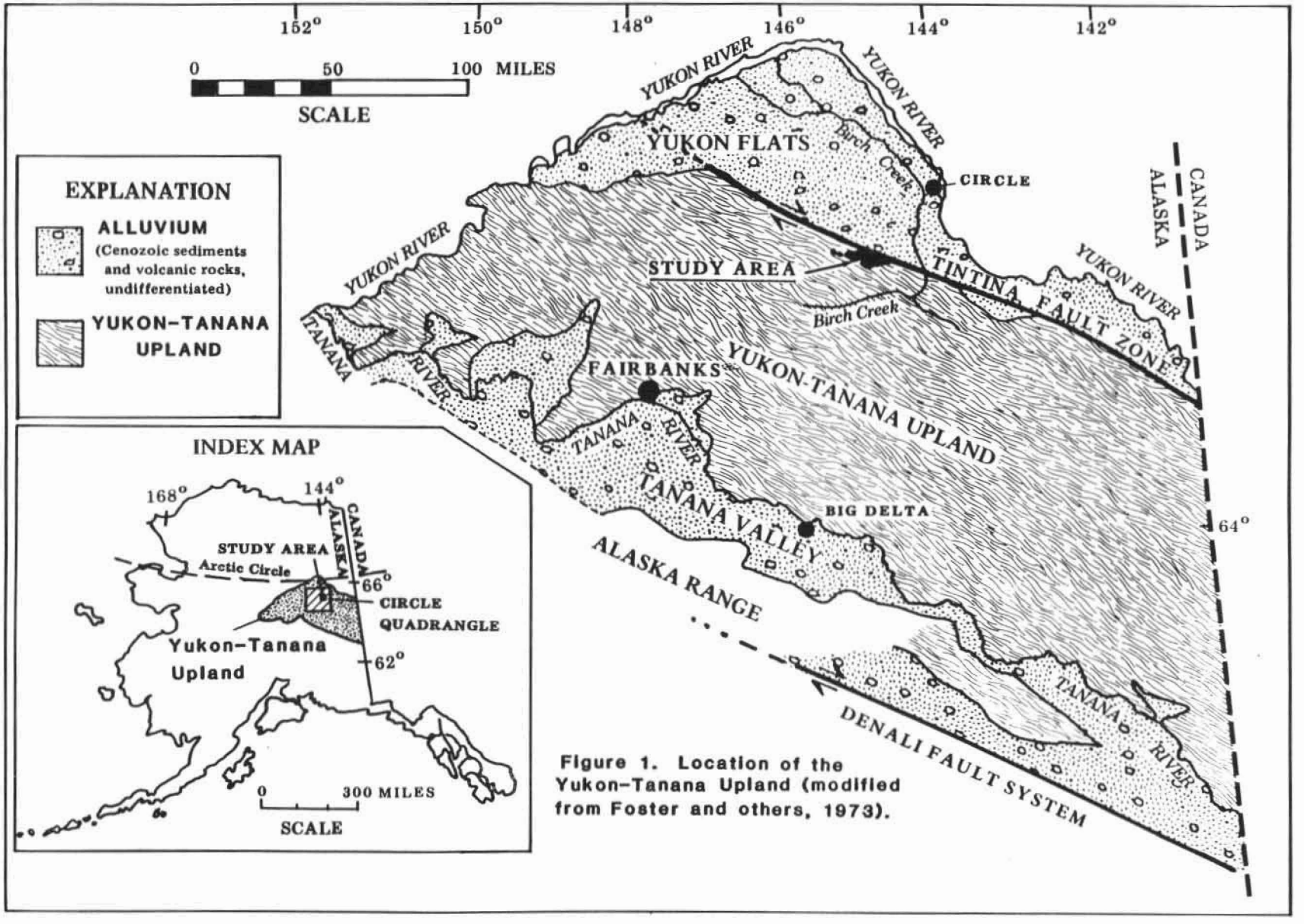

Figure 1. Location of the Yukon-Tanana Upland (modified from Foster and others, 1973).

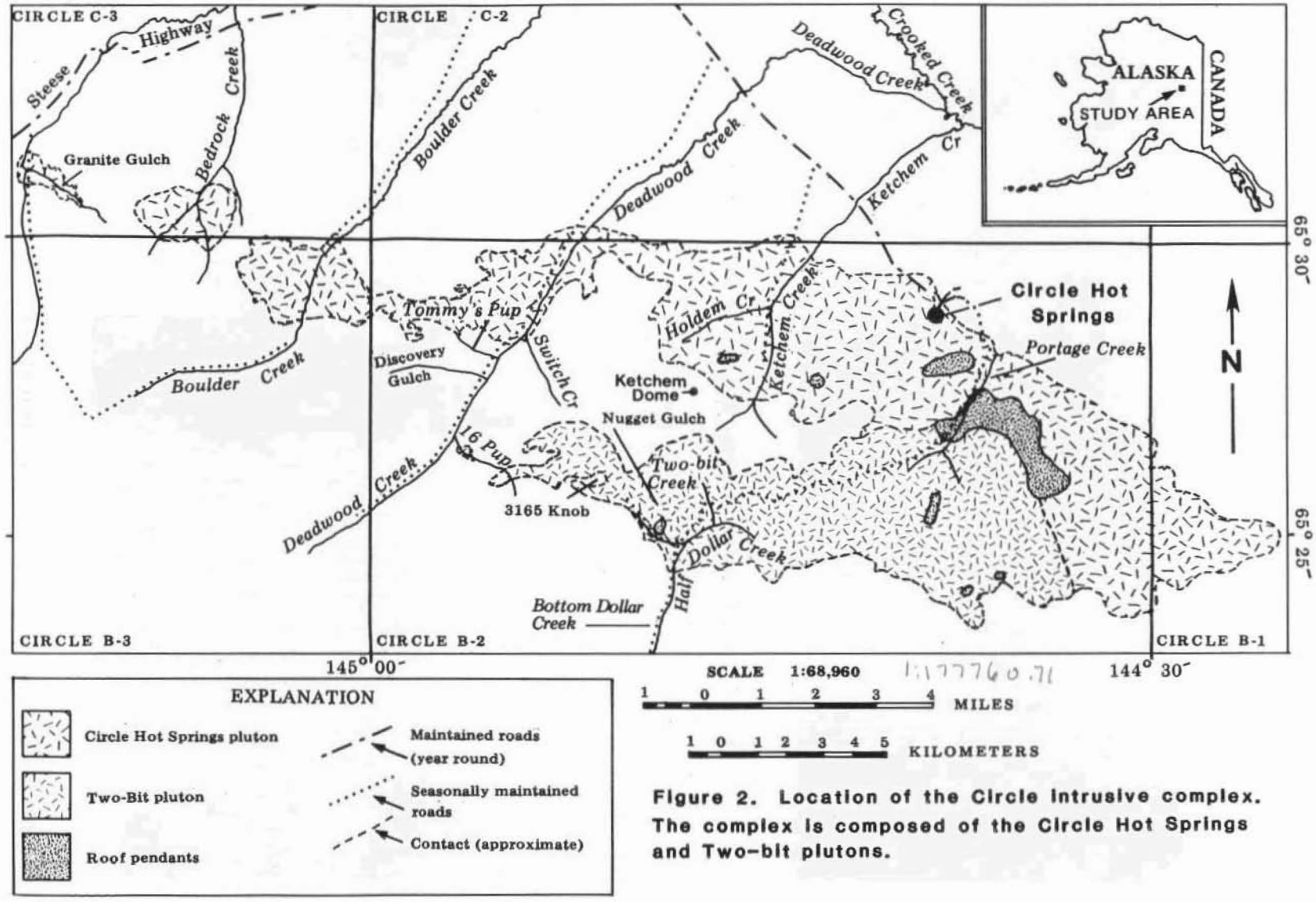

Figure 2. Location of the Circle intrusive complex. The complex is composed of the Circle Hot Springs and Two-bit plutons.

Plate I

A. Looking northeast from the headwaters of Deadwood Creek.

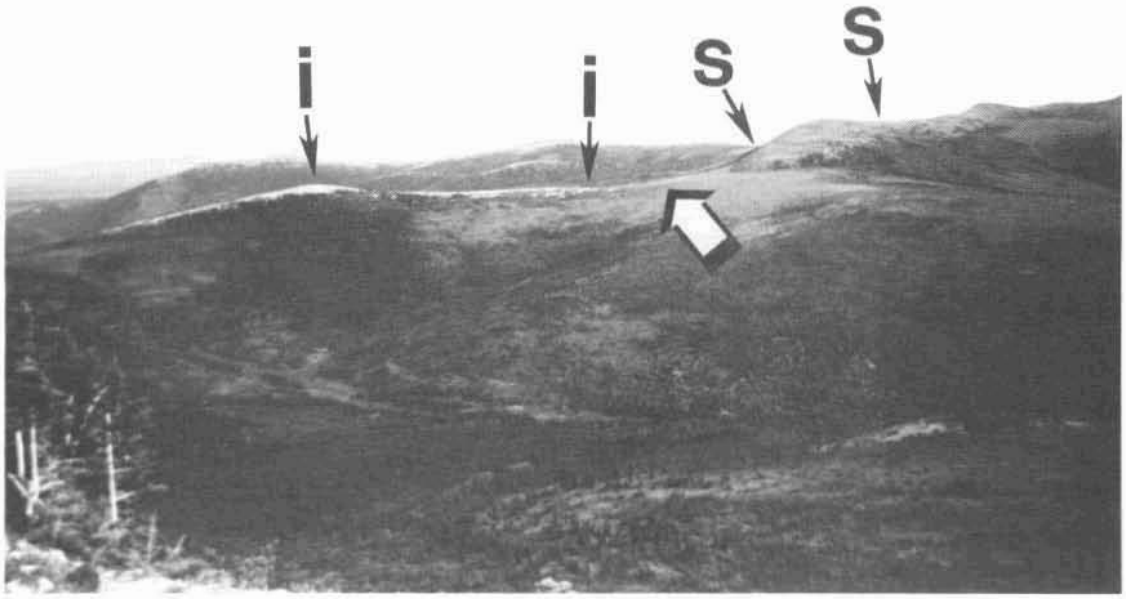

B. Intrusive (i) contact with schist (s) just south of the Portage Creek headwaters.

Plate II

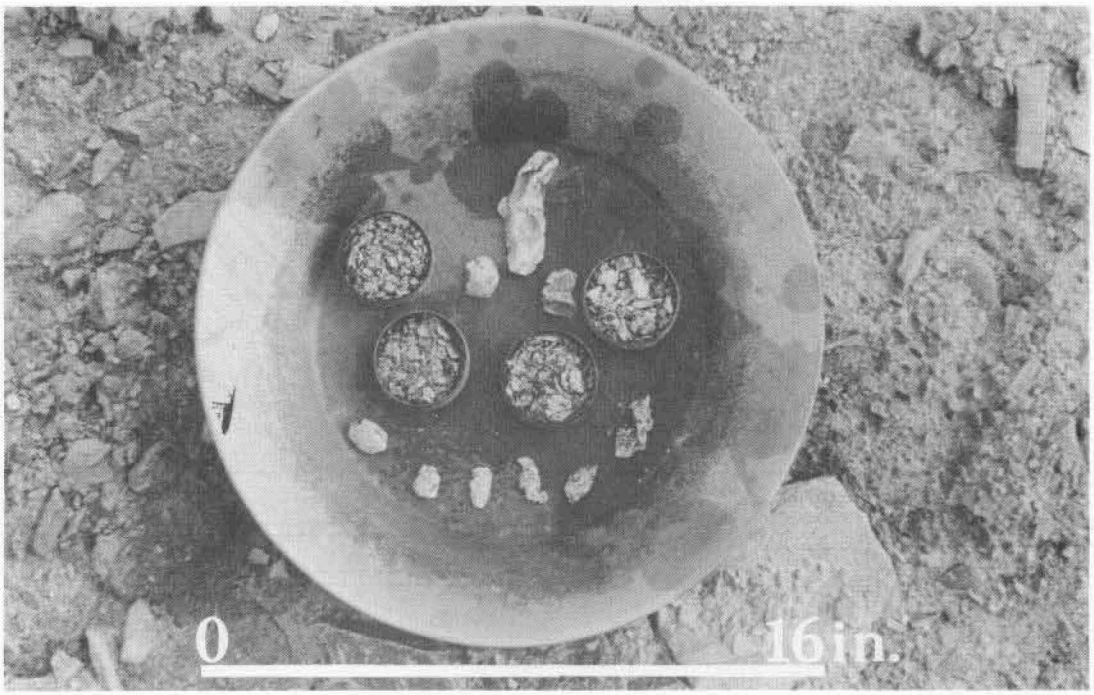

A. Placer gold mined on Deadwood Creek in 1984.

B. Placer mining operation on Deadwood Creek (Photos by R.H. Wilkinson).

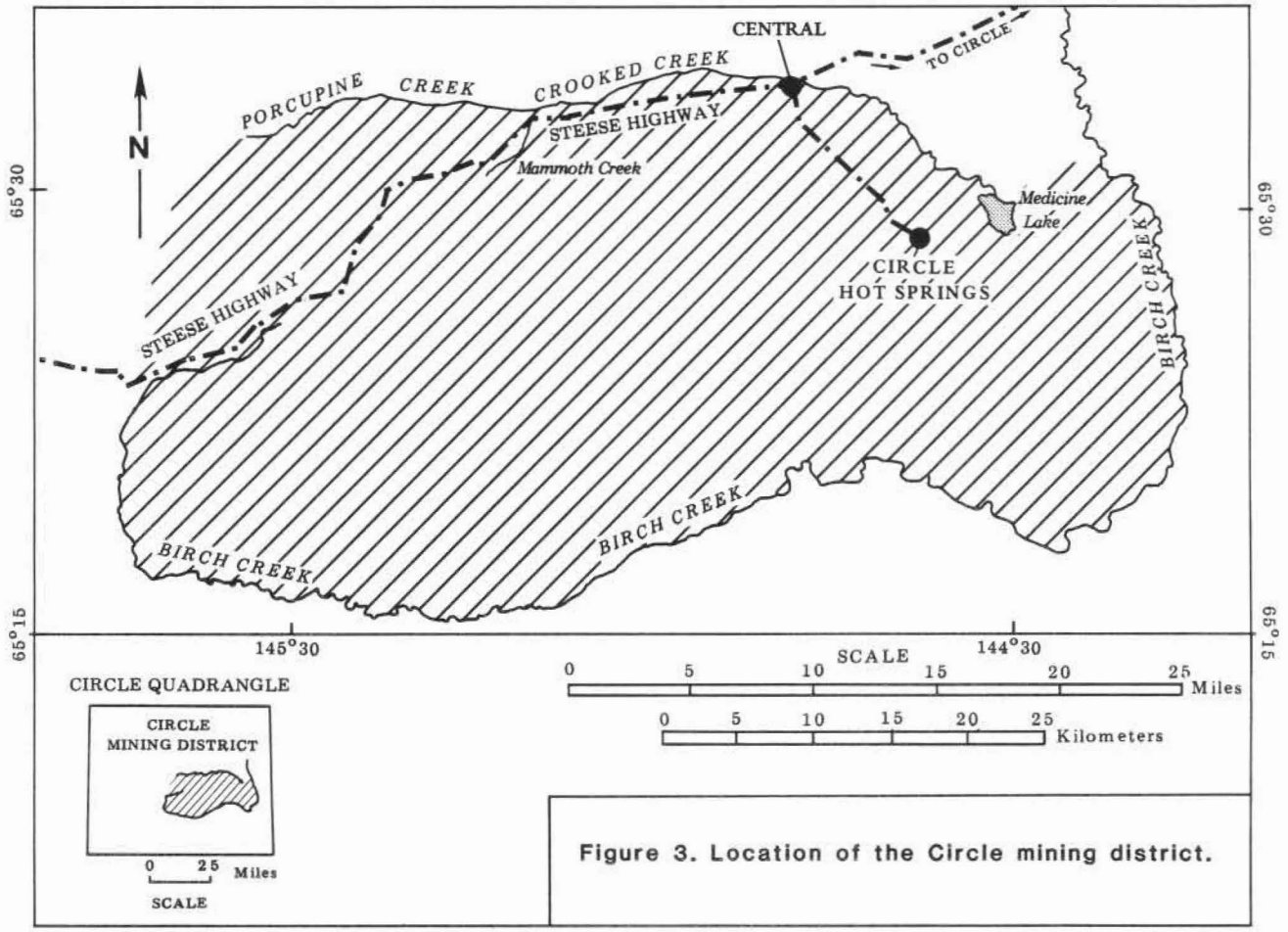

Figure 3. Location of the Circle mining district.

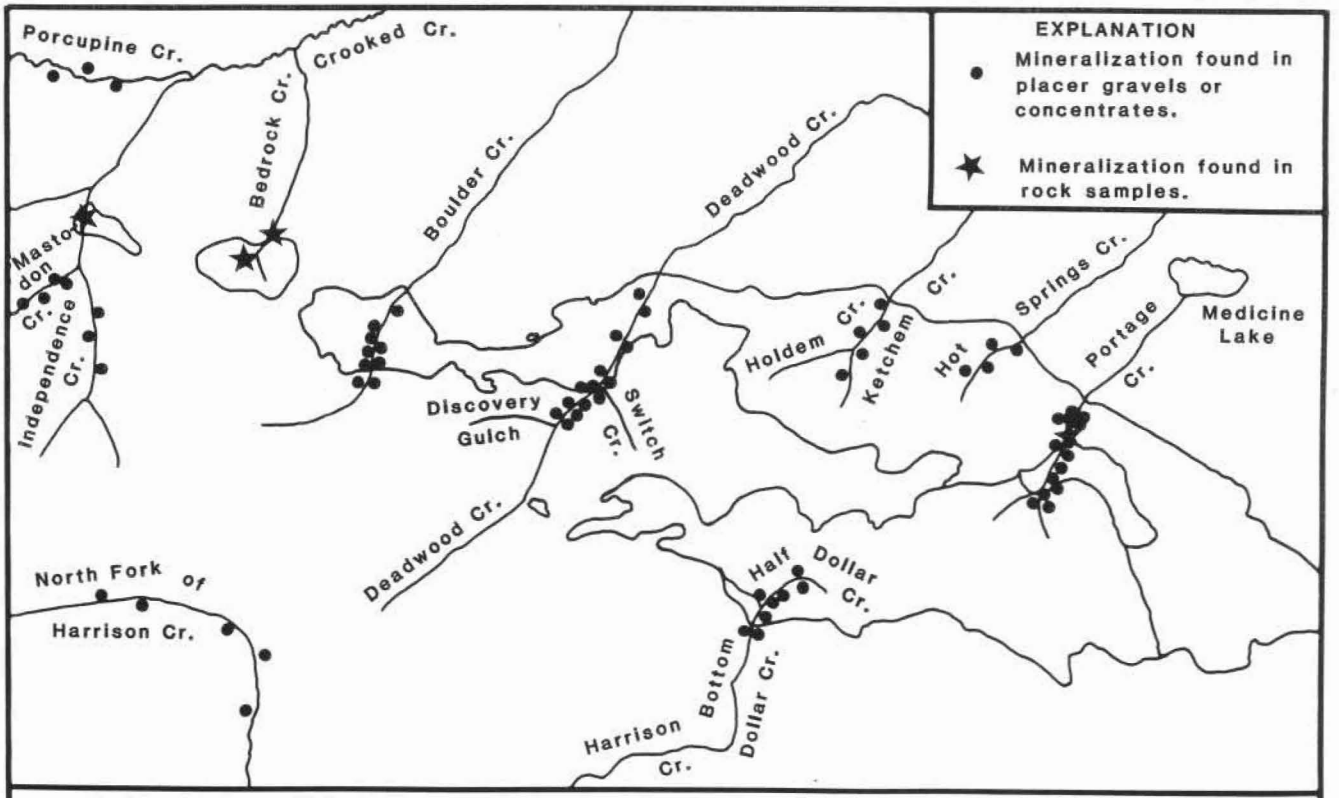

Figure 4. Generalized locations of reported occurrences of tin and tungsten in the area of the Circle intrusive complex (See Table 1 for summaries and references of these occurrences).

Table 1.

References and Brief Summaries of Tin and Tungsten Occurrences in the Area of the Circle Intrusive Complex (see fig. 4) (listed in alphabetical order by creek.)

Bedrock Creek	Scheelite in granite sample, (Berg and Cobb, 1967). Granite bedrock contained 10% monazite and a trace of scheelite (Nelson and others, 1954).
Boulder Creek	Minor cassiterite and scheelite found in quartz and schist cobbles; anomalous amounts of tin and tungsten found in granite sample (20 ppm-Sn, 22 ppm-W); heavy concentrations of cassiterite found in placer gravels (Barker, 1979).
Deadwood Creek	Wolframite vein discovered (Brooks, 1909). Abundant placer cassiterite and wolframite found (Brooks, 1910; Hess, 1912; Prindle, 1913; Wedow and others, 1952). Wolframite shipped for processing (Brooks, 1918). Quartz and mica wolframite placers and cassiterite placers found upstream of Switch Creek; none found in Switch Creek (Mertie, 1938). Small amounts of placer scheelite found (Joesting, 1942). Schist and granite samples contain cassiterite, scheelite and wolframite (Nelson and others, 1954).
Half Dollar Creek	Abundant cassiterite and a fair amount of scheelite in placers (Joesting, 1943). Granite samples contain scheelite (Nelson and others, 1954).
Hot Springs Creek	Scheelite present (Wedow and others, 1954).
Independence Creek	Placer gravels contain cassiterite, scheelite and wolframite (Nelson and others, 1954).
Ketchem Creek	Placer scheelite and cassiterite present (Wedow and others, 1954).
Mammoth Creek	Presence of scheelite in granite talus (Nelson and others, 1954).
Mastodon Creek	Scarce placer cassiterite (Joesting, 1942).
North Fork of Harrison Creek	Scarce placer cassiterite (Joesting, 1942).
Porcupine Creek	Some cassiterite in placer concentrates (Mertie, 1938).
Portage Creek	Common cassiterite in placers (Joesting, 1942). Granite bedrock and placer concentrates contain cassiterite, scheelite and wolframite (Nelson and others, 1954).

Plate III

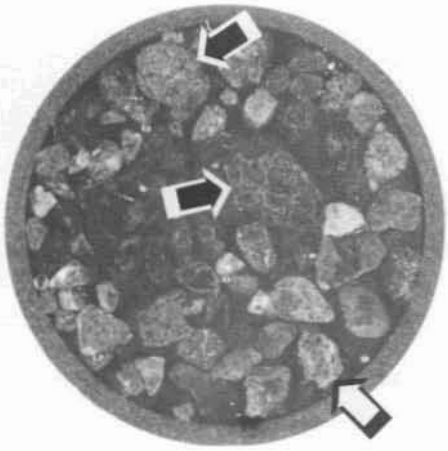

A. A polished section containing Deadwood Creek placer tin (1.25 inch Ring Form).

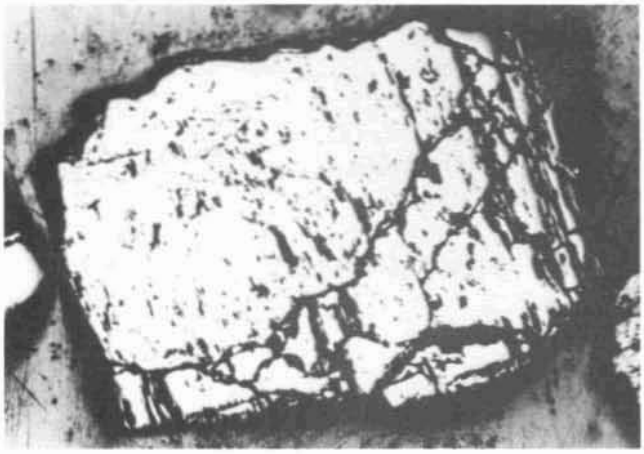

B. A single grain of Deadwood Creek placer tin. Photo taken in normal incident light, width of field 1750 microns.

Deadwood Creek tin placer and a photograph of one grain of placer tin.

Previous Geologic Mapping

The most comprehensive early geologic publications on Alaska's interior were written by J.B. Mertie in 1930 and 1937 titled, "Geology of the Eagle-Circle District, Alaska" and "The Yukon-Tanana Region, Alaska". Currently, the only geologic map available of the Circle quadrangle is at the 1:250,000 scale and can be found in the U.S.G.S. open-file report 83-170A (Foster and others, 1983). The U.S.G.S. open-file report 83-170B (Menzie and others, 1983) outlines descriptive and grade-tonnage models of deposit types that may occur in the Circle quadrangle and can provide additional references. This study will focus on the geology of the Circle intrusive complex and the relationship between tin mineralization and the intrusive bodies.

II. SAMPLE COLLECTION

Accessibility and Sample Location

Most of the Circle intrusive complex is accessible from mid-June through mid-September by dirt roads (Fig. 2). The majority of rock samples were collected from available rubblecrop. The exposed rubblecrop occurs on ridges or in stream-cut valleys with long, gently sloping tundra covered hills in between. Due to the lack of outcrop, virtually all contact relations are based on rubblecrop exposures (Plate I-B). Therefore all the contacts between the intrusive bodies and the metamorphics are inferred (Fig. 2). For all the following figures these inferred contacts will be shown in solid lines. Minor roof pendants will not always be shown in the following figures.

In the Circle Hot Springs pluton, intrusive spires occur at the head of Bedrock Creek, on a ridge just east of Boulder Creek (see Appendix A-1, Sample KM74), on Deadwood Creek near the Switch Creek confluence and in the area adjacent to Holdem and Ketchem Creeks (Fig. 2). Plate IV-A shows a Boulder Creek intrusive spire. The least accessible portions of the Circle Hot Springs pluton include the Bedrock Creek spires and the rubblecrop exposed in the eastern end (Fig. 2).

In the Two-bit pluton most of the samples were collected from continuous rubblecrop that is well exposed along the main dirt road (Fig. 2). Striking intrusive spires outcrop near the confluence of Half Dollar Creek and Bottom Dollar Creek (Plate IV-B). The least accessible portions of the pluton include the area adjacent to 3165 Knob and the eastern end (Fig. 2). A sample location map shows the areal distribution of samples that were collected (Fig. 5). The sample site location figures are in Appendix A-1 through A-5.

III. METHODS OF ANALYSIS

Macrocrystalline Textural Variation Analysis

The samples selected for analysis are representative of the main intrusive phases (i.e. biotite syenogranite). Minor intrusive phases (aplite and mafic dikes) are not used. The feldspar and quartz crystals of each rock sample were measured in millimeters (mm) with the use of a hand lens and a binocular microscope. These crystal measurements were categorized under three headings; large quartz crystals, large feldspar crystals and groundmass. The measurements from this study are listed in Appendix B.

Due to the inherent variation of crystal sizes in any given specimen, size ranges of the maximum crystal length were recorded. For example, if a sample had five large feldspars,

Plate IV

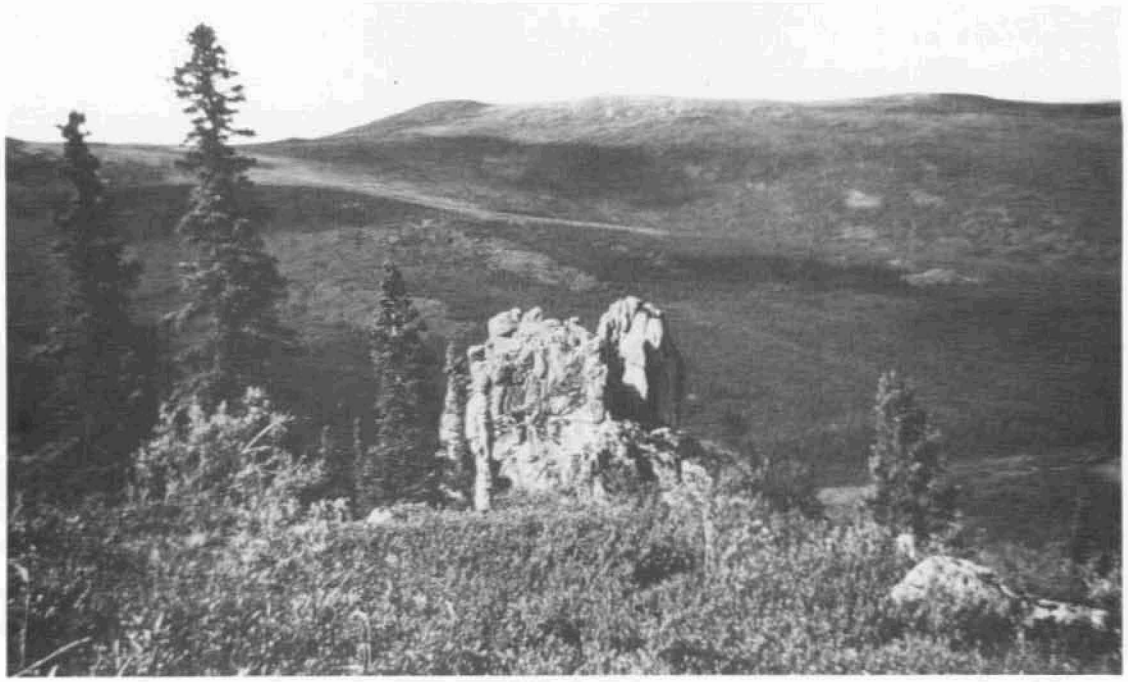

A. A Boulder Creek intrusive spire. Boulder Creek is toward the west, located in the lower right of the photograph.

B. Intrusive spires are located just west of the confluence of Half Dollar and Bottom Dollar Creeks on the north side of the road.

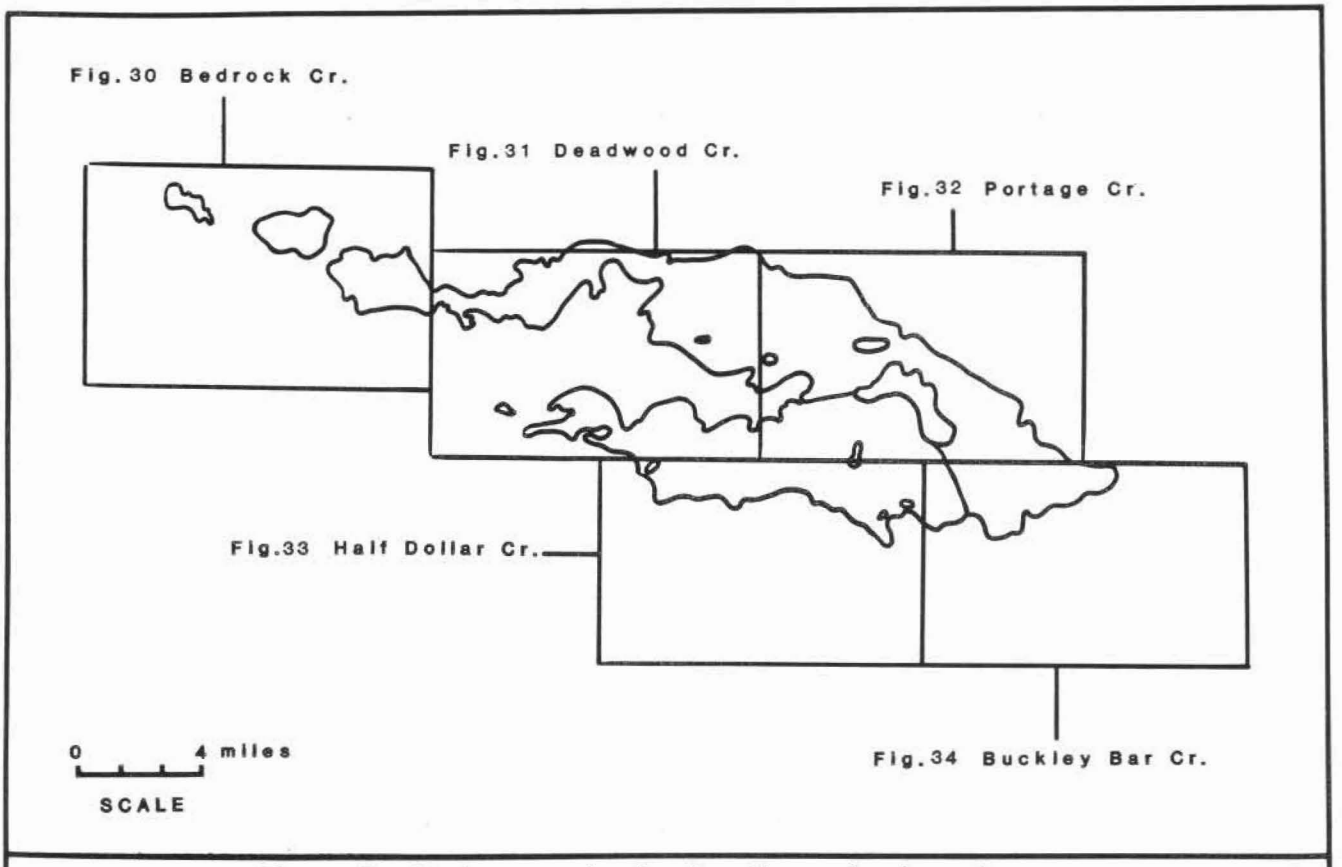

Figure 5. Study area showing locations of enlarged maps.
(See Appendix A-1 through A-5, p.57)

each was measured and the resultant range was recorded (20-30 mm).

In addition to the measurements of size ranges, the volumetric percentages of each crystal category was estimated for 72 of the 104 samples by visual estimation and modal point-count methods. For example, the sample KM 147 was found to have zero percent large quartz crystals, two percent large feldspars and 98 percent groundmass.

Modal Analysis

Ninety-nine representative rock samples were selected for modal point-count analysis. The rocks were cut with a Pistorius cut-off saw using a 14" Buehler diamond blade. Each slabbed surface was then ground flat using 120 grit to remove saw marks and rough edges. The slabs were then placed on aluminum foil on a hot plate set at approximately 350 degrees fahrenheit. A thin layer of epoxy was spread across the slabs to fill all cracks, large and small. After the epoxy hardened, a 220 grit was used to polish off any residual epoxy. The slabs were then polished down to 600 grit using 220 and 400 as intermediate grits. Next, the slabs were stained using the accepted techniques. These procedures are discussed by Meade B. Norman II in an article titled, "Improved Techniques for Selective Staining of Feldspar and Other Minerals Using Amaranth" (1974).

In modal analysis, a clear, acetate grid is placed over a rock slab or thin section that has been color stained to define potassium feldspar (yellow) from plagioclase (red). Point-counting is simply counting how many points of plagioclase, potassium feldspar, quartz and mafics there are in a given sample using a grid as a point guide. This data can be used to determine the volumetric percentages of the counted minerals in each specimen which can be used to determine the composition of the rock.

There is an important relationship between the number of points counted and the accuracy of the point-counting results. The number of points obtained on a given sample is a result of the size of grid used and the area of the sample counted. According to Van der Plas and Tobi (1965), the chosen distance between points should be greater than the largest grain encountered in a given specimen.

The Circle intrusive complex is composed primarily of medium-grained rocks containing medium to large phenocrysts. In the Two-bit pluton, the largest grains range in size

from 20-47 mm. Because only a few points could be counted on most of the rocks, a high maximum error of estimate, given a 95 percent confidence level would result.

To circumvent this problem it was necessary to come up with a separate procedure for point-counting the samples with large potassium feldspar phenocrysts. The grid sizes used were 1, 3 and 5 mm for the groundmass, and 15, 30 and 45 mm for the phenocrysts. The procedure is exemplified in Appendix C.

Statistical Reliability Study Summary

Two samples were point-counted, one from the Circle Hot Springs pluton (a medium-grained sample) and one from the Two-bit pluton (a medium-grained sample containing large phenocrysts). Each sample was point-counted three times per day on four separate days. Using these 12 point-counts for each specimen, the means and standard deviations were calculated for the percentages of plagioclase, potassium feldspar and quartz.

Given that 315 points were counted for sample SM 241 (from the CHS pluton) in 95 cases out of 100 the true volume percentages for plagioclase will lie between 48.58 percent and 28.58 percent, 43.87 percent and 19.79 percent for potassium feldspar and between 33.5 percent and 26.5 percent for quartz.

Given that 175 points were counted for sample SM76-C (Two-bit pluton), in 95 cases out of 100 the true volume percentages for plagioclase will lie between 15.96 percent and 10.2 percent, 56.91 percent and 45.59 percent for potassium feldspar and between 40.26 percent and 31.06 percent for quartz.

The large standard deviation is in part due to the low number of total points counted. The low number of total points counted is due to the coarse size of the grains in the samples. In order to decrease the standard deviation of the mineral percentages in each sample, larger areas of sample would have to be counted.

Geochemical Analysis

Whole-rock

Fourteen samples were prepared and analyzed for the major oxides. These results are listed in Appendix D. SiO_2, Al_2O_3, Fe_2O_3, MgO, CaO, Na_2O, K_2O, TiO_2, P_2O_5, MnO and Fe_2O_3T were analyzed by x-ray fluorescence at the Division of Geological and Geophysical Survey's (ADGGS) state laboratory located at the University of Alaska in Fairbanks. FeO was analyzed by titration methods using the hydrofluoric acid decomposition technique (Johnson and Maxwell, 1981). CIPW norms were also determined and are listed in Appendix D.

Trace-element

Eighteen samples were sent to the Bondar-Clegg laboratory in Vancouver, British Columbia, Canada for trace-element analysis. Beryllium and lithium were analyzed using atomic absorption methods with lower detection limits of 0.5 and 1 ppm respectively. Fluorine was analyzed using the specific ion electrode method with a lower detection limit of 20 ppm. Tungsten was analyzed using the colorimetric method with a detection limit of 2 ppm. Both tin and rubidium were analyzed using x-ray fluorescence with lower detection limits of 1 ppm. Boron was analyzed using a direct current plasma atomic emission spectrometer with a lower detection limit of 10 ppm. These trace element results are listed in Appendix E-1.

Fourteen samples were prepared and analyzed for Pb, Au, Ag, Mo, Sb, As, Cu, Zn, Co, Ni, Fe, Mn, and Cr in the ADGGS lab, Fairbanks, Alaska. Pb, Au, Ag, Mo, Sb, and As were analyzed using atomic absorption. Cu, Zn, Co, Ni, Fe, Mn, and Cr were analyzed using an inductively coupled plasma atomic emission spectrometer (Beckman ICP 2500). These trace-element analyses and the detection limits are listed in Appendix E-2.

Geochronology

Seven potassium-argon (K-Ar) ages were determined at the Alaska Cooperative Geochronology laboratory, Geophysical Institute in Fairbanks, Alaska. The calculation constants used are as follows:

$$K_{capture} = 0.581 \times 10^{-10}\ yr^{-1}$$

$$\text{Beta decay} = 4.962 \times 10^{-10}\ yr^{-1}$$

$$^{40}K/K_T = 1.167 \times 10^{-4} mol\ ^{40}K/K_T$$

The K-Ar analytical data results are presented in Section V.

IV. ANALYSIS OF MACROCRYSTALLINE TEXTURES

The purpose of this section is to examine the macroscopic igneous textures of the Circle intrusive complex. Since field relations are difficult to unravel in an area with little exposure, the scattered pieces of rubblecrop provide the only key to unlocking the history of the igneous rock. Invaluable information will always be provided by the uncrushed or undissolved field specimen.

Increasingly evident in geologic literature is the reported occurrences of particular macrotextures that appear to be coincidental with mineralization. It is therefore

becoming a growing necessity for workers to state briefly what textural set of standards they used. In this way, comparisons among intrusive rocks by various workers, can be made with a higher degree of accuracy. Standardization is difficult to achieve with the complex diversity that occurs in natural systems. Some standardized formats are either oversimplified, others cumbersome and biased, with the end result concealing important textural relationships. Commonly, there are several textural classifications that workers may select. These, combined with the various igneous rock classifications available, make it evident that one individual's subhedral, porphyritic biotite granite is another's equigranular, quartz monzonite porphyry. Until everyone subscribes to the same set of descriptive guidelines, it is very important to define the format which is being used for textural and rock classifications.

In this study, the analysis of macrocrystalline igneous textures provided the first clue that two texturally dissimilar bodies composed one larger body. This led to replotting modal data and plotting other chemical parameters to see if these two bodies were compositionally different. The main discovery was that commonly used textural terminology obscured textural differences between two plutons having different compositions and crystallization histories.

Bates and Jackson (1980) define texture as, "the general physical appearance or character of a rock, including the geometric aspects of, and the mutual relations among, its component particles or crystals." In igneous rocks, textural terms should describe, "the crystallinity, granularity, and fabric of the constituent elements," (Bates and Jackson, 1980). Hyndman (1972) states, "The granularity or grain size, of a rock is governed by the rate of cooling, composition and viscosity of the magma, number of crystal nuclei and movement of the magma." These processes that govern grain size provide direct evidence for the origin or petrogenesis of the rock (Hyndman, 1972). Therefore, since textures provide evidence of the petrogenesis of a rock, descriptive textural terms should distinguish between rocks that are petrogenetically different.

Some widely used textural terms include prophyritic, aphanitic, phaneritic, fine-grained, medium-grained, and coarse-grained. According to Cox, Bell and others (1976), if large crystals (phenocrysts) are set in a finer grained matrix (groundmass) the rock has porphyritic texture. Hyndman (1972) states that aphanitic rocks are those in which the grain sizes are too small to see and phaneritic rocks are those with visible coarser grains. He has further subdivided phaneritic rocks on the basis of grain size:

Fine-grained: less than 1 mm to aphanitic

Medium-grained: 1 to 5 mm

Coarse-grained: greater than 5 mm

According to these definitions most of the Circle intrusive rocks could be described as medium-grained porphyritic rocks. This also implies that most of the intrusive rocks have the same general appearance, composition and conditions of crystallization. Analysis of the macrocrystalline textures of 104 rock samples has shown that there are specific differences among groups of rocks. In addition, these groups of rocks have been found to differ in composition, appearance, age and geographic extent.

Shown in Plate V are three hand samples that could be described as medium-grained, porphyritic biotite granites. On closer examination, the rock in the middle and bottom photo has consistently larger feldspar phenocrysts set in a slightly larger grained groundmass (although still medium-grained by Hyndman's definition). Are the differences in size of feldspar phenocrysts, between the top photo and middle and bottom photos important enough, in terms of petrogenesis to distinguish by descriptive textural terms? If the rocks are described as being porphyritic biotite granites, this implies they are petrogenetically similar. In fact, the top photo shows a 57 million year old syenogranite and the middle and bottom photos are of 70 million year old monzogranites. To answer the posed question, "Yes, the differences in the size of the large feldspar phenocrysts provide an important clue to rocks that have a different composition, cooling history and, in this case, age". Therefore distinguishing textural terms should be used to describe these rocks.

Textural Terms: Redefined for the Circle Intrusive Complex

Porphyritic versus Mediophyric and Megaphyric

To determine if the macrocrystalline measurements (Appendix B) show any textural trends, a simple plot was devised. In Figure 6 the large feldspar values were plotted against the size of the groundmass to determine if any obvious groupings of rocks with similar textures resulted. This particular plot was chosen because the measurements of the large feldspars and the groundmass grains are the most straightforward and can be easily reproduced.

The plot shows that some samples do not have large feldspars. These rocks became Group A. A few samples have groundmass grains that are one to less than one mm. These rocks became Group B. The C and D Group division was less readily apparent and familiarity with the samples aided in setting the resultant boundary. For example, in the area of Nugget Gulch, Bottom Dollar Creek and part of Portage Creek, the large feldspars increased notably in size (20-47 mm). Other areas, including Deadwood Creek and Boulder Creek, had rocks with smaller, large feldspars (5-17 mm). In Figure 6, the boundary is drawn between 17 and

Plate V

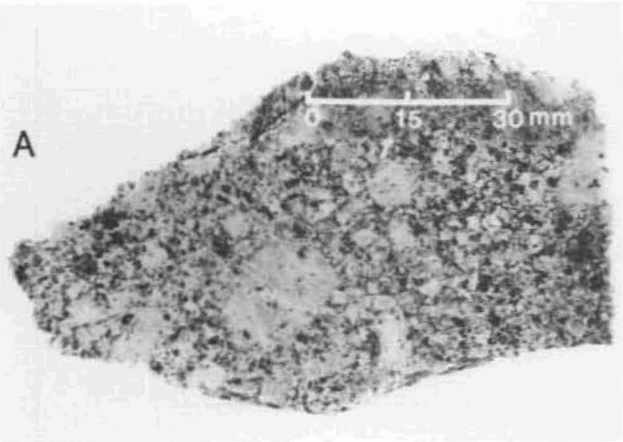

A. A 57 m.y. old syenogranite (see p. 21 for plutonic rock classification).

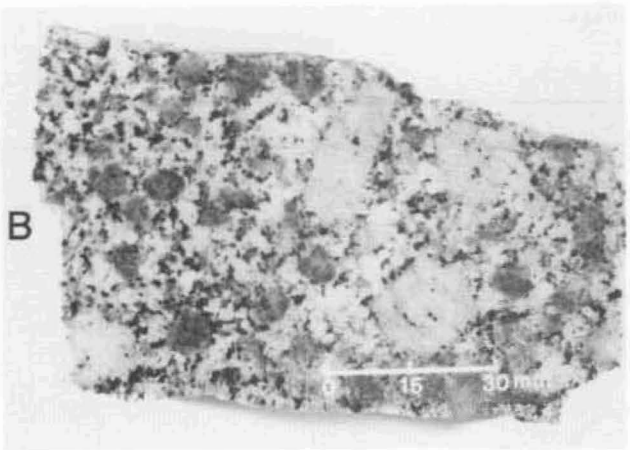

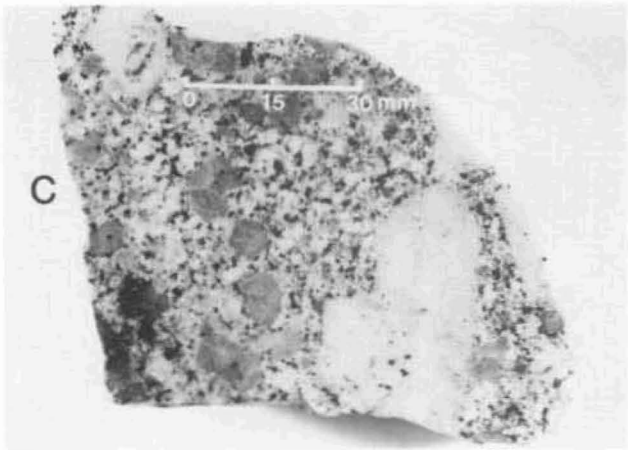

B. and C. 70 m.y. old monzogranites.

20 mm to separate the two groups. The C Group samples share a similar groundmass size with the D Group samples but the D rocks have consistently larger feldspars.

In Figure 7, Groups A, B, C and D were plotted by sample location to determine if they represented any regional textural trends across the plutonic complex. Figure 7 shows that the predominant texture in the northern lobe of the complex is Group C. The predominant texture in most of the southern lobe of the complex is Group D. Group A apparently represents an intrusive contact border phase. Group B represents a small area of local variation.

The difference between Group C and Group D is primarily in the size of the large feldspars. In current textural terminology, both groups would be lumped together and described as medium-grained porphyritic rocks. This is a true, general description but on closer examination the textural differences between Groups C and D provide important insight to compositional variation across the plutonic complex.

Figure 8 was created as a result of the Group C and D textural trends. Neither modal point-count work nor whole-rock geochemistry suggested such a clear-cut difference between the northern and southern lobes of this complex. It was the major textural trends (Fig. 7) that keynoted the possibility of compositional differences between the northern and southern lobes. Figure 8 shows the modal composition of the northern lobe rocks to be more potassic whereas the southern lobe rocks are less potassic and richer in the plagioclase component.

Other plots were devised to further analyze the difference between the two intrusive lobes. Rubidium is a trace-element that is similar to potassium and will extensively replace potassium in the micas and feldspars. In Figure 8, the northern lobe is shown to be more potassium rich. Hence, rubidium values should be higher here. Figure 9-A shows that the northern lobe has distinctly higher rubidium values than the southern lobe.

The differentiation index values of 14 rocks from the batholith were determined. According to Bates and Jackson (1980), the differentiation index expresses the extent to which a magma has differentiated, and it represents the sum of the weight percentages of normative kalsilite, nepheline, leucite, albite, orthoclase, and quartz. Figure 9-B shows that the northern lobe has higher differentiation index values than the southern lobe. Because the samples are sparse, this diagram is only suggestive that northern and southern areas are compositionally different.

In addition, Figure 9-C shows a plot of tin analyses for the same samples used in plotting Figure 9-A. This is an

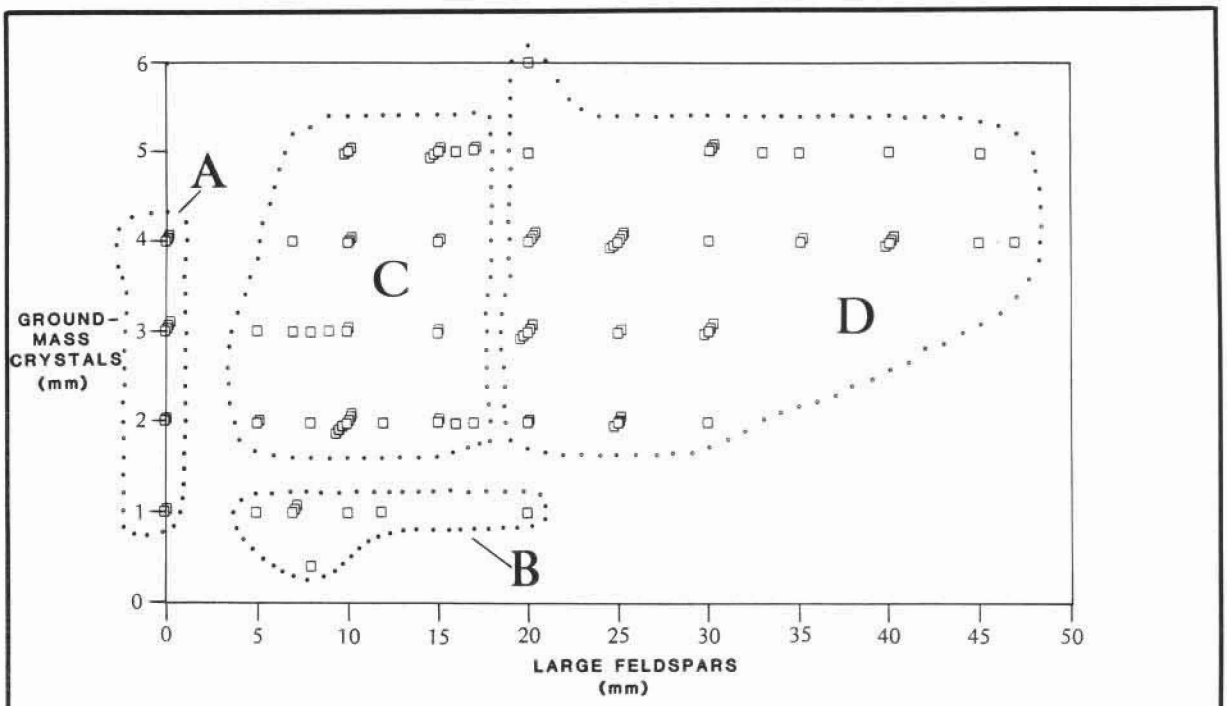

Figure 6. Textural variation of 104 rocks from the Circle intrusive complex. For each sample, the size of the largest feldspar and the size of the largest crystal in the groundmass was plotted. Each of the four groups represents rock samples that share textural similarities. The division between Groups C and D is based on field observations.

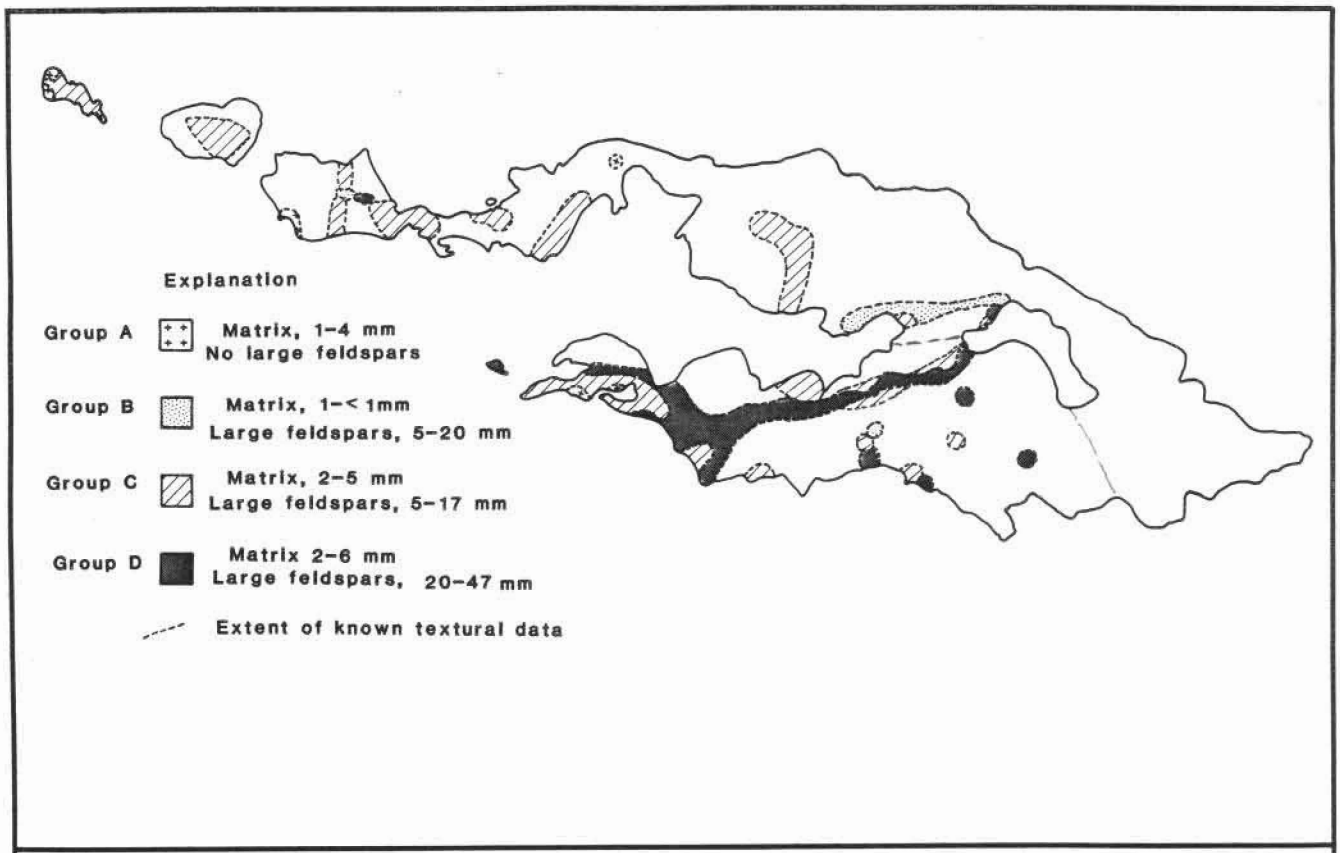

Figure 7. Geographic locations of four distinct textures that compose the Circle intrusive complex.

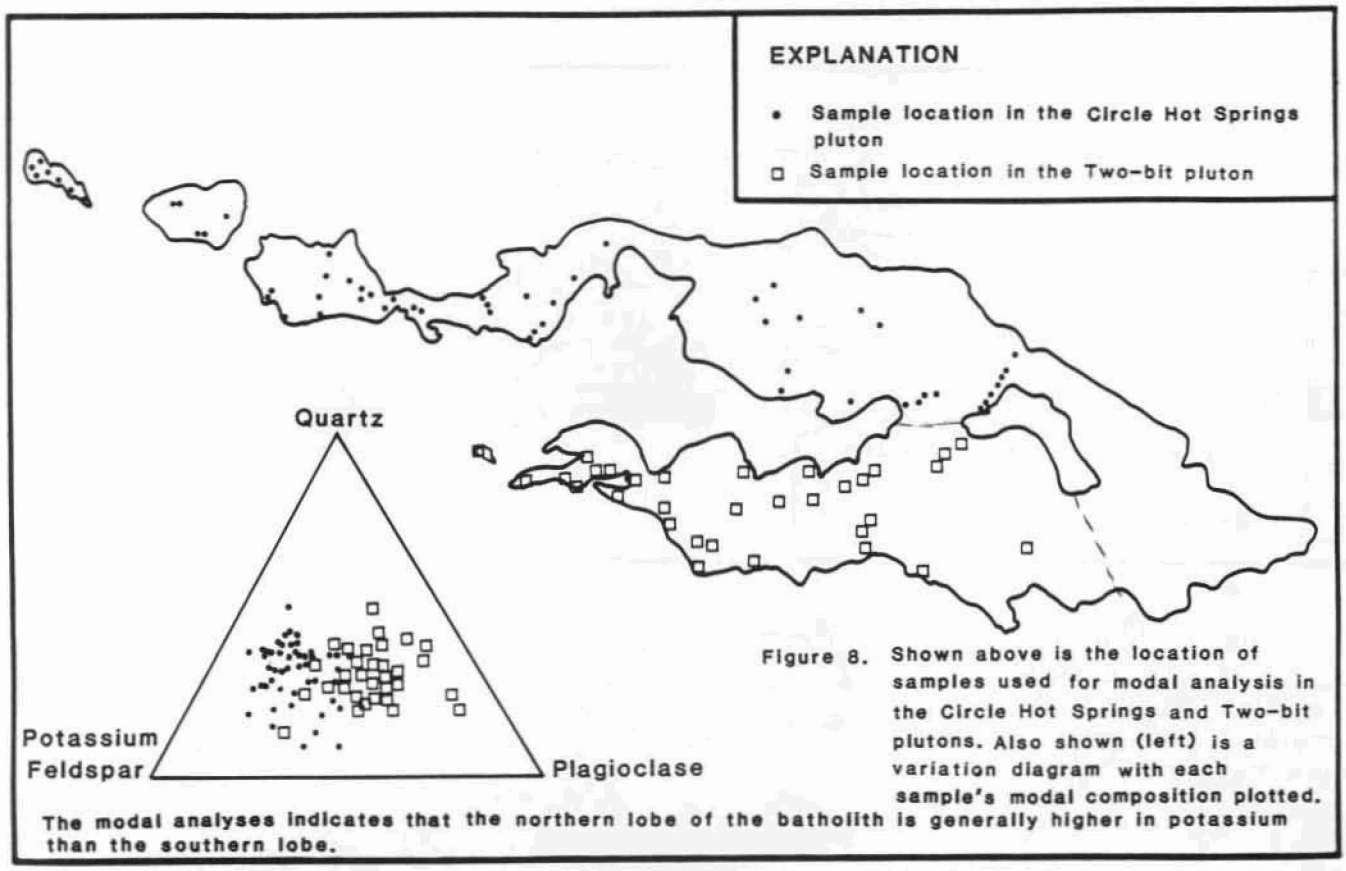

Figure 8. Shown above is the location of samples used for modal analysis in the Circle Hot Springs and Two-bit plutons. Also shown (left) is a variation diagram with each sample's modal composition plotted. The modal analyses indicates that the northern lobe of the batholith is generally higher in potassium than the southern lobe.

interpretive diagram but the general trends indicate low tin values in the southern areas and higher tin values in the northern areas. Based on the general trends of these chemical parameters (modal composition, trace-element and differentiation index), it appears that there is a compositional difference between the northern and southern intrusive lobes of the complex.

The "size" of the large feldspars provides the first and most readily available clue that the northern and southern intrusive lobes are different. It would be too general to describe all the rocks from both lobes as "porphyritic". For this study, the term porphyritic will be redefined for the Circle intrusive complex as follows: Any rock with large feldspars (phenocrysts) that range in size from 5-17 mm will be described as mediophyric. Rocks with large feldspars of the size range 20-47 mm will be called megaphyric.

The Importance of the Volume Percentage of the Large Feldspars

A rock containing three percent large feldspars has a different appearance than a specimen containing 40 percent large feldspars. They "look" so different that is does not seem correct to describe them with the same textural term. To some workers, the term 'porphyry' would be used to describe a rock with a greater percentage of large feldspars and a rock with less would be described as 'porphyritic'. Is the number of large feldspars contained in a specimen important in providing clues to the perogenesis of the specimen? Should there be textural terms to distinguish between a rock containing one percent large feldspars versus a rock that contains 50 percent large feldspars? It has already been suggested that based on textural trends and chemical parameters, two intrusive bodies compose the batholith. The purpose of this section is to determine if the percentage of large feldspars across the complex provides additional evidence that two plutons exist. For example, do the rocks in the northern lobe consistently contain ten percent large feldspars versus the rocks of the southern lobe that may consistently contain 40 percent large feldspars? If so, textural terms should be used to distinguish between the petrogenetically different suites of rocks.

Based on the volume percentages of 72 samples (Appendix B), four divisions were formed. These divisions consisted of the following; samples with no large feldspars, samples with 1-10 percent large feldspars, 11-40 percent feldspars, and those with greater than 40 percent feldspars. These divisions were determined by listing the volume data and choosing the percentage groupings by visual estimation.

In Figure 10 the samples within the four, large feldspar divisions were plotted on the sample site locations. Figure

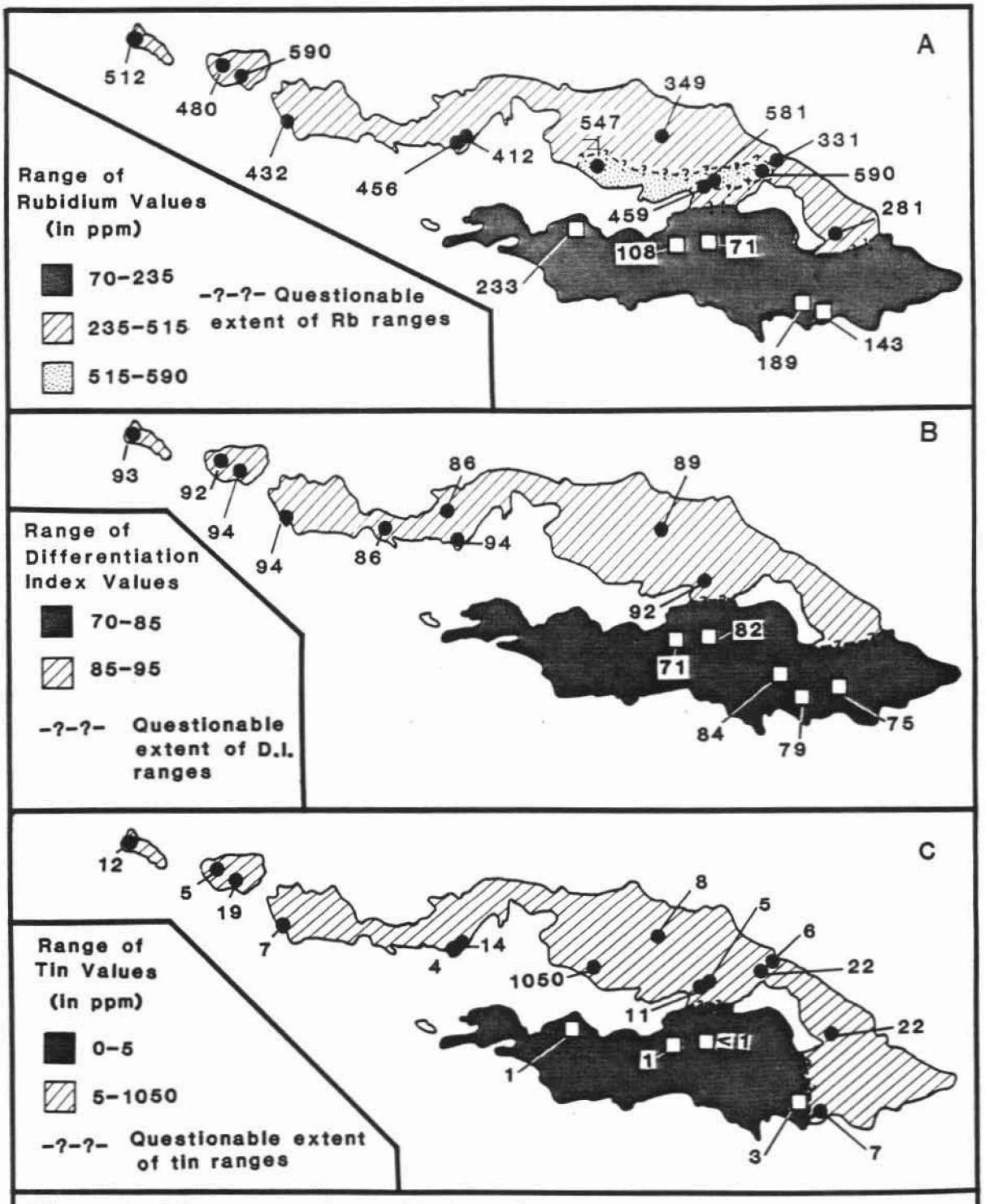

Figure 9. The maps show the location of samples with their corresponding rubidium, differentiation index and tin values plotted. The range of values suggest that the batholith is composed of two compositionally different intrusives.

10 shows that although rocks containing one to ten percent large feldspars somewhat correspond to the northern lobe, discrepancies and variations occur that impair a clear trend. Lack of data makes it difficult to determine textural relationships in the northern lobe. Rocks containing 11-40 percent large feldspars appear to correspond to the southern lobe.

Several problems are inherent in a volume-percentage study of the large feldspars. There are extraneous variables that directly affect the percentage of large feldspar recorded. One factor is the amount of sample available at each site. The final percentage of large feldspars measured is directly related to the amount of sample obtained. This amount varies from site to site depending on outcrop availability and accessibility. Also, the fewer the points that are available on a rock slab to point-count, the greater the error in the final volume proportions.

Based on the variation of large feldspar percentages in the rocks of the northern lobe, in conjunction with sample collection and modal point-count error, it is not clear that volumetric percentages of the large feldspars provide ready clues to the petrogenesis of a given specimen. For this study, textural terms will not be used to distinguish between rocks that fall into one of the four divisions shown in Figure 10.

Groundmass: Fine-grained, Medium-grained and Coarse-grained

On the basis of macrocrystalline measurements (Appendix B), the matrix or groundmass of most of the Circle plutonic rocks range from 2-6 mm, a few specimens have a matrix of 1 to less-than-1 mm, and only a very few have a matrix of greater than 6 mm. With these measurements as criteria, the following groundmass grain-size subdivisions are defined for the Circle intrusive rocks:

Fine-grained: 1 mm to aphanitic

Medium-grained: greater-than-1 mm to 6 mm

Coarse-grained: greater-than-6 mm

This classification closely resembles Hyndmans' subdivision of phaneritic rocks (1972).

Groundmass: Equigranular Versus Subequigranular

An equigranular groundmass is composed of equant crystals. In many of the Circle intrusive rocks the minerals

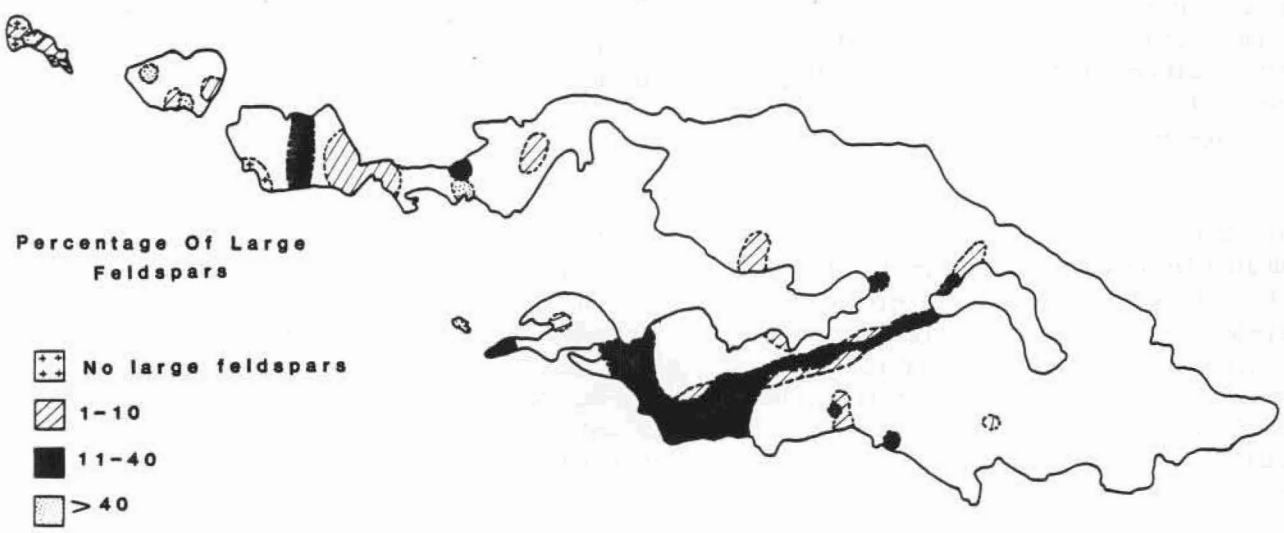

Figure 10. Map shows geographic distribution of the large feldspars.

in the groundmass reflect differential growth rates that appear to be consistent and specific to each mineral. For example, in many samples the quartz grains are consistently smaller than the feldspars. The potassium feldspar typically grows larger than the plagioclase and often occurs in two distinct grain sizes within the groundmass. It is important to note that each mineral is fairly equal in size to other minerals of the same composition. Quartz is equigranular with respect to other quartz crystals. But quartz crystals within the groundmass are not often equigranular with respect to the potassium feldspar or plagioclase crystals. To describe the rocks with these characteristics, the term "subequigranular" is used.

Large Quartz Crystals: Phenocryst Versus Groundmass

Exactly how large a crystal must be, relative to the groundmass to be considered a phenocryst is largely based on personal opinion. One convention followed is that a crystal must be approximately ten times the size of the groundmass to be called a phenocryst.

Many of the Circle intrusive rocks have large subhedral to euhedral quartz crystals. They are generally 1-4 mm larger than the groundmass but three to four times smaller than the large feldspars that occupy the same rock (Fig. 11). They are definitely not ten times the size of the groundmass. Are they phenocrysts or are they part of the groundmass? Since these quartz crystals do not seem to be part of the groundmass and are not large enough to be called phenocrysts they are ignored by textural classifications currently in use.

Figure 12 shows that the large, subhedral quartz crystals are consistently bigger in the southern lobe of the batholith. There appears to be a direct relationship between the size of the large feldspars and the size of the large quartz crystals. It has already been established that it is important to distinguish between the size of the large feldspars (Fig. 6, Group C and D). Based on this proportional relationship between the large quartz and feldspar it is not necessary to distinguish the quartz texturally.

Summary

Macroscopic textures provide the first clues to the petrogenesis of a rock and descriptive textural terms should distinguish between rocks that are significantly different. In the Circle intrusive complex, the size of the feldspar phenocrysts provides the first clue that two, dissimilar intrusive bodies compose the batholith. Contemporary textural terminology can effectively obscure these important differences due to oversimplification. For this study, 'mediophyric' and 'megaphyric' textures are defined for the Circle intrusive complex and texturally describe rocks which are also different in composition, geographic extent and age.

V. GEOCHRONOLOGY

Potassium-argon (K-Ar) radiometric ages were determined for six samples of biotite and one sample of white mica from the Circle intrusives. Figure 13 shows the locations of the samples dated and the analytical data. Macrocrystalline textural variations were the first clue that two plutons composed the batholith. Modal analysis, whole-rock and trace-element data supports this hypothesis. Finally, K-Ar age dates confirm it.

Four age dates ranging from 56.35 ± 1.69 to 57.75 ± 1.73 million years were determined for samples from the Circle Hot Springs pluton. One age of 54.17 ± 1.63 million years was obtained for an aplite dike crosscut by a tourmaline rich veinlet. K-Ar dates of 69.71 ± 2.09 and 70.92 ± 2.13 million years were determined for samples from the Two-bit pluton. Deuteric alteration of the biotites make it difficult to date rocks in the western portion of the Two-bit pluton. The association of these K-Ar ages to rock types and crosscutting relationships will be discussed in the following section. According to Wilson and others (1985), based on a compilation of metamorphic and plutonic K-Ar ages of the Yukon-Tanana Upland, it is doubtful that there have been any regional thermal metamorphic events with enough heat to reset the K-Ar ages of the Circle intrusive complex. Therefore, since crystallization of the plutons, the temperature of the surrounding metamorphics probably did not exceed the biotite blocking temperature for argon.

VI. ROCK TYPES

The purpose of this section is to describe the rocks of the Circle intrusive complex. Each pluton will be examined separately. The rock types have been named based on modal analysis data. Each rock type will be briefly described by their macroscopic characteristics which include color and alteration. Minerals identified microscopically are also discussed. This includes major minerals, accessory minerals and secondary minerals.

A discussion section at the end of this chapter summarizes the main rock types of each pluton, macroscopic textural variation and mineralogical differences, along with crosscutting relationships based on field evidence, thin section work and K-Ar age dates. The final summary figure is a composite of four structural cross sections showing the area in the Circle intrusive complex thought to have the greatest tin potential based on mineralogy and rock types.

The Circle Intrusive Complex

Streckeisen's classification (1973) of plutonic rocks based on actual mineral composition is used for this report (Fig. 14). Another boundary has been added to separate

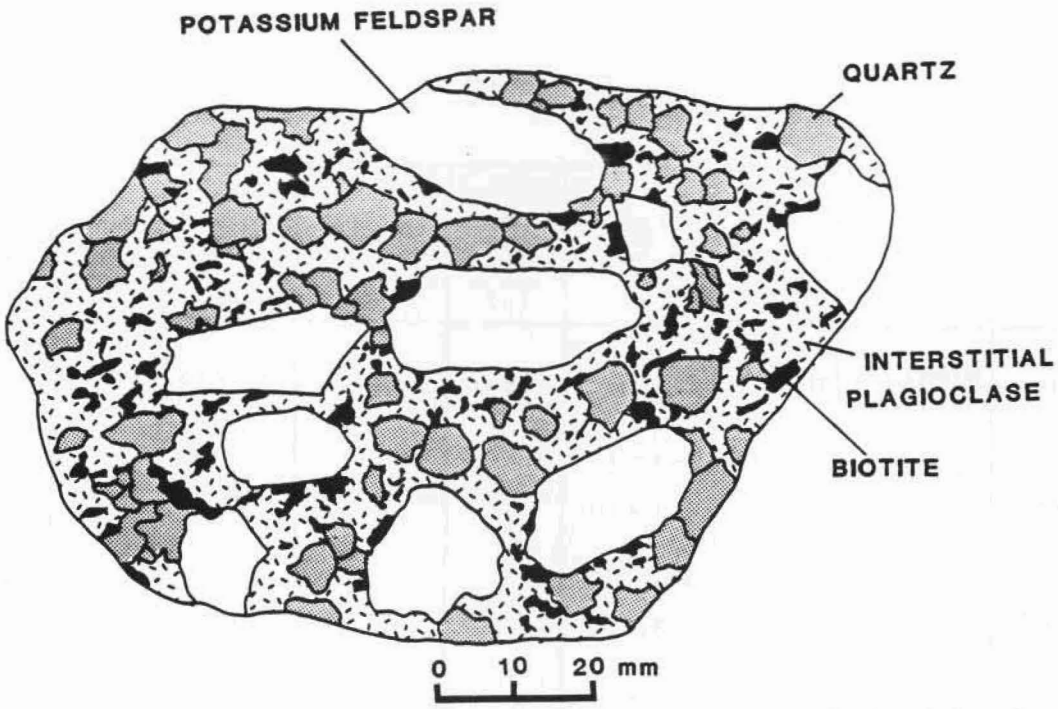

Figure 11. This drawing shows the textural relationship between the large potassium feldspar crystals, interstitial plagioclase and biotite, and the large, subhedral quartz crystals.

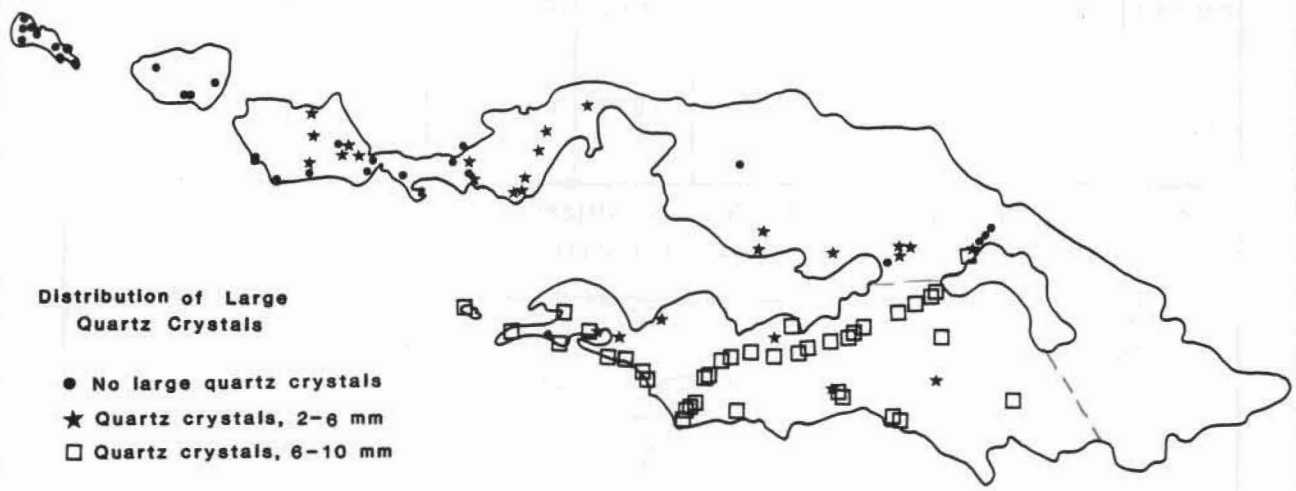

Figure 12. Map shows geographic distribution of the large quartz crystals.

Sample Number	Rock Type	Mineral	K_2O (wt%)	Sample Weight (g)	40ArRad (mol/g) x 10E-11 *	40ArRAD / 40K x 10E-3 *	%40Ar RAD *	Age +/- Sigma (M.Y.) *
CH59	Monzo-granite	Biotite	Mean = 8.779	.1544	73.3599	3.3729	89.47	57.14 +/-1.71
CH61	Syeno-granite	Biotite	Mean = 8.410	.1155	71.0429	3.4094	86.84	57.75 +/-1.73
KM114	Grano-diorite	Biotite	Mean = 3.242	.3545	33.1723	4.1294	91.92	69.71 +/-2.09
KM133	Mineral-ized Aplite Dike	Biotite	Mean = 8.682	.1316	68.7262	3.1949	88.71	54.17 +/-1.63
KM147	Syeno-granite	Biotite	Mean = 8.899	.0793	73.3209	3.3256	82.91	56.35 +/-1.69
PM250	Pegmatite Dike	White Mica	Mean = 10.264	.1517	106.8952	4.2023	79.92	70.92 +/-2.13
1933	Grano-diorite	Biotite	Mean = 8.113	.1073	67.9719	3.3814	87.56	57.28 +/-1.72

* These values are valid to three significant figures.
RAD = radiogenic Sigma = standard deviation

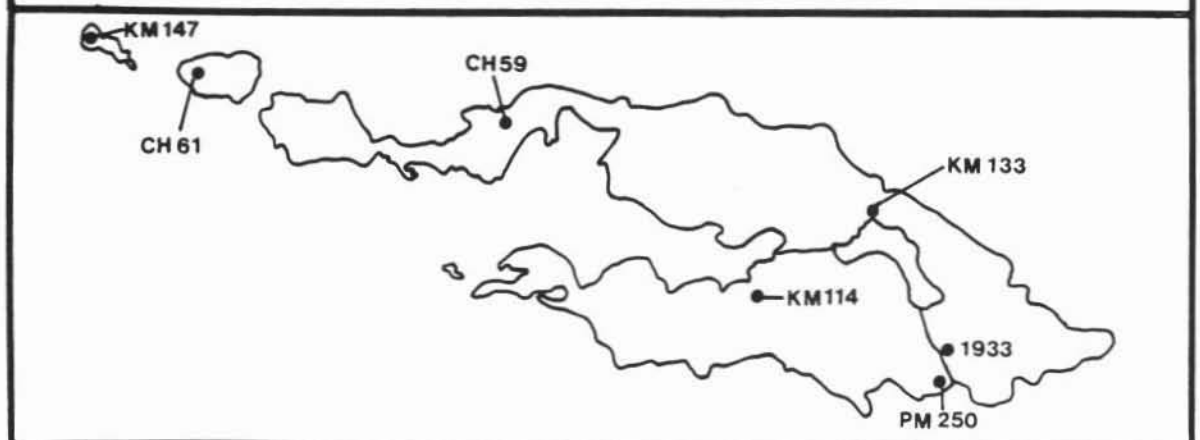

Figure 13. Analytical data for potassium-argon ages of the Circle intrusive complex. Map shows sample locations.

syenogranites from monzogranites (Clarke and others, 1980).

Figure 15 is a modally-derived composition map. All the composition contacts are inferred based on individual sample compositions and apparent trends. Although K-Ar dates support that the eastern end of the complex is part of the Circle Hot Springs pluton, insufficient modal data are available to extrapolate composition. For both the Circle Hot Springs and Two-bit plutons, plagioclase, potassium feldspar and quartz are the major mineral constituents with biotite as the dominant mafic mineral. For easy reference, Figure 16 is a location map of the rocks that were examined petrographically. Additionally, the distribution of enclaves, aplite-pegmatite and mafic dikes is shown.

Circle Hot Springs Pluton

The Circle Hot Springs pluton is composed of syenogranite, monzogranite and quartz monzonite. Only two samples of granodiorite were identified. Generally, the rocks are light-colored. They have black specks set against a grey and white matrix. Occasionally they are covered by a thin coat of red-brown iron stain. The feldspars are white, the quartz crystals are translucent, milky or smoky and the biotites, black-brown. In some samples the biotites are green as a result of chloritization.

The main distinction between the rock types is the relative percentages of potassium feldspars to the plagioclase feldspars. Quartz and mafics are not visibly significant enough to use as discriminators between the rock types. It would be difficult to impossible to distinguish among the four rock compositions in hand specimens without the aid of modal point-counting (Plate VI).

Most of the Circle Hot Springs pluton is composed of rock with a medium-grained, subequigranular groundmass and varying percentages of subhedral potassium feldspar phenocrysts. Some of the rocks near the contact zones have a fine-grained groundmass.

Enclaves are inclusions. Inclusions can represent

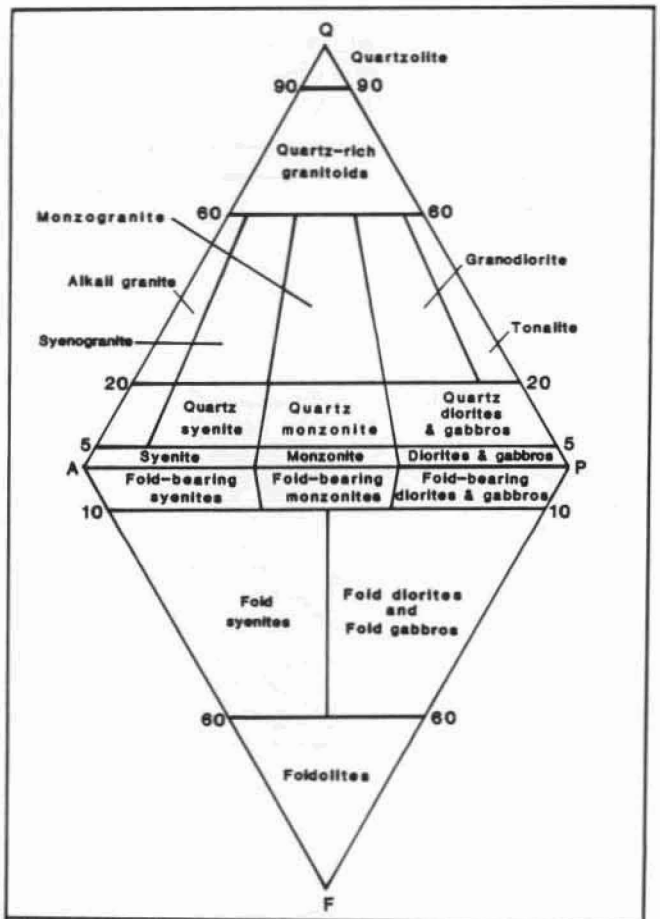

Figure 14. Classification of plutonic rocks based on their actual mineral composition (adapted from Figure 1, Geotimes, October 1973, p. 26). Q-Quartz, A-Alkali feldspar, P-Plagioclase, F-Feldspathoid (abr. "foid")

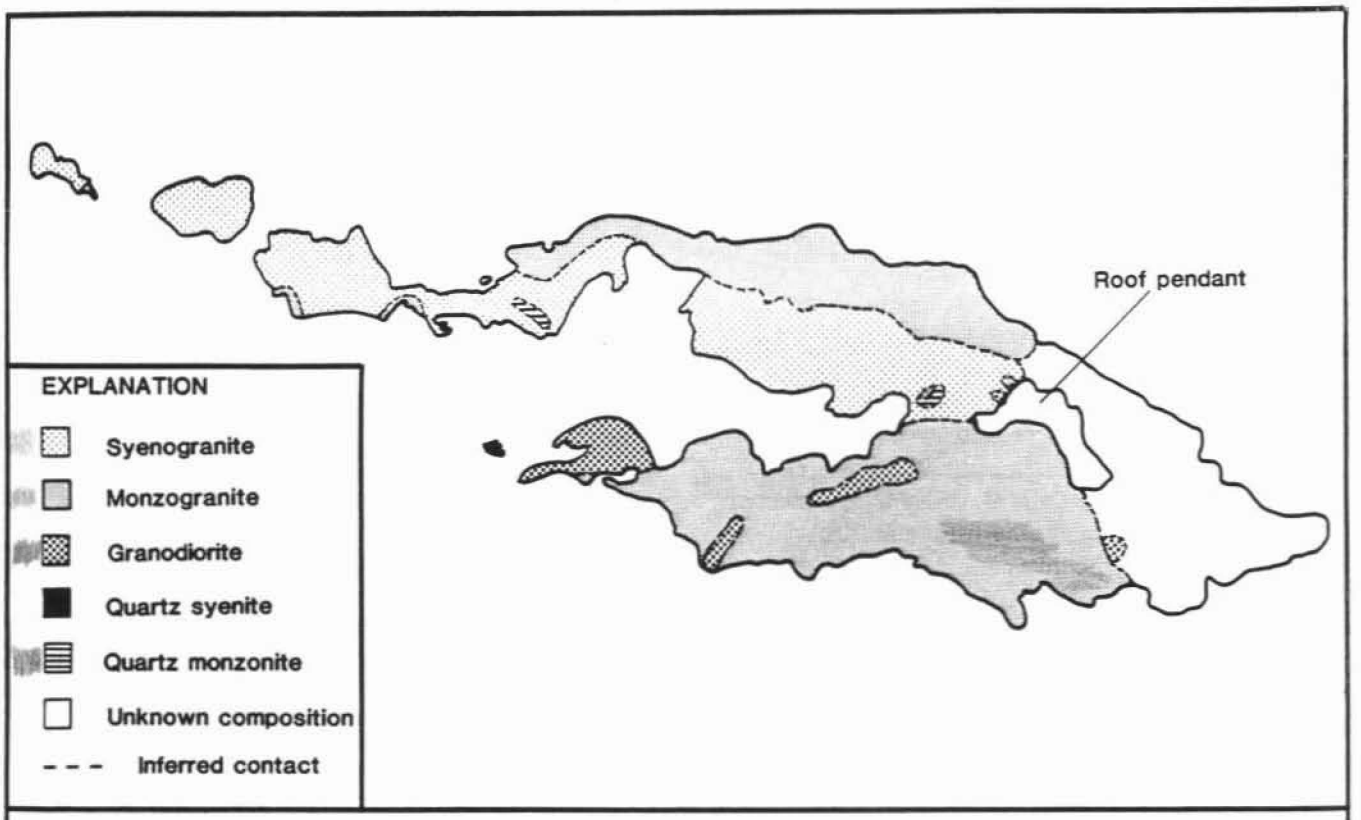

Figure 15. Shown above is a composition map of the Circle intrusive complex that is based on modal analysis data. The compositions have been determined by using the modified Streckeisen's classification previously discussed (p.18).

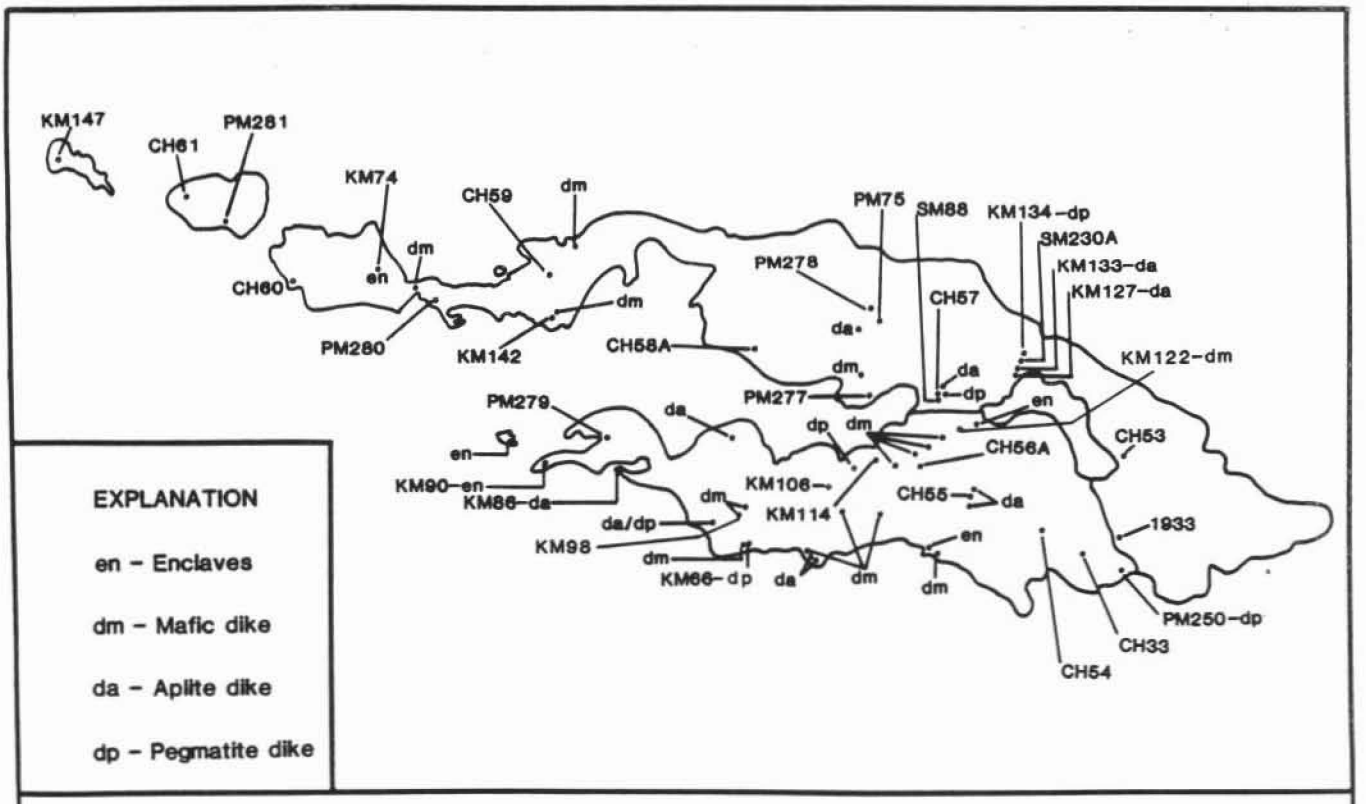

Figure 16. Location of samples that were examined in thin section. Also shown is the distribution of enclaves and aplite, pegmatite and mafic dikes.

Plate VI

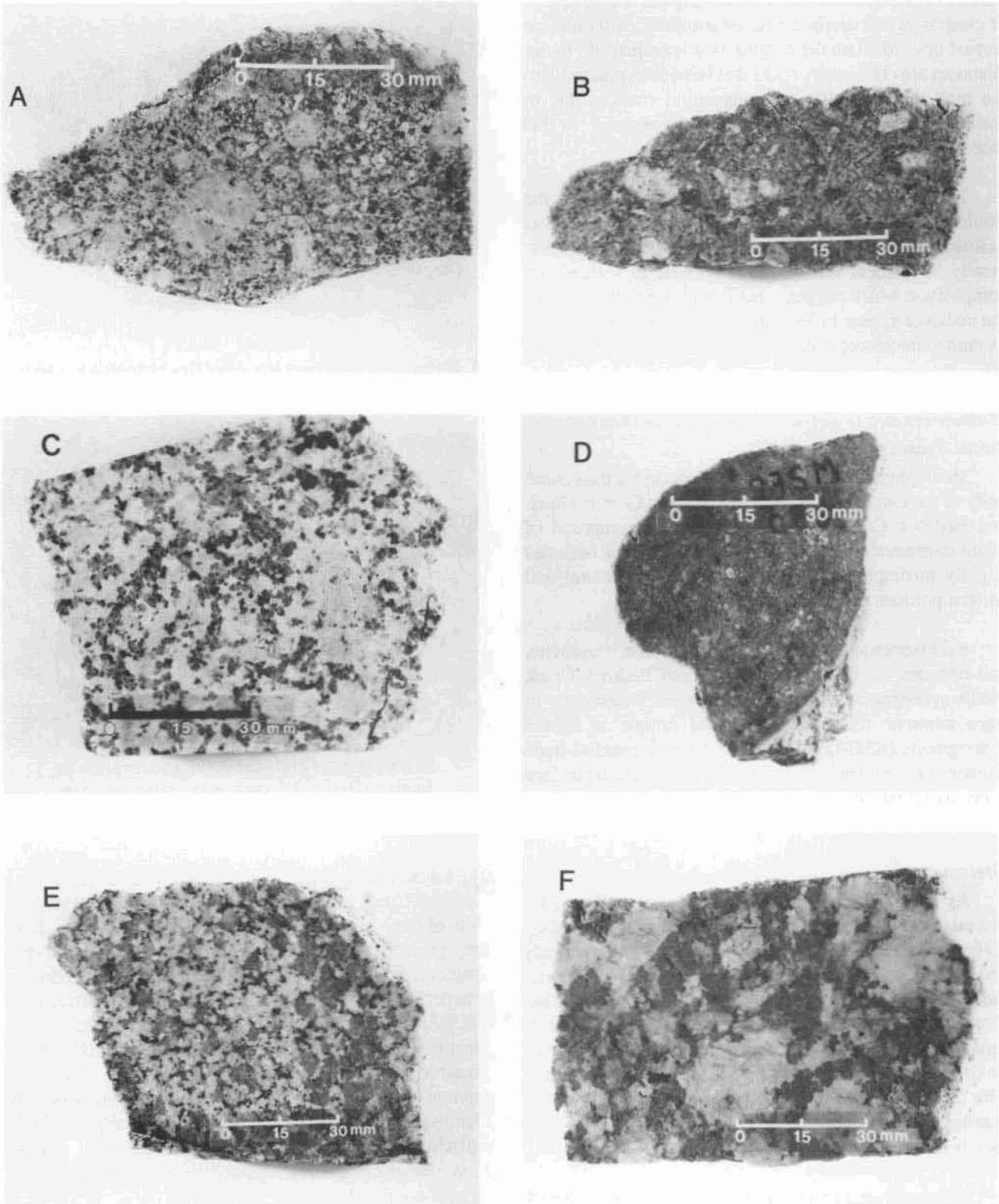

Representative rock types of the Circle Hot Springs pluton.
A - SM319, syenogranite B - BC68, quartz monzonite
C - KM147, syenogranite D - SM88, quartz monzonite
E - 1933, granodiorite F - KM139, monzogranite

groups of early-formed crystals that are more mafic but have a similar composition to the granitic magma. These groups or clusters of this origin are called autoliths. Autoliths are carried upwards with the magma as it is emplaced. Inclusions can also be country rocks that have been plucked into the melt thereby suffering composition changes due to assimilation and reequilibration with the magma. In this case they are referred to as xenoliths.

The only conspicuous appearance of enclaves is in the Boulder Creek spires (Plate IV-A, p. 9). One enclave was examined in thin section and was found to contain approximately 25 percent biotite. It is igneous in texture and composition which suggests that it is an autolith. Some of the enclaves appear to have foliated textures but were not examined microscopically to verify their origin (Plate VII-A).

Medium-grained to Slightly Mediophyric to Mediophyric Biotite Syenogranite

Mediophyric biotite syenogranite occupies the central body of the Circle Hot Springs pluton. The Granite Gulch and Bedrock Creek exposures are mostly composed of medium-grained, subequigranular rock. The rock becomes slightly mediophyric to mediophyric in the central and eastern portions of the body.

Accessory minerals include zircon, apatite, muscovite, and opaques. In the Granite Gulch and Bedrock Creek biotite syenogranites, tourmaline is present interstitially in trace amounts (Plate VII-B). One sample of biotite syenogranite (KM142) in Deadwood Creek contains trace amounts of hornblende. Chlorite and sericite are secondary minerals found throughout the intrusive body.

Greisen

As a magma cools to a crystalline state, it can be essentially solid but still hot. Associated with the cooling magmas are residual, hot, aqueous fluids (hydrothermal) and/or gaseous emanations (pneumatolytic) that rise through intergranular pore spaces, fissures or cracks. Contact zones provide especially favorable sites for these fluids and gases to migrate. Sometimes these postmagmatic fluids or gases are mineralized. When they come into contact with the hot, granite rock, earlier-formed minerals in the granite can be partially or wholly replaced. In this way the rock becomes altered or changed.

Pneumatolyzed rocks are those that have been altered by hot, gaseous emissions. Greisens are pneumatolyzed rocks that are generally located near granite pluton boundaries (Williams and others, 1982). They occur in beltlike strips and as veins of varying width that grade into unaltered granite.

Plate VII

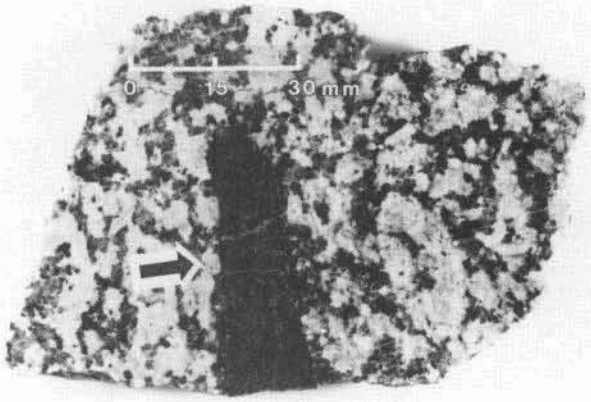

A. Sample taken from Boulder Creek intrusive spire (Plate IV-A). KM74, enclave in syenogranite.

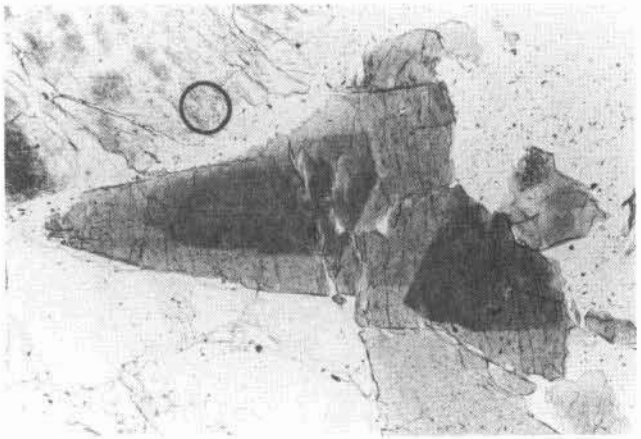

B. Sample CH61, interstitial tourmaline in syenogranite. Photomicrograph taken in plain light, width of field 1330 microns.

Located on two topographically high areas adjacent to Ketchem Creek is altered rubblecrop (CH58A and PM75). Both of these samples are greisen. The rock appears dark, grey-green in hand sample. Accessory minerals include apatite, zircon, rutile(?), magnetite, allanite(?), granular sphene(?), and cassiterite. A polished section was made for CH58A. Cassiterite in trace amounts and magnetite were identified based on Vicker's microhardness test (Craig and Vaughan, 1981) and on reflectance properties. X-ray diffraction was also performed and cassiterite was positively identified (Plate VIII). Secondary minerals include chlorite and white mica. In both of these samples, the feldspars have been almost completely replaced by white mica and the biotites are mostly altered to chlorite.

SM230A is located adjacent to Portage Creek. This altered biotite syenogranite is not greisen but the rock has been changed by postmagmatic emissions. This sample has tiny veinlets (5mm in width) of granitic material that appear

Plate VIII

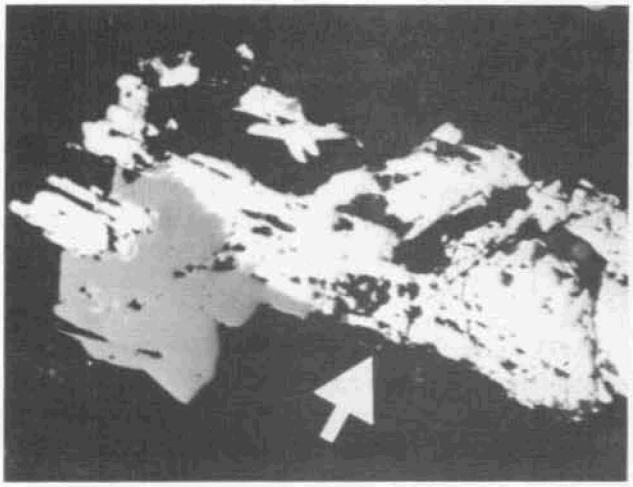

A. CH58A, magnetite. Photo taken in normal incident light, width of field 440 microns.

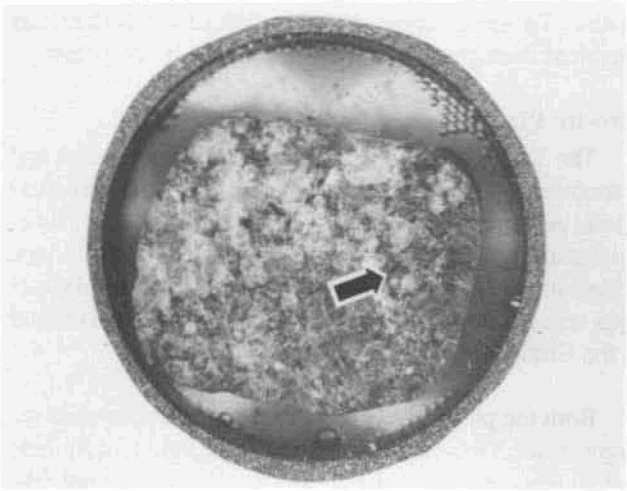

B. CH58A, a polished section containing cassiterite and magnetite in greisen (1.5 inch Ring Form).

as dark, grey stringers in hand specimen. Included in the veinlets are plagioclase, potassium feldspar, quartz, chlorite, magnetite, and cassiterite. The cassiterite has been only identified by Vicker's microhardness test (Craig and Vaughan, 1981) and on reflectance properties (Plate IX).

Slightly Mediophyric to Mediophyric Biotite Monzogranite

The biotite monzogranite predominates along the northern side of the Circle Hot Springs biotite syenogranite with the exception of two small occurrences that outcrop between Tommy's Pup Creek headwaters and Boulder Creek (Fig. 15). The western exposures of the biotite monzogranite have medium-grained, subequigranular groundmass with occasional potassium feldspar phenocrysts. The biotite monzogranites in the Ketchem to Portage Creek areas have medium-grained to coarse-grained subequigranular groundmass and are slightly mediophyric to mediophyric. The mineral constituents are generally the

Plate IX

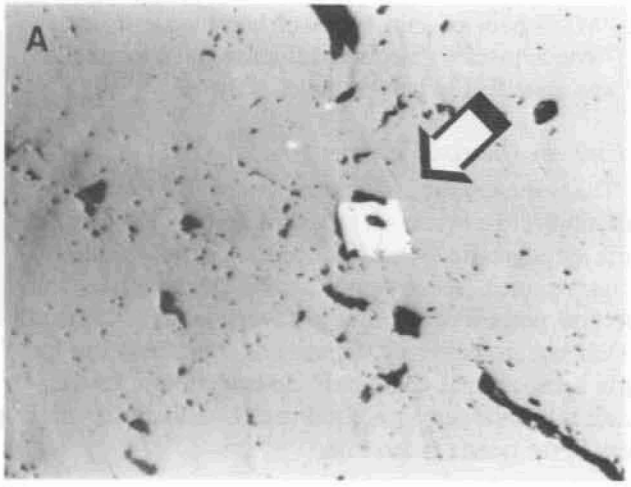

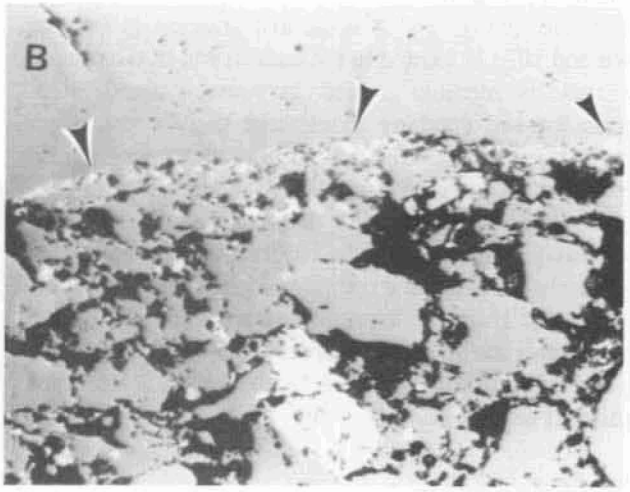

A. and B. SM230A, cassiterite. Photo taken in normal incident light, width of field 440 microns.

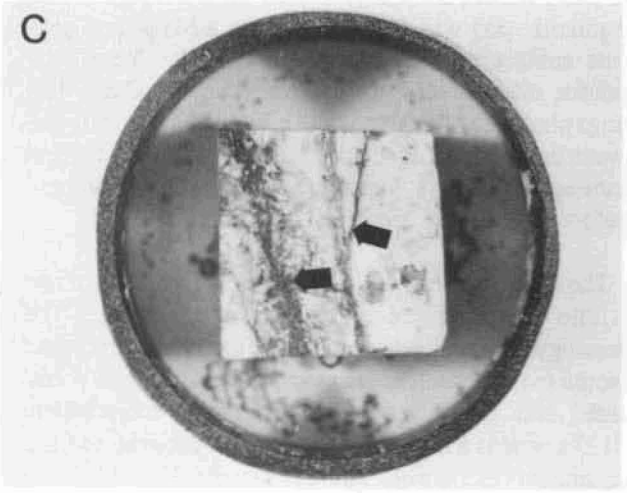

C. SM230A, small veinlets in sample containing cassiterite (1.5 inch Ring Form).

same as those in the biotite syenogranites. Samples CH59 and PM280 both contain traces of hornblende. Sample CH57 contains trace amounts of fluorite and a tourmaline pod was identified in hand sample.

Mediophyric Quartz Monzonite

The two exposures of quartz monzonite are relatively small, fairly close to contact zones and both are found in the biotite syenogranite (Fig. 15). The rock is fine-grained to medium-grained, subequigranular and mediophyric with subhedral potassium feldspar phenocrysts. The mineral constituents are generally the same as those found in the biotite syenogranites and biotite monzogranites. One difference is that the percentage and size of the biotite crystals is less in the quartz monzonite.

Slightly Mediophyric Granodiorite

Only two samples were identified as granodiorites (PM98 and 1933). PM98 is located adjacent to Portage Creek and 1933 is located in the eastern end of the pluton. The rock is medium-grained to coarse-grained subequigranular and contains about three percent potassium feldspar phenocrysts. The granodiorite looks very similar to the other rocks in the pluton (Plate VI-E). The groundmass contains minor amounts of potassium feldspar (approximately 7 percent) and the biotite grains are relatively large, fairly unaltered and compose about 15 percent of the groundmass. Hornblende occurs in trace amounts. Accessory minerals include sphene, apatite, zircon, and opaques. The feldspars are only slightly sericitized and a few biotites are altered to chlorite.

Aplite-Pegmatite Dikes

The only aplite dike material found, occurs as rubblecrop. It is generally located between Ketchem Creek and Portage Creek with most of the aplitic intrusive rock concentrated adjacent to Portage Creek. Near Portage Creek, a pegmatitic pod was found in sample KM124 and pegmatitic rubblecrop was found near CH57. Very little pegmatite dike rubblecrop was found in the Circle Hot Springs pluton. Although no field relationships were found between the aplite dikes and the pluton, K-Ar dates suggest that the aplite dikes are younger (Section V, this report) and therefore crosscut the biotite syenogranite.

The aplite rubblecrop is light-colored, fine-grained and has little to no coating of red-brown iron stain. The mineralogy is basically the same as the biotite syenogranites or biotite monzogranites. One sample (KM127) was point-counted and has a biotite monzogranite composition. KM127 contains a higher percentage of muscovite and has trace amounts of fluorite. Another sample (KM133) has a small (1 mm) mineralized veinlet crosscutting it. The veinlet is black in hand sample and contains mostly tourmaline, quartz, white mica and fluorite, but does not contain cassiterite.

Mafic Dikes

Mafic dike rubblecrop was found sporadically from near the headwaters of Tommy's Pup Creek to the Ketchem Creek area (Fig. 16). There were no crosscutting relationships evident in the field in the Circle Hot Springs pluton. In hand sample the dike material is fine-grained and dark green. Some samples contain small, white laths set in the matrix.

PM73, located in the Ketchem Creek area, was examined and found to contain approximately 35 percent hornblende and 60 percent plagioclase (Plate X). Minor amounts of biotite and laths of opaques are also present. Some of the hornblende is altering to biotite. The feldspar is very fresh and unaltered. This might suggest that the mafic dike material is younger than the surrounding Circle Hot Springs pluton. To some degree, sericitization of the feldspars is prevalent throughout the other rock types in the pluton.

Two-Bit Pluton

The Two-bit pluton is composed of monzogranite and granodiorite. Only one sample of quartz syenite was identified. All three rock types have a medium-grained, subequigranular groundmass with large, subhedral to euhedral potassium feldspar phenocrysts. The presence of phenocrysts is much more consistent and distinctive than is found in the Circle Hot Springs pluton.

Both the phenocrysts and the groundmass crystals are larger in the Two-bit rocks than in the Circle Hot Springs rocks. Fine-grained rocks are not prevalent even near the contact zones in the Two-bit pluton. The occurrence of enclaves, aplite-pegmatite and mafic dikes near the contact zones is higher in the Two-bit pluton (Fig. 16).

Megaphyric Biotite Monzogranite

The megaphyric biotite monzogranite occupies the main portion of the Two-bit pluton (Fig. 15). It is easily recognizable by its large, white, sub- to euhedral potassium feldspars set against a grey and white groundmass. Quartz (milky-white to grey) crystals occur in the groundmass that are noticeably sub- to euhedral and slightly larger than the surrounding groundmass crystals. Megaphyric biotite monzonites near the metamorphic contact zones and the intrusive contact zones with the megaphyric granodiorite, have pervasive green specks in the matrix and fine-grained green zones throughout the rock. The green is due to chloritization caused by deuteric alteration. Deuteric is a comprehensive term that does not separate whether hydrothermal or pneumatolytic processes changed the primary magmatic minerals in the postmagmatic cooling history (Williams and others, 1982). Trace amounts of hornblende are present. Accessory minerals include zircon, apatite,

Plate X

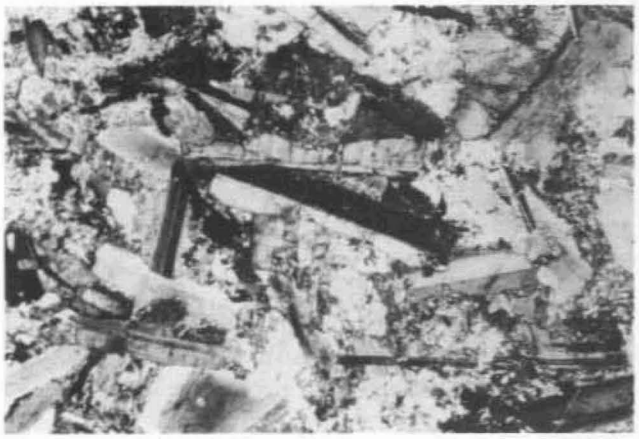

A. PM73, mafic dike. Photomicrograph taken under crossed nichols, width of field, 3400 microns.

B. PM73, hornblende. Photomicrograph taken in plain light, width of field 1330 microns.

opaques and monazite(?). Secondary minerals include sericite, epidote(?), chlorite and sphene.

The rocks examined in the eastern end of the pluton (CH33 and CH54) are relatively free of sericitization (Fig. 16). Some of the plagioclase crystals have altered to epidote(?). Moving west from CH54 to CH55, sericitization of the feldspars becomes more pervasive. In CH55, the outline of relict hornblende encloses chloritized biotite. Granular sphene occurs along the cleavage traces of the mica. In this case, the alteration scenario is: hornblende altered to biotite, biotite altered to chlorite which produced sphene as a byproduct.

Megaphyric Granodiorite

Megaphyric granodiorite outcrops in three separate sections in the Two-bit pluton. The megaphyric granodiorite varies slightly in each of the three exposures. The eastern exposure contains rocks that have fine-grained to medium-grained, subequigranular groundmass with approximately five percent sub- to euhedral potassium feldspar phenocrysts. Conspicuous sub- to euhedral quartz crystals stand out in the groundmass. The middle megaphyric granodiorite body contains zones of biotite-rich layers.

The largest and farthest west occurrence of the megaphyric granodiorite is composed of two, different-appearing megaphyric granodiorites. PM279 and SM195 are similar to the rocks of the central and eastern granodiorites. KM90, SM180, SM183, and SM196 have a slightly finer grained groundmass and the rocks contain small, isolated red-brown spots where sulfides (pyrite?) have weathered out.

The mineralogy of the megaphyric granodiorite rocks is similar across the complex. The rock contains trace amounts of hornblende and accessory minerals include apatite, sphene, zircon, monazite(?) and allanite(?). Secondary minerals include sericite, chlorite, sphene, opaques, and epidote(?). Sericitization of the plagioclase feldspars is pervasive in some specimens (KM106 and PM279).

Megaphyric Quartz Syenite

In 16 Pup Creek is a small exposure of megaphyric quartz syenite. It is similar in texture, appearance and composition to the megaphyric biotite monzogranite. A few hundred yards from the mouth of 16 Pup is bedrock which outcrops alongside the stream for easy examination.

Aplite-Pegmatite Dikes

The aplite and pegmatite dikes are primarily located near the contact zones. Most of the rock is rubblecrop but there is an excellent exposure of aplite-pegmatite dikes crosscutting intrusive spires just west of the confluence of Half Dollar Creek and Bottom Dollar Creek (Plate IV-B, p. 9). The texture of the dikes grade from fine-grained (aplitic)

to coarse-grained (pegmatitic) (Plate XI-A).

Throughout the pluton most of the aplite dike rubblecrop is fine-grained with a light grey and white groundmass. The major minerals are potassium feldspar, quartz and plagioclase. In KM86 there is no mafic component (Fig. 16). The plagioclase crystals are thoroughly sericitized. Trace amounts of muscovite occur interstitially.

The major constituents of the pegmatite, PM250, are quartz, potassium feldspar and muscovite. Less significant is plagioclase. The potassium feldspar is slightly sericitized. No biotite or opaques are present. In the pegmatitic rubblecrop KM66, the major minerals are potassium feldspar, quartz and plagioclase. Biotite occurs in trace amounts and is altered to chlorite and sphene. Metamict zircon occurs in the biotite. Trace amounts of muscovite are also present.

Mafic Dikes

Mafic dike rubblecrop is prevalent throughout the Two-bit pluton. Located at the KM122 sample site (Fig. 16) is a 15 foot road cut with mafic dikes crosscutting the pluton (Plate XII). This field relationship suggests that the mafic dikes are younger than the Two-bit pluton. Plate XIII-A is of KM122 showing the mafic dike intrusive contact. Plate XIII-B is a photomicrograph of the contact and shows the quenched texture of the dike as it intruded and cooled against the megaphyric monzogranite. From KM122, traveling further west along Portage Creek road approximately one mile, mafic dikes that are horizontal to slightly inclined occur at the road level.

The dike rock found throughout the pluton is fine-grained to aphanitic and dark green. Some samples have 1 to 4 mm, white laths (plagioclase feldspars) in the matrix. A few of the samples have a red-brown coat of iron stain. KM122 contains calcareous veinlets.

In KM98 (Fig. 16), the major mineral constituents are plagioclase and augite. Minor quartz and potassium feldspar are present. Additionally, opaques, secondary sphene and a fibrous chlorite are present.

Enclaves

The appearance of enclaves is more prevalent in the Two-bit pluton than in the Circle Hot Springs pluton. They are often ovoid in shape, fine to medium-grained, dark grey to black with subhedral to anhedral white laths (plagioclase feldspar) set in the matrix. Also black clusters of mafic components occur in the matrix.

The major minerals are hornblende (approximately twenty-five percent) and plagioclase. Quartz and potassium feldspar are present interstitially. Biotite is present in fresh and altered conditions. Selective sericitization of the zoned plagioclase crystals' cores is prevalent. Accessory minerals include zircon, apatite, sphene, and opaques. Secondary minerals include sericite, chlorite, sphene, and clinozoisite(?). The igneous texture and composition of KM90 suggest that it is an autolith.

Discussion and Summary

The Two-bit pluton is primarily composed of megaphyric biotite monzogranite and megaphyric granodiorite. Potassium-argon dates indicate that a pegmatite dike (PM250) and a sample of megaphyric granodiorite (KM114) are both approximately 70 million years old. This suggests that the pluton and the aplite-pegmatite dikes were intruded within a narrow margin of geologic time. The mafic dikes are younger than the pluton but how much younger was not determined.

Potassium-argon dates indicate that the Two-bit pluton is at least 13 million years older than the Circle Hot Springs pluton so it is not surprising to find greater alteration effects on the plagioclase crystals and a higher degree of chloritization in the older pluton. Opaques and zircons are far less prevalent. Hornblende is more prevalent and monazite(?) along with epidote(?) occur primarily in the eastern end of the intrusive. The aplite and pegmatite dikes do not have mineralized veinlets and there is no evidence of greisen in the older pluton.

The Circle Hot Springs pluton is primarily composed of the biotite syenogranite and the biotite monzogranite. The porphyritic character in both rock types increases in the eastern portion of the pluton. With the exception of the contact zones where some rocks are fine-grained, the majority of the CHS pluton rocks have a medium-grained subequigranular groundmass.

Potassium-argon dates indicate that both the biotite monzogranite and the biotite syenogranite are approximately 57 million years old. This suggests that the emplacement and crystallization of the two intrusive phases occurred within the same geologic time frame.

The biotite syenogranite is the most interesting mineralogically. Trace amounts of interstitial tourmaline only occur in the Granite Gulch and Bedrock Creek exposures (Plate VII-B, p. 24). From Granite Gulch to Hot Springs Creek, the biotite crystals typically enclose anywhere from 2 to 30 zircons that are often metamict (Plate XIV-A). In contrast, the greisen contains large, euhedral, zoned zircons (Plate XIV-B). The only occurrence of hornblende is between the headwaters of Tommy's Pup Creek and Deadwood Creek. Sphene, allanite(?), rutile(?), and cassiterite first appear in the Ketchem Dome-Ketchem Creek vicinity on topographically high areas. Moving east, fluorite appears in trace amounts. Finally in Portage Creek, aplite dikes

Plate XI

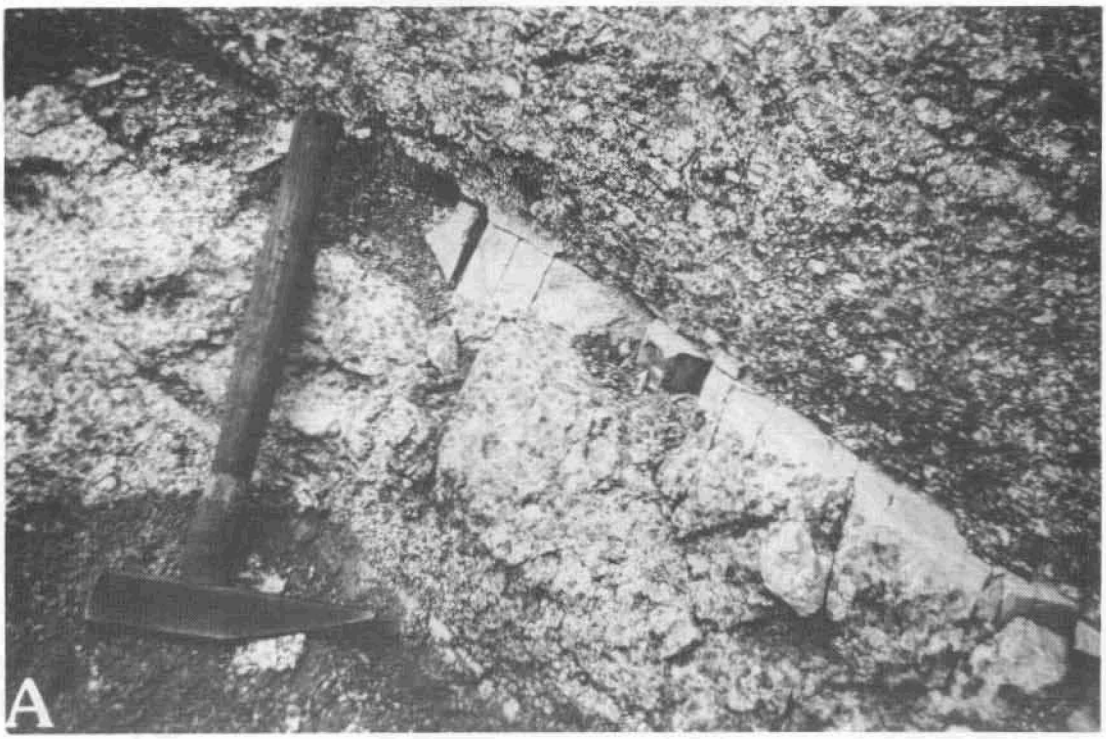

A. and B. Aplite-pegmatite dikes crosscutting intrusive spires located a short distance west of the confluence of Half Dollar Creek and Bottom Dollar Creek (Plate IV-B).

Plate XII

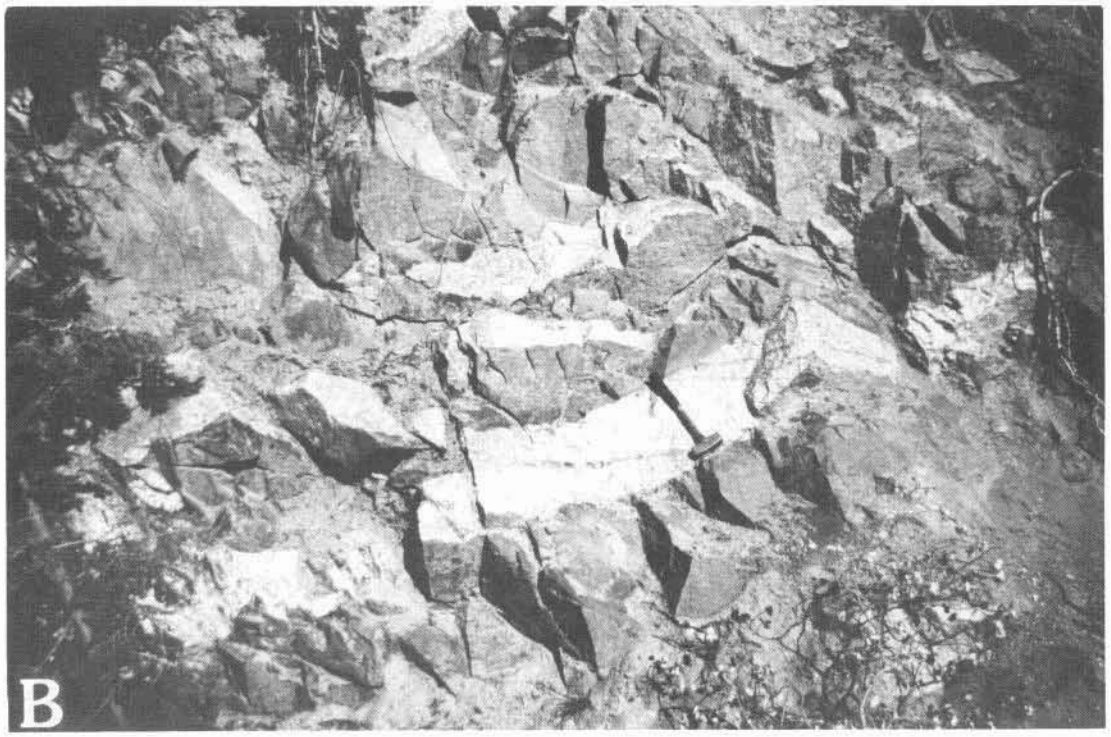

A. and B. Located near KM122 (Figure 16, p. 22), mafic dikes crosscutting megaphyric biotite monzogranite.

Plate XIII

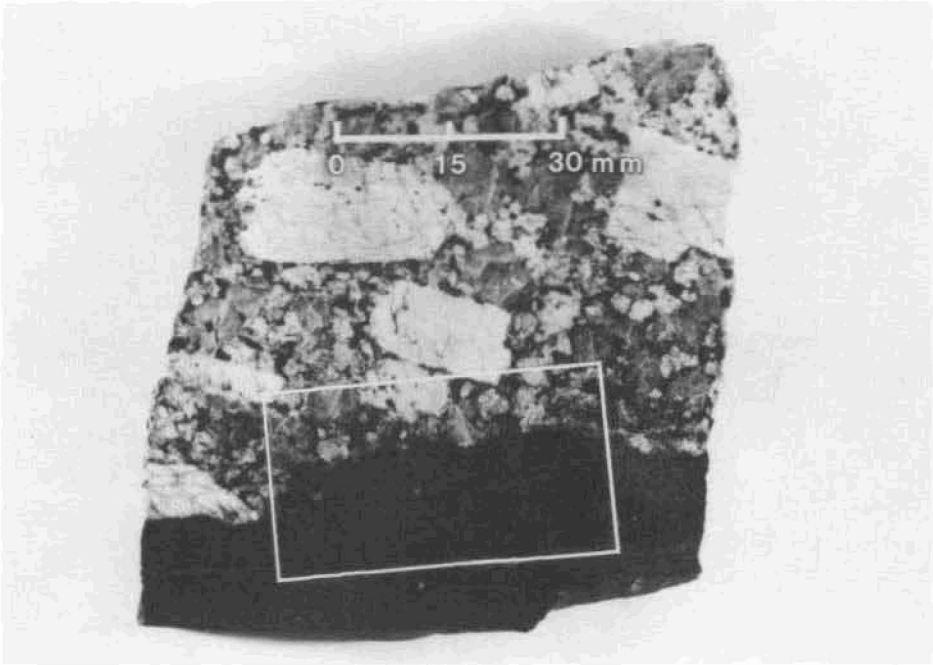

A. KM122, megaphyric biotite monzogranite contact with mafic dike.

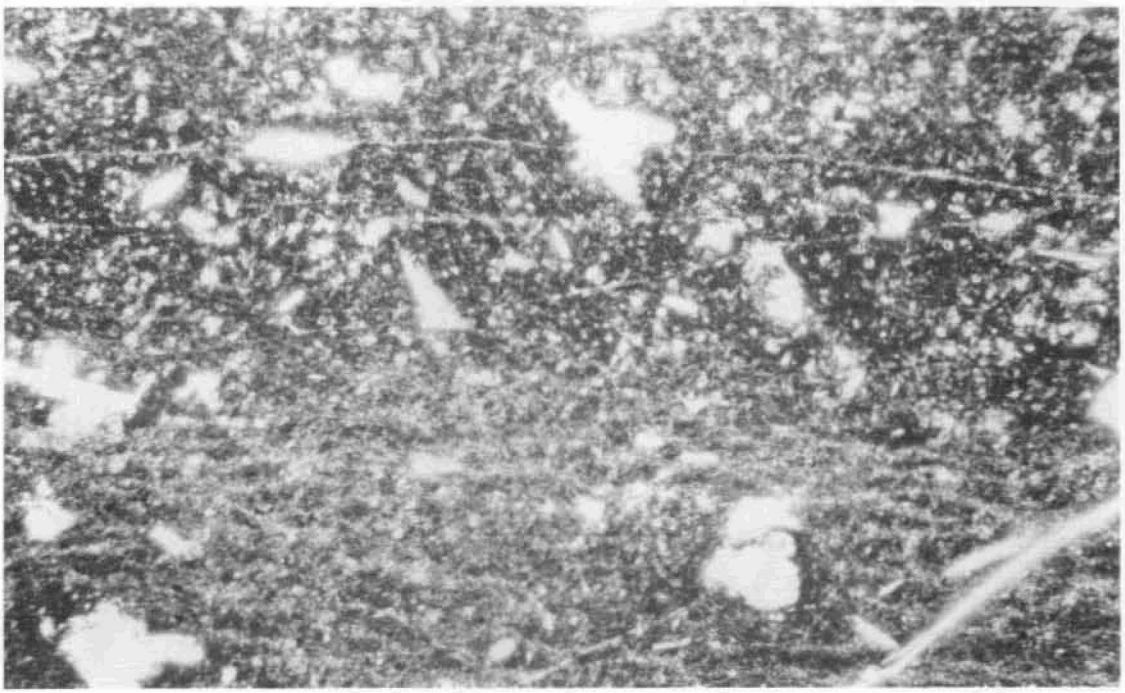

B. KM122, mafic dike with increasing grain size away from the contact. Photomicrograph taken in plain light, width of field 3400 microns.

Plate XIV

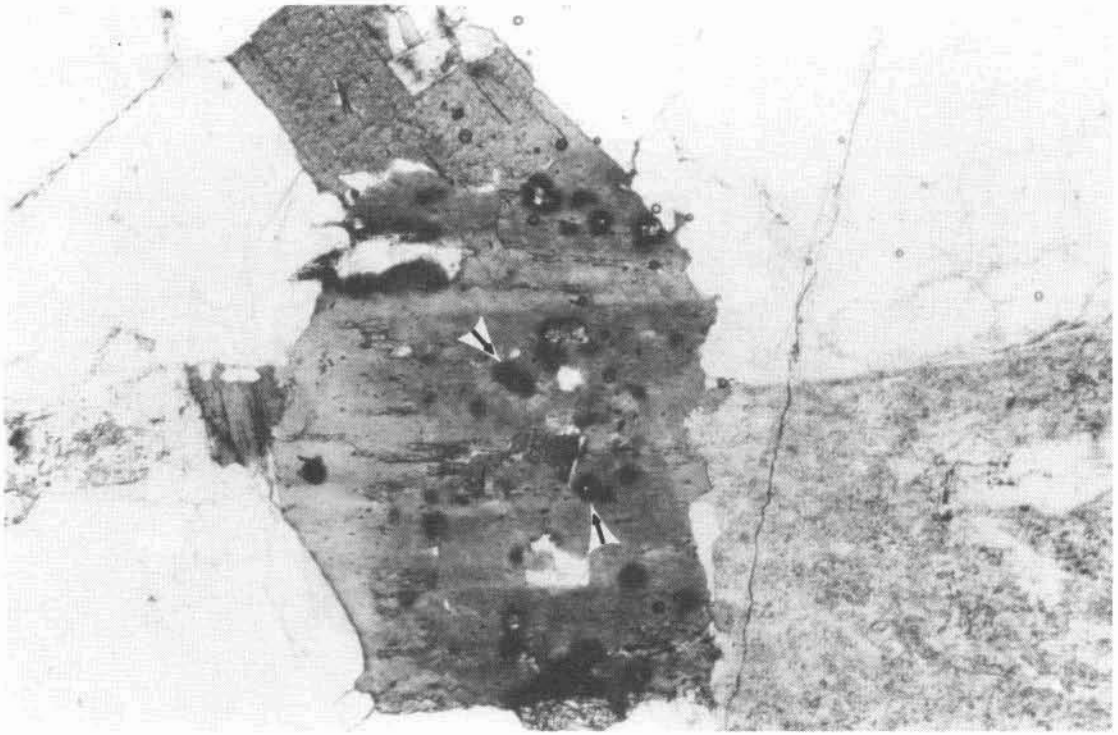

A. KM147, metamict zircons enclosed by biotite in a slightly mediophyric, biotite syenogranite. Photomicrograph taken in plain light, width of field 3400 microns.

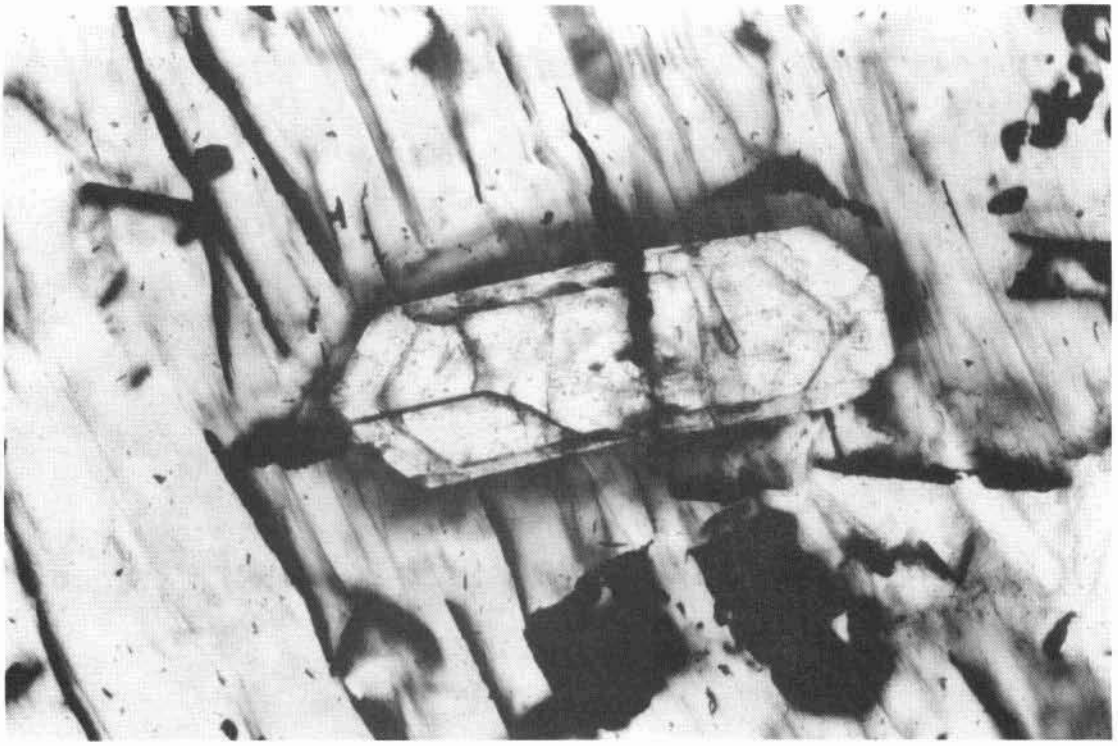

B. PM75, zoned zircon enclosed by chlorite in greisen. Photomicrograph taken in plain light, width of field 520 microns.

occur containing veinlets of tourmaline and altered granite crosscut by veinlets containing cassiterite is present.

From Portage Creek, an aplite dike containing a tourmaline veinlet was K-Ar dated and found to be approximately 54 million years old. This suggests that approximately three million years after the CHS pluton was emplaced, the aplite dike was intruded. The Portage Creek area in the CHS pluton may represent a fracture zone or structurally weak area. On a detailed scale there are perplexing textural variations and it is difficult to decipher the field relations with little to no bedrock available.

Figure 17 is a summary diagram showing general topography and projected structural cross sections to approximately ground level from the highest point in the area (Ketchem Dome). The dip of the rocks is based on metamorphic foliations and conjecture.

Cross section A-A' shows where the greisen is located in relation to the contact zone and elevation. Cross section B-B' shows that nearby on another hilltop, greisen occurs but at the lower elevation cassiterite is not in the samples examined. Cassiterite may have been present higher in the system before erosion cut this hilltop to its present level. Along cross section C-C' no greisen was found. At approximately 2800 feet in elevation, cross section D-D' shows the presence of minerals often associated with tin. In Portage Creek, altered intrusive was found that contains cassiterite (Plate IX, p. 25).

Specific areas of the greatest tin potential appear to be either in greisen on the flank of Ketchem Dome (cross section A-A') or in altered intrusive found near Portage Creek (cross section D-D'). Tin mineralization was not found in the aplite dikes examined. This suggests that the mineralization was primarily associated with postmagmatic pneumatolytic alteration and although mineralization may be associated with the younger aplite dikes it does not appear to be as significant or obvious. More detailed work is necessary to confirm this.

Importantly, the biotite syenogranite in the Circle Hot Springs pluton is the rock type that contains tin-bearing rocks and associated minerals. Based on present-day exposures of rock, the middle and eastern portion of the pluton appear to be more deeply eroded than the western end (Granite Gulch and Bedrock Creek exposures). This could be the result of greater uplift and erosion. Much of the greisen may have already been eroded freeing the cassiterite to become placer tin in the creeks nearby (Plate III, p. 8). The examination of the rocks and minerals of the Circle intrusive complex in this report suggests that further tin exploration should be concentrated in the Circle Hot Springs biotite syenogranite (Fig. 15, p. 22).

VII. MODAL ANALYSIS

The purpose of this section is to examine chemical trends within each pluton based on rock types assigned by modal analysis. In order to propose an explanation for the chemical trends exhibited within the Circle intrusive complex, a few geologic concepts are addressed and briefly explained.

According to Barker (1983), the mode is the mineralogic composition of a rock. To classify a rock based on its composition it is necessary to determine the relative proportions of minerals it contains. For this study, the percentages of quartz, potassium feldspar and plagioclase were determined using point-counting methods. A variation diagram is used to plot the composition of each rock with respect to its mineral proportions. Streckeisen's classification of plutonic rocks is superimposed on this diagram in order to assign rock names to compositional fields. Ninety-nine rocks from the Circle intrusive complex were analyzed and the mode for each rock was determined. Figure 18 shows the compositions and rock names of the samples collected from the two plutons.

Crystallization and Bowen's Reaction Series

The processes by which a gas or a fluid (i.e. magma) become solid is called crystallization (Bates and Jackson, 1980). According to Putnam and others (1971), N.L. Bowen determined that as a magma cools, crystallization follows an orderly sequence. This is summarized in Figure 19.

According to William Putnam (1971):

> "If conditions are favorable, minerals may crystallize from a magma in a dual sequence in the order shown in Bowen's reaction series. The plagioclase feldspars crystallize in what is known as a continuous reaction series, which means that the early-formed crystals change continuously in their composition by reaction with the changing composition of the fluid magma still remaining. The other minerals, such as pyroxene, hornblende, and biotite, make a discontinuous series, so that an early-formed mineral reacts with the remaining fluid to form a completely new mineral with a quite different composition and crystal form, rather than an isomorphous series such as the plagioclases.
>
> According to the Bowen reaction series, the first minerals to come out of solution in a magma are olivine and calcium-bearing plagioclase. Were the entire magma to crystallize at this stage, the resulting rock would be a basalt if it were volcanic, and a gabbro if it were plutonic. Should, however,

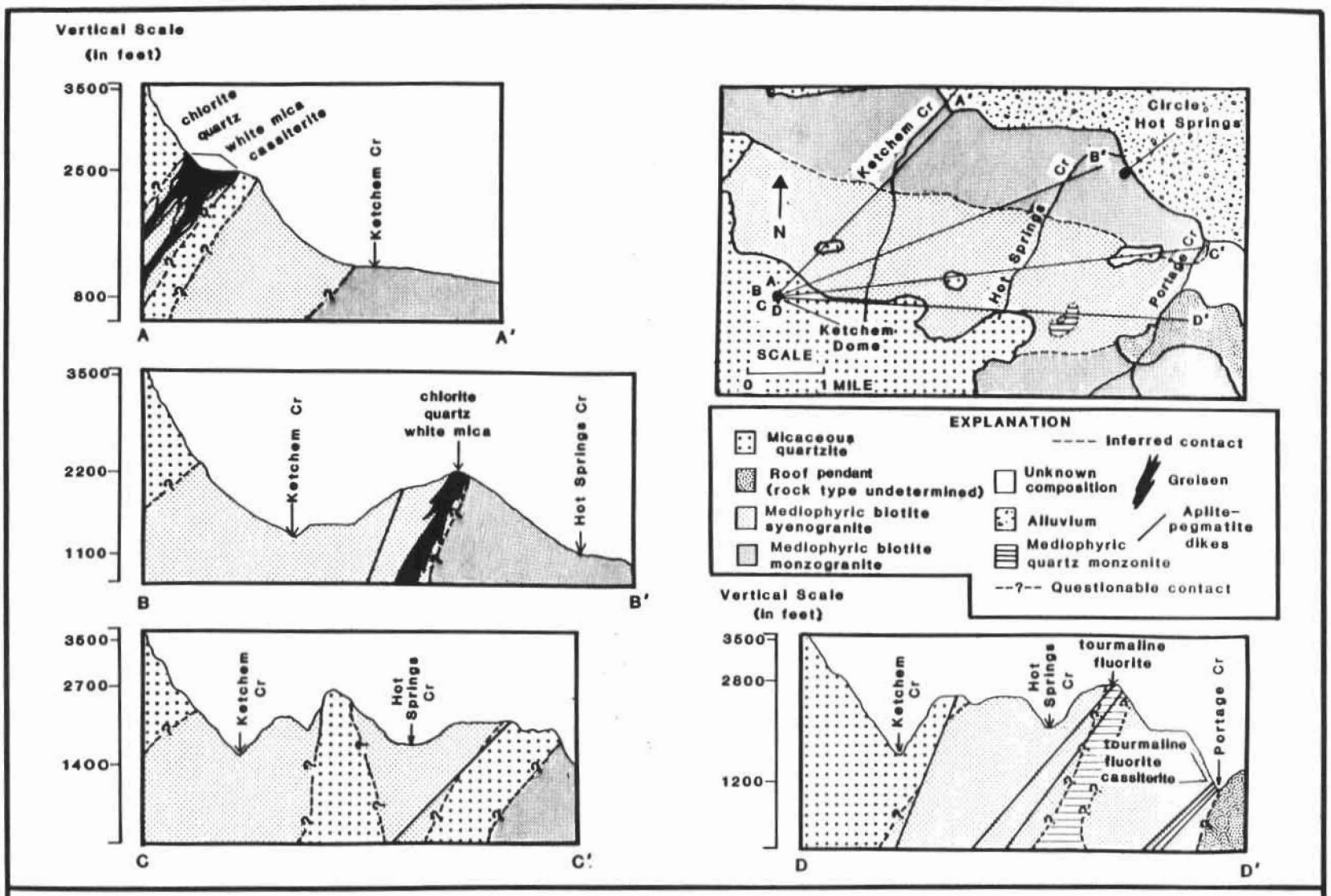

Figure 17. Four structural cross sections of a portion of the Circle Hot Springs pluton showing topography and mineralized areas.

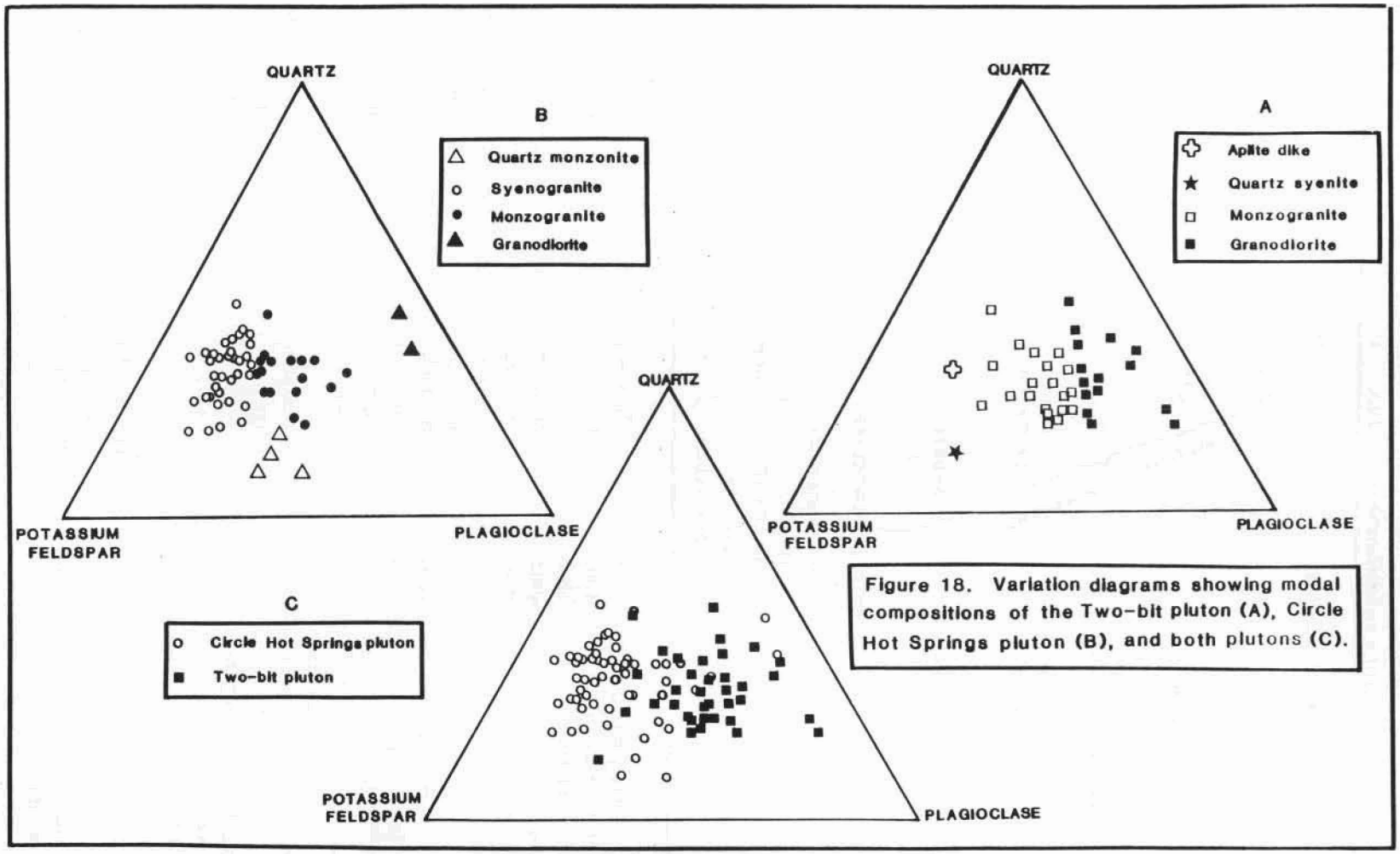

Figure 18. Variation diagrams showing modal compositions of the Two-bit pluton (A), Circle Hot Springs pluton (B), and both plutons (C).

Figure 19. Bowen's igneous reaction series (adapted from Williams and others, 1982).

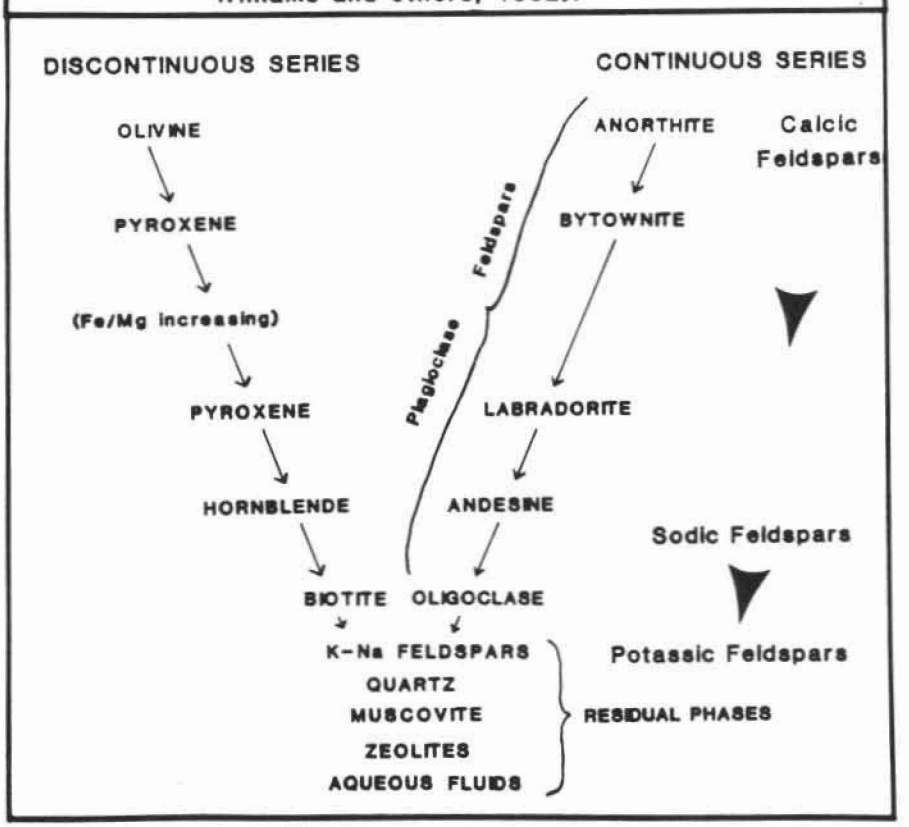

these early-forming minerals settle out, then the remaining magma will have lost much of its iron, magnesium, calcium, and some silicon. With a progressive decrease in these elements the magma will be correspondingly enriched in potassium, sodium and silicon.

The next minerals to crystallize are the plagioclases of intermediate composition along with pyroxene and hornblende. Should the magma congeal at this point, it would yield rocks of intermediate composition, such as andesite if fine-grained and diorite if coarse-grained. Should these earlier crystallizing minerals be separated from the magmatic solution, the remaining minerals to crystallize will be sodium-rich followed by potassium-rich plagioclase and the two micas. Last of all to solidify is quartz, and then only if free silica is left over in solution after all the metallic ions are used up and none are left to enter into combination. Quartz is an interstitial mineral since it fills in the voids or spaces among the earlier-forming crystals. Typical rocks with a mineral composition of quartz, mica, orthoclase, and minor amounts of sodium-bearing plagioclase and hornblende are granite if plutonic and rhyolite if volcanic.

The so-called Bowen reaction series does explain how a magma of originally basaltic composition (one that on crystallizing yields olivine and calcium-bearing plagioclase) might go through a process of differentiation to yield a granitic magma from which quartz, biotite, and orthoclase crystallize. It is necessary to realize, however, that an original magma may have a composition different from Bowen's idealized starting one. That is, a magma may begin with a composition about halfway through the series.

Unfortunately, the origin of the massive bodies of granite that crop out so broadly in the heartlands of the world's continents is almost certain to be vastly more complex than this simple explanation."

Magmatic Differentiation

Magmatic differentiation covers any process whereby different rocks have evolved from the same parental magma (Raguin and others, 1965). The fractionation of a magma as a result of crystallization (fractional crystallization) is thought to be the most significant process that accounts for differentiation (Williams and others, 1982). Modal analysis of the Circle intrusive complex suggests that magmatic

differentiation, as a result of fractional crystallization, could be a viable explanation for the diversity of rocks seen within each pluton.

In Figure 18, variation diagrams A and B show compositional trends occurring within each pluton, reflecting a decrease in plagioclase and an increase in potassium feldspar across the diagram from right to left. Figure 20 shows variation diagrams of quartz, total feldspar and mafics. In Figure 20, diagrams A and B do not clearly suggest that mafic mineral proportions decrease in the rocks as the percentages of potassium feldspar increase.

In order to determine if kindred rocks crystallized from a common parent magma, it is important to establish that the rocks are about the same age (Williams and others, 1982). For the Circle Hot Springs pluton, K-Ar are dates of the two main intrusive phases (syenogranite and monzogranite), are approximately 57 m.y. old. In the Two-bit pluton, the K-Ar age dates of a granodiorite and a pegmatite are approximately 70 m.y. old. Based on the compositional trends shown in Figure 18 A and B, and the similar ages of the main intrusive phases of each pluton, fractional crystallization from a parent magma could explain the diversity of rocks seen within each pluton.

Were the two plutons comagmatic? Did the Two-bit granodiorites originate from the same magma as the CHS syenogranites? Two possible scenarios are proposed:

1) From Figure 18-C, the compositional trend from the Two-bit granodiorites to the CHS syenogranites with a slight overlap in the monzogranite range might suggest fractional crystallization from a common parent magma. From Figure 20-C, it is evident that there is a slight decrease in mafics and a slight increase in quartz in the CHS pluton, supporting the chemical trend shown in Figure 18-C and the comagmatic theory.

2) There are two compositionally distinct groups of rocks that share similar compositional phases expressed by the monzogranites. Additionally the CHS pluton has granodiorites that are similar in composition, though slightly higher in quartz to the Two-bit granodiorites. If the two plutons were comagmatic, it is difficult to explain why some of the CHS rocks are as calcium-rich as the Two-bit rocks. Given the statistical error in the point-counting method already discussed p. 11, the trend of decreasing mafics and increasing quartz between the Two-bit and CHS plutons may not be significant. According to K-Ar dates, there is a span of at least 13 m.y. between the emplacement and crystallization of the two plutons. This time period may be too great for a comagmatic theory to be convincing.

Discussion and Summary

Plagioclase and mafics are high temperature minerals that first crystallize from a magma. As the magma fractionates due to the crystallization of these early-formed minerals it becomes enriched in silicon and potassium which can solidify to form quartz and potassium feldspar. If fractional crystallization did cause the modal variation across the Two-bit pluton then the megaphyric granodiorite was the first to crystallize. It was followed by the megaphyric quartz syenite and next was the megaphyric biotite monzogranite. The aplite and pegmatite dikes were the final phases to crystallize in the Two-bit pluton. All of the Two-bit intrusive phases crystallized approximately 70 m.y. ago. At least 13 m.y. passed before the first CHS intrusive phase crystallized. If fractional crystallization caused the modal variation across the CHS pluton then the mediophyric granodiorite was the first to crystallize followed by the mediophyric monzogranites, then the mediophyric quartz monzonites with the last intrusive phase of the same age being the biotite syenogranite. Aplite-pegmatite dikes intruded approximately three million years later.

Based on the different ages of the two plutons, the compositional overlap in the monzogranite range, the appearance of granodiorite in the CHS pluton and petrographic differences, it is likely that the two plutons originated from separate parent magmas that were derived from similar sources. The proximity of the plutons could also be evidence that the parent magmas were from closely associated sources.

VIII. DISCRIMINANT ANALYSIS

A continuing objective throughout this study has been to verify, with supporting evidence, that the Circle intrusive complex is composed of two separate plutons. Towards this end, a stepwise discriminant analysis was run using the modal percentages of quartz, potassium feldspar and plagioclase as variables and BMDP-7M software (Dixon and others, 1983). A variable entered into the discriminant function if it was significant (F test) in distinguishing between the two populations (Two-bit and Circle Hot Springs plutons). The discriminant function was evaluated using a "jackknife method" to compute the apparent error rate (APER) for the analysis.

For the Circle intrusive complex, only the variables, plagioclase and potassium feldspar, were considered significant in distinguishing between the two plutons and only one

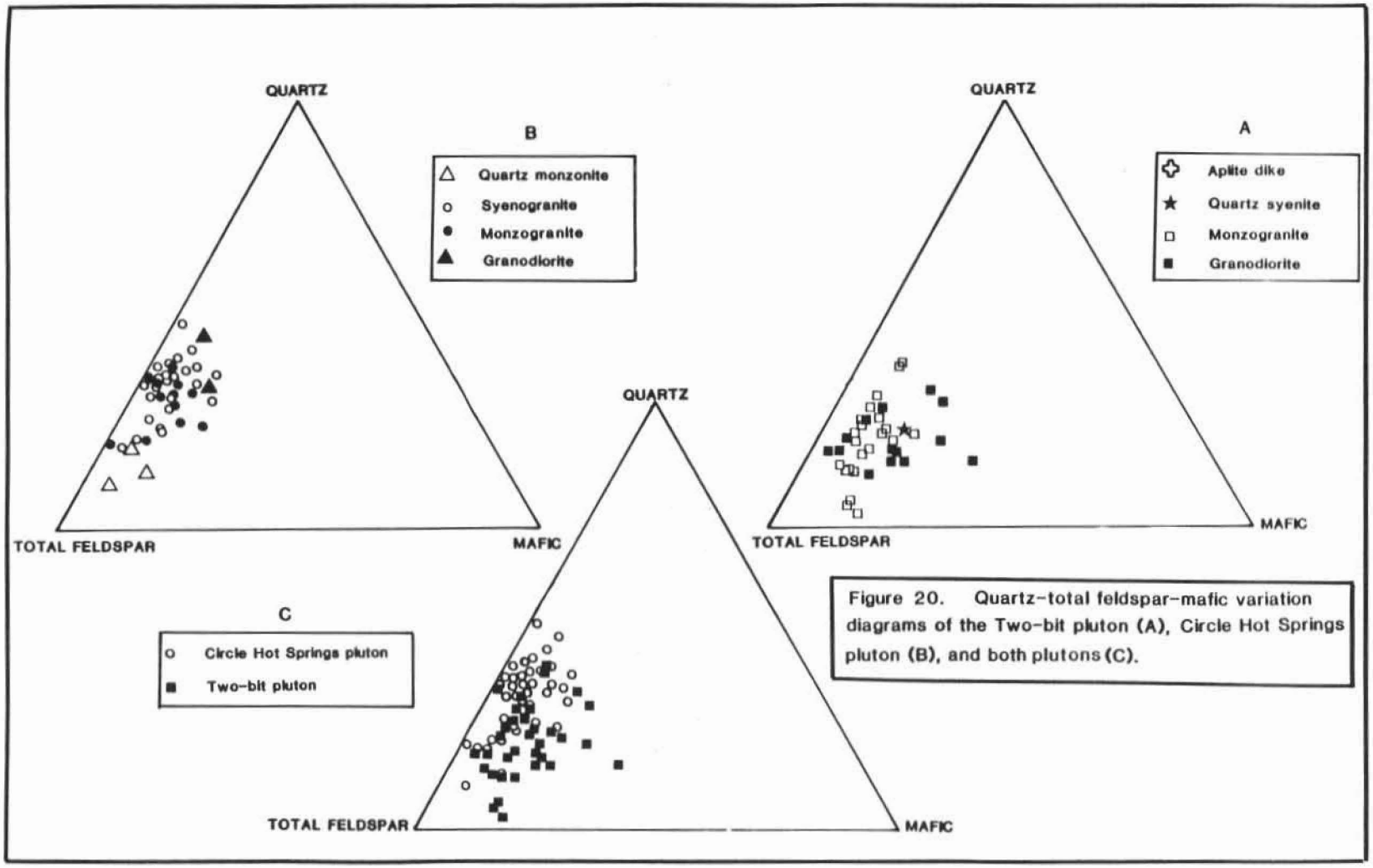

Figure 20. Quartz-total feldspar-mafic variation diagrams of the Two-bit pluton (A), Circle Hot Springs pluton (B), and both plutons (C).

of these variables was required to yield a good discriminant function. A discriminant function using only potassium feldspar as a discriminant variable gave an APER of 10.2 percent, i.e. 10.2 percent of the samples were misclassified. An APER of 16.3 percent was obtained when only plagioclase was used as a discriminant variable. Figure 21 shows a plot of the two plutons classified according to the variable plagioclase. Subscripted C's (12) and T's (5) distinguish the samples misclassified by the discriminant function. These are plotted by sample location in the Circle intrusive complex in Figure 21. The misclassified cases are not generally representative of the main intrusive phases but are minor phases (i.e. quartz monzonite) or located near contact zones where contamination from the wall rocks can affect composition.

Figure 22 shows a plot of the two plutons classified according to the variable potassium feldspar. Subscripted C's (7) and T's (4) distinguish the samples misclassified by the discriminant function. These are also plotted by sample location in the Circle intrusive complex in Figure 22. The classification function and rule obtained by discriminant analysis using the variable potassium feldspar are given below.

Function:

$$D_1 = [0.45\ (\%\ \text{K-spar})] - 10.94$$

$$D_2 = [0.28\ (\%\ \text{K-spar})] - 4.57$$

Rule:

If D_1 is greater than D_2, then the sample is classified as Circle Hot Springs. Otherwise, it is classified as Two-bit.

In spite of the misclassified cases, the results of the discriminant analysis support the hypothesis that the Circle intrusive bodies are composed of two separate plutons.

Figure 21. BMDP-7M classification of samples from Two-bit and Circle Hot Springs pluton using plagioclase as the discriminant variable. Map shows location of misclassified cases.

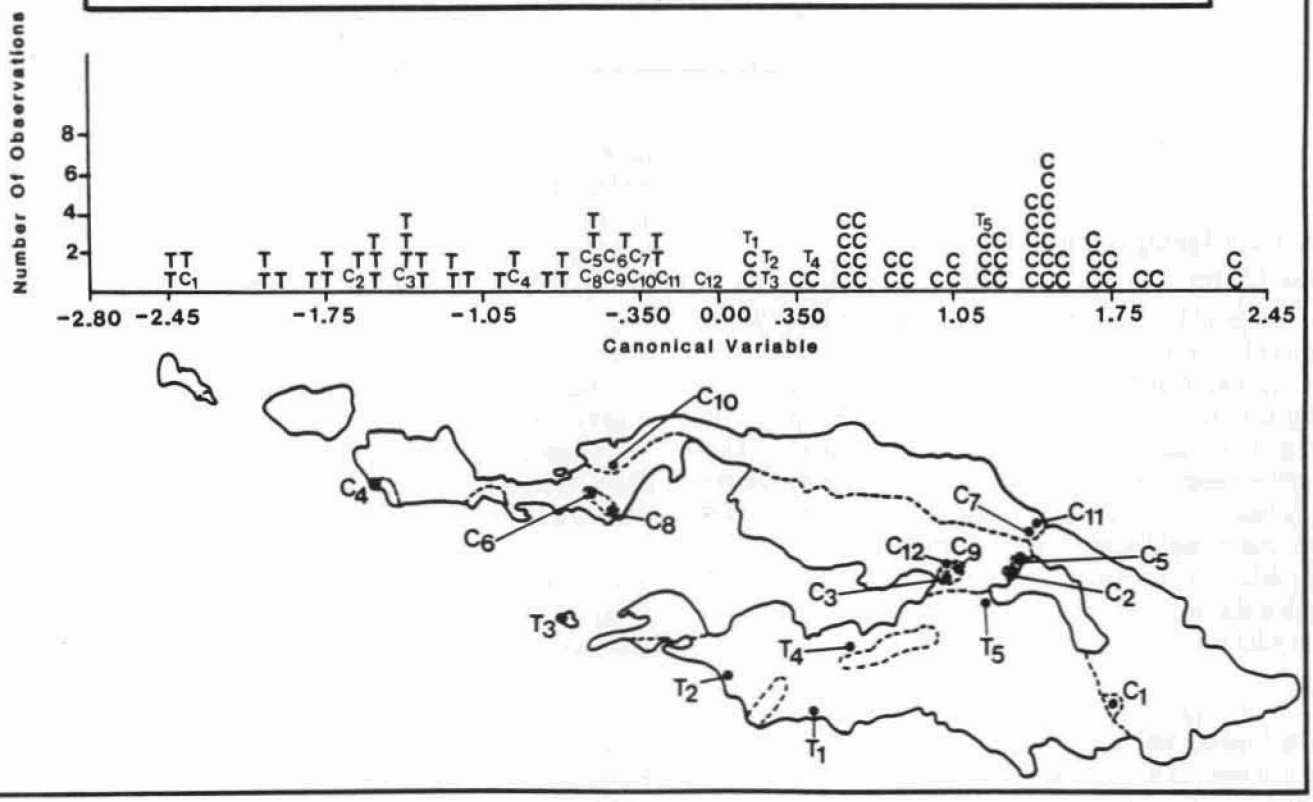

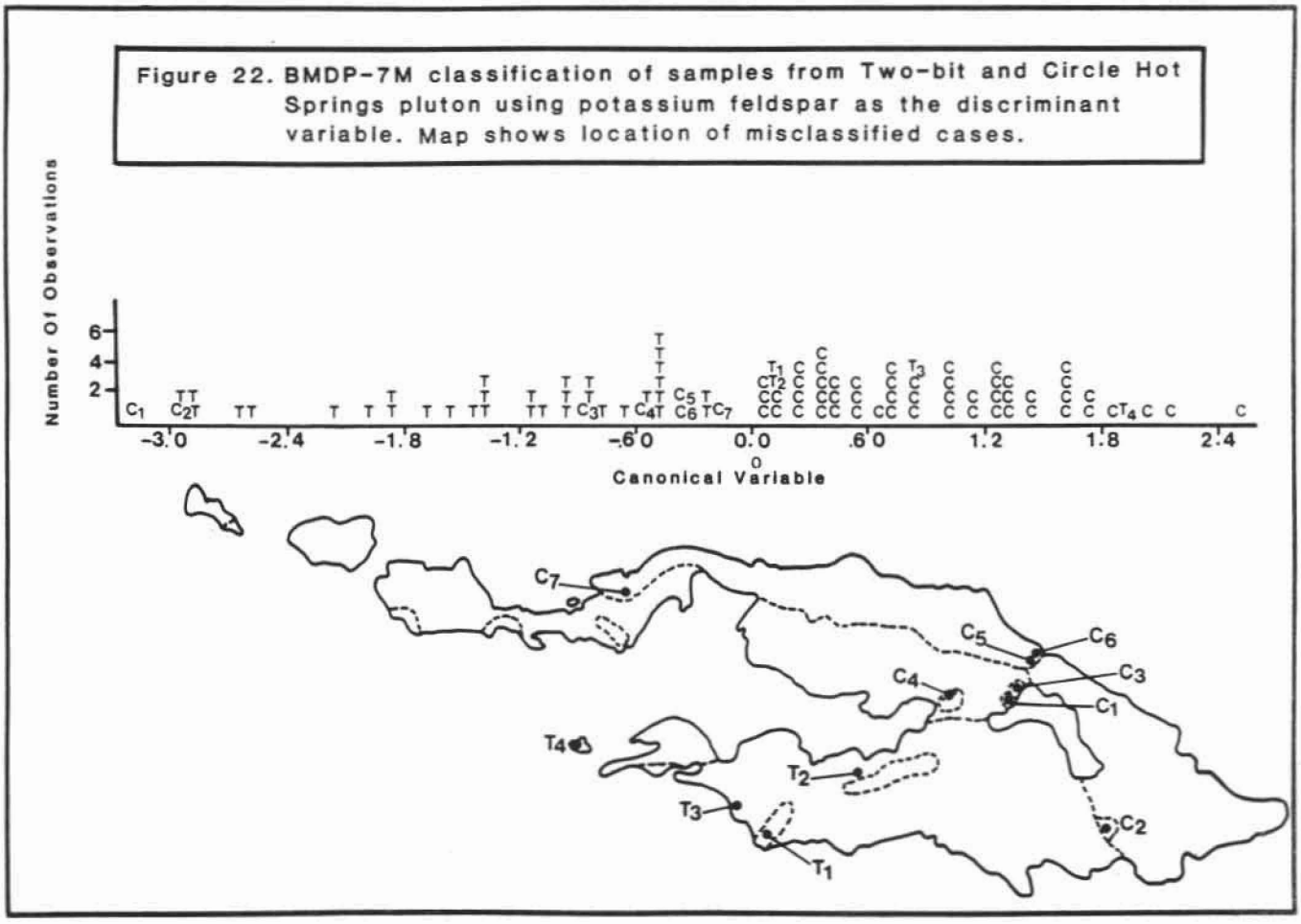

Figure 22. BMDP-7M classification of samples from Two-bit and Circle Hot Springs pluton using potassium feldspar as the discriminant variable. Map shows location of misclassified cases.

IX. MINERALOGY

Circle Hot Springs Pluton

Major Mineral

Albite and albite-Carlsbad twinning is present in the plagioclase crystals throughout the pluton. Albite and pericline twin lamellae are occasionally present (Plate XV). Using the Michel-Lévy method (Griffin and Phillips, 1981) the anorthite content was estimated to be An_{22} to An_{25}. This anorthite range suggests that the plagioclase feldspars are oligoclase. The plagioclase feldspars examined in the biotite syenogranite and the mediophyric biotite monzogranite are unzoned. However, in a quartz monzonite near Portage Creek and in a granodiorite (1933) in the eastern end, zoned plagioclase crystals occur (Plate XVI).

In the potassium feldspars, Carlsbad twinning is common along with perthitic texture. Micrographic textures are also present sporadically throughout the pluton (Plate XVII-A). Granophyric textures (MacKenzie and others, 1982) are found in the Bedrock Creek and Boulder Creek areas (Plate XVII-B). Optic figures combined with twinning and textures suggest that the potassium feldspars are orthoclase. Quartz is a primary constituent throughout the pluton and mostly occurs interstitially. The quartz grains exhibit straight extinction in the Granite Gulch and Bedrock Creek exposures but undulose extinction becomes more prevalent in the middle and eastern portions of the pluton.

Mafic Minerals

The biotite grains exhibit strong pleochroism and usually contain inclusions of zircon, apatite and opaques. The grains are fairly fresh although chloritization does occur to some degree in most samples. In the Ketchem Creek-Ketchem Dome area, biotites also enclose allanite(?), rutile(?) and sphene. The grains are predominantly subhedral to euhedral. The exceptions are in the Ketchem Dome-Ketchem Creek area where alteration has affected the biotite grain shapes.

Trace amounts of hornblende occur in both the mediophyric biotite monzogranite and biotite syenogranite. Hornblende occurs in the area between Deadwood Creek and the headwaters of Tommy's Pup Creek. The hornblende grains have green to light brown pleochroism and are anhedral. They contain opaques and occur spatially close to biotite grains and appear to be altering to biotite.

Plate XV

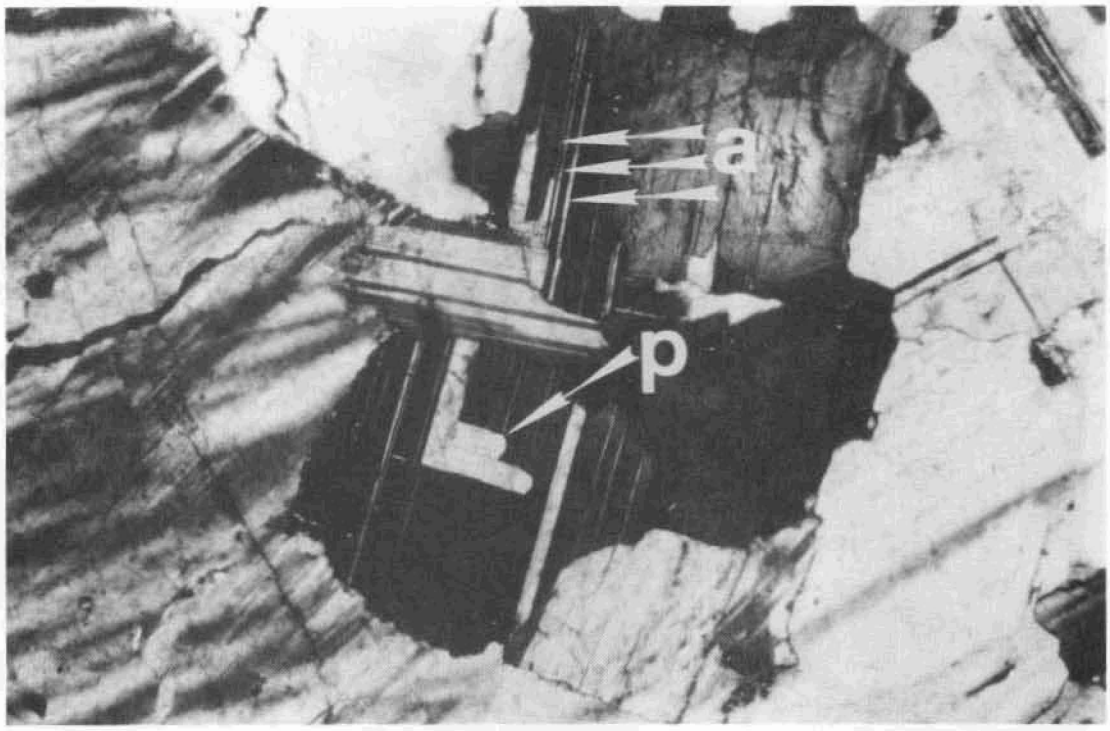

Sample 1933, albite (a) and pericline (p) twin lamellae in a plagioclase feldspar. Photomicrograph taken under crossed nichols, width of field 3400 microns.

Plate XVI

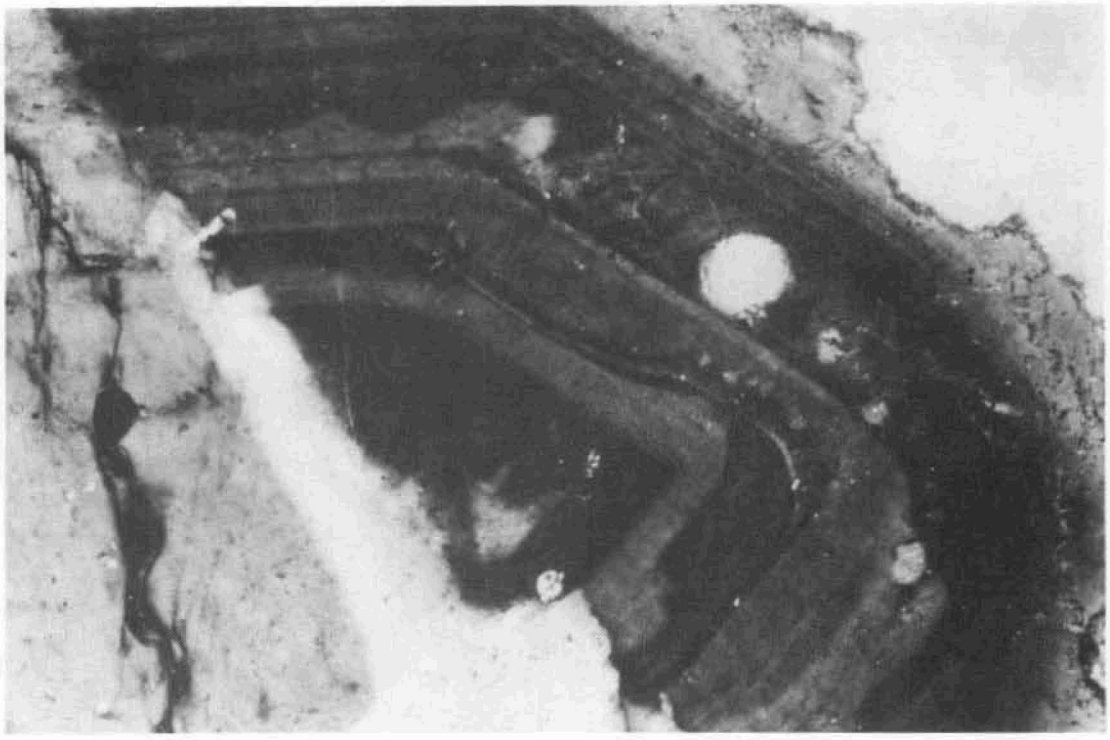

Sample 1933, a zoned plagioclase feldspar in a granodiorite. Photomicrograph taken under crossed nichols, width of field 1330 microns.

Plate XVII

A. PM280, micrographic texture in biotite syenogranite. Photomicrograph taken under crossed nichols, width of field 3400 microns.

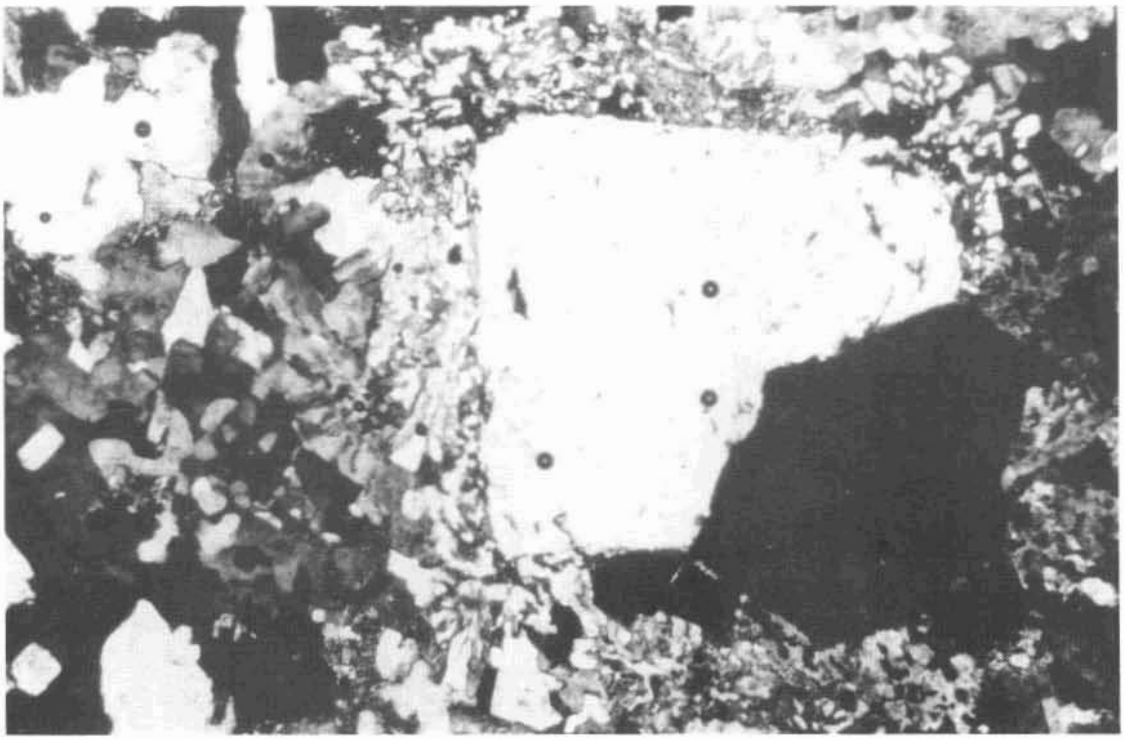

B. PM281, granophyric texture in a biotite syenogranite. Photomicrograph taken under crossed nichols, width of field 3400 microns.

White Mica

Trace amounts of muscovite occur interstitially throughout the pluton. Secondary white mica or sericite occur as small scales or flakes in the feldspars. Small laths of white mica occur in significant amounts in the altered rocks of the Ketchem Dome-Ketchem Creek area. White mica is present in tourmaline-rich veinlets that crosscut aplite dikes in Portage Creek.

Accessory Minerals

Accessory minerals include zircons, apatite, tourmaline, and opaques. The zircons are strongly pleochroic and many of the crystals are metamict (Plate XIV-A, p. 32). As many as 10 to 30 zircons per biotite grain is common in the western intrusive exposures (Granite Gulch and Bedrock Creek). The prevalence of zircons decreases in the Deadwood Creek area but is generally pervasive throughout the eastern portion of the pluton. In greisen in the Ketchem Dome-Ketchem Creek area (PM75), relatively large, euhedral, zoned zircons are found contained in chlorite (Plate XIV-B, p. 32). Zircons also occur containing rounded cores.

Additional accessory minerals are found in the Ketchem Dome-Ketchem Creek area. These include rutile(?), allanite(?), sphene, magnetite and cassiterite. Adjacent to and in Portage Creek, fluorite and tourmaline are found in trace amounts. Sphene was found only in the Ketchem Creek-Portage Creek areas. It is diamond shaped and enclosed by unaltered biotite grains. Sphene also occurs as granules associated with chlorite. Allanite(?) occurs in biotite grains which exhibit pleochroic halos. The occurrence of allanite appears to be restricted to the Ketchem Creek area. Rutile(?) occurs as tiny, brown, anhedral grains associated (usually touching) with opaques and enclosed in chlorite. Fluorite is subhedral, and usually found near biotite grains. Tourmaline is found interstitially in the Granite Gulch and Bedrock Creek exposures (Plate VII-B, p. 24). It is also found near Portage Creek either as pods in the granite or in veinlets crosscutting aplite dikes. It has blue-brown pleochroism and occurs as stubby laths in the veinlet. Cassiterite occurs in greisen in the Ketchem Dome area (Plate VIII-B, p. 25) and in altered intrusive that is present alongside Portage Creek (Plate IX, p. 25).

Two-bit Pluton

Major Minerals

Albite and albite-Carlsbad twinning are dominant in the plagioclase feldspars with only occasional albite-pericline twins occurring. The plagioclase feldspars predominantly exhibit zoning (Plate XX-A, p. 46). Selective sericitization of the cores of the plagioclase grains is a pervasive feature throughout the granodiorite phase. The megaphyric biotite monzogranites in the eastern portion of the pluton were examined microscopically and these were found to be less sericitized than the granodiorite.

Zoning and sericitization make it difficult to determine plagioclase composition based on the Michel-Lévy method. The Michel-Lévy method was performed on KM86, an aplite dike, and a granodiorite (KM114) (Fig. 16, p. 22). The anorthite content was An_{35} and An_{30} respectively. This suggests that the plagioclase feldspars in the most residual phase of the Two-bit pluton are slightly more calcic-rich than the rocks examined in the Circle Hot Springs pluton. This also suggests that the plagioclase composition in the Two-bit pluton does not vary significantly between the early crystallized phases (granodiorite) to the later phases (aplite dikes).

In both the megaphyric biotite monzogranite and megaphyric granodiorite, based on twinning and textures, the potassium feldspars appear to be microcline and perthitic microcline. An occasional grain will manifest only perthic texture. In the pegmatite dike (PM250), the potassium feldspars exhibit myrmekitic textures. Macrographic texture is also found in the pegmatites (Plate XVIII).

Quartz occurs both interstitially and as discrete sub- to euhedral grains slightly larger than the surrounding groundmass. Undulose extinction occurs in most of the quartz grains, especially in the eastern portion of the pluton. Straight extinction occurs more commonly in the western end.

Mafic Minerals

Chloritization of the biotite grains is fairly pervasive in the megaphyric granodiorite and less prevalent in the megaphyric biotite monzogranite. The biotites are often completely altered to chlorite with sphene and magnetite occurring as alteration byproducts. Inclusions found in the biotite grains throughout the pluton, are zircon, apatite, allanite(?) and opaques. Hornblende occurs in both the granodiorite and monzogranite phases. It is occasionally found as an isolated subhedral crystal but more often it is found altering to biotite.

White Mica

Trace amounts of muscovite occur in the aplite dikes examined. Large laths of muscovite occur in the pegmatite dike, PM250. In one granodiorite sample, KM106, trace amounts of white mica occurred in subparallel laths with biotite and chlorite. The predominant form of white mica occurs as sericite.

Accessory Minerals

Accessory minerals include zircon, sphene, apatite, allanite(?), epidote(?) and opaques. None of these minerals are especially pervasive. Anywhere from zero to four zircons (usually metamict) may be found in the biotite grains. Sphene generally occurs as a byproduct of chlorite alteration but is found in distinctive diamonds in the grano-

Plate XVIII

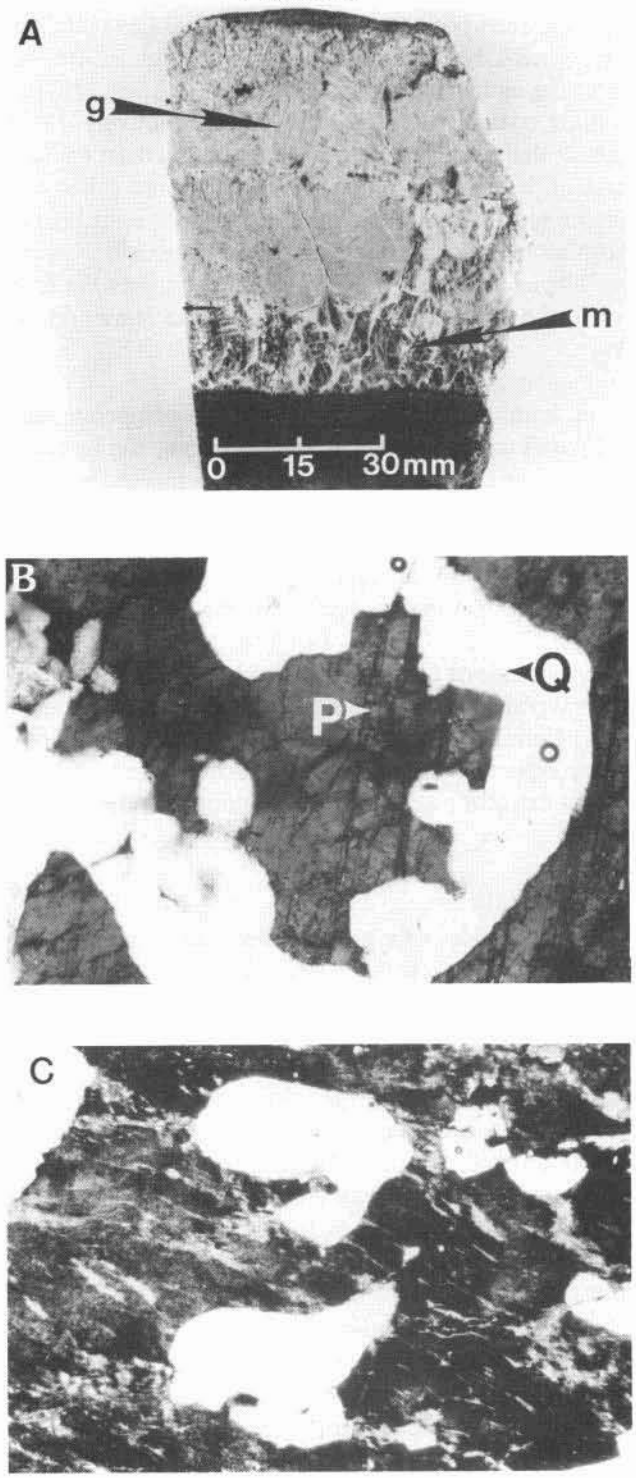

A. KM66, myrmekitic (m) and graphic (g) textures in a pegmatite vein.
B. KM66, myrmekitic texture. Quartz labeled (Q) and plagioclase (P). Photomicrograph taken under crossed nichols, width of field 1300 microns.
C. KM66, graphic texture. Two quartz blebs are enclosed by perthitic alkali feldspar. Photomicrograph taken under crossed nichols, width of field 3,400 microns.

diorite KM114 (Plate XIX). Monazite(?) occurs usually touching biotite grains in sub- to euhedral crystals. Epidote occurs as an alteration product of the plagioclase feldspars. It is primarily found in the monzogranites and is often spatially adjacent to biotite grains.

Discussion and Summary

The minerals in the rocks examined across the intrusive complex could support the theory that two compositionally different plutons compose the batholith. The plagioclase compositions of the examined Two-bit rocks are slightly more calcic (andesine) than the examined Circle Hot Springs plagioclase grains (oligoclase). Zoning in the Two-bit plagioclase feldspars is a prevalent feature as opposed to a predominance of unzoned feldspars in the Circle Hot Springs pluton. This suggests that the two magmas forming the plutons crystallized under different conditions (Plate XX). Additionally, perthic microcline is the predominant alkali feldspar in the Two-bit rocks whereas the Circle Hot Springs alkali feldspars are typically perthitic with Carlsbad twins (orthoclase) (Plate XXI).

A detailed study of the minerals and specifically the feldspars is not in the scope of this study. However, an in-depth look at the minerals could provide additional insight to the conditions of crystallization that each pluton underwent.

X. CHEMICAL ANALYSIS

Major Oxides

Harker Variation Diagrams

To determine the bulk composition of a rock it is necessary to analyze for the major oxides that compose it. The major oxides represent at least 95 to 99 percent of the chemical composition of a rock. Fourteen rocks were selected to be analyzed for the major oxides (Appendix D). These rocks were analyzed prior to the discovery that the Circle intrusive complex was composed of two plutons. Therefore, syenogranites in the Ketchem Dome-Ketchem Creek area are not represented.

Chemical variation diagrams are one way to show compositional trends within a given province (Williams and others, 1982). SiO_2 is the oxide element that shows the most numerical variation so Harker (1909) devised a plot of SiO_2 versus the weight percentages of other major oxides (Barker, 1983). According to Barker (1983), the trends exhibited can show how each rock type chemically varies in relation to the other rock types of a province, but do not necessarily confirm how one rock is genetically related to another. The model diagram that arranges rocks in a genetic sequence has yet to be developed. The difficulties of variation diagram

Plate XIX

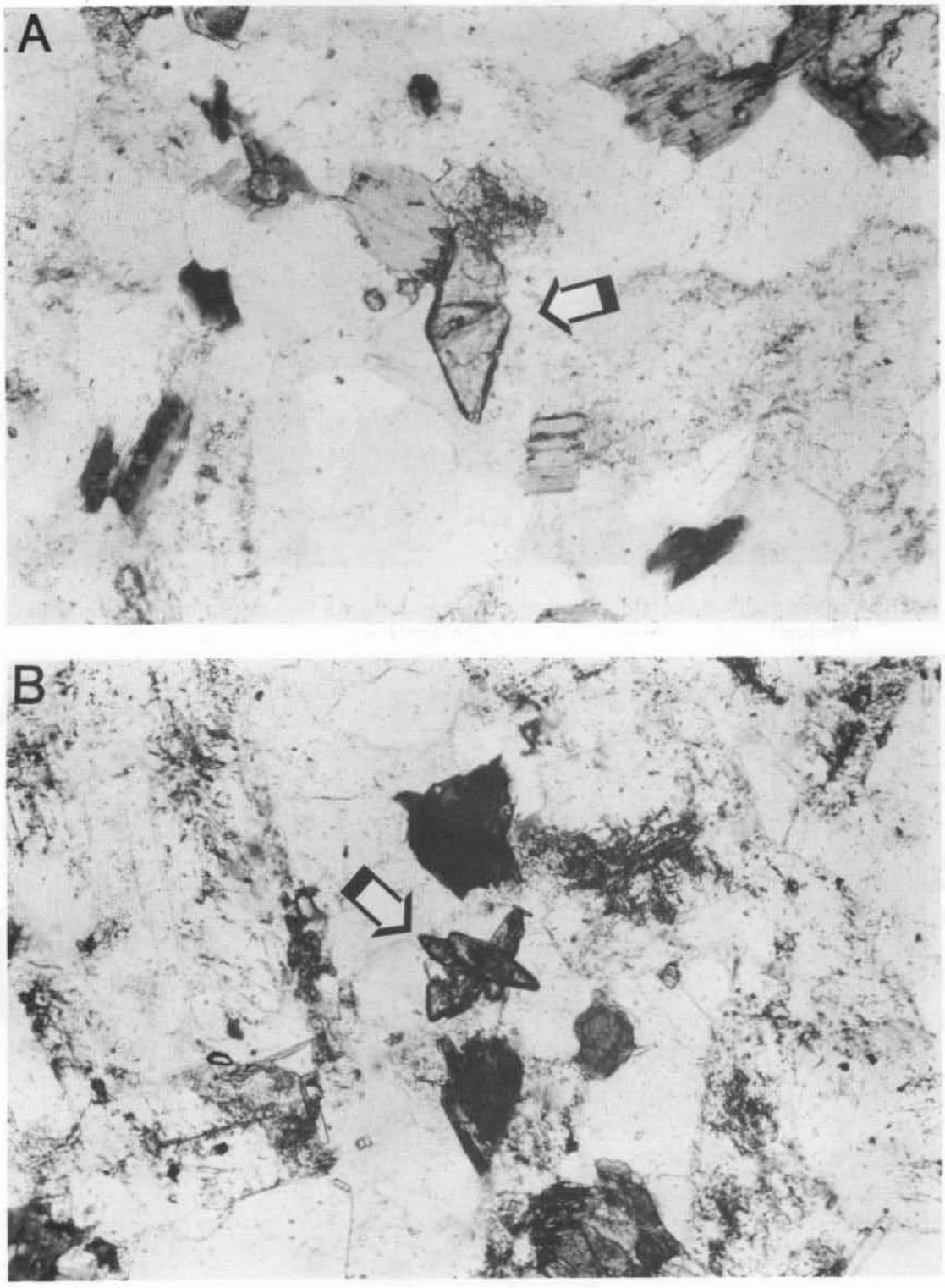

A. and B. KM114, sphene crystals in a megaphyric granodiorite. Photomicrographs taken in plain light, width of field 1330 microns.

Plate XX

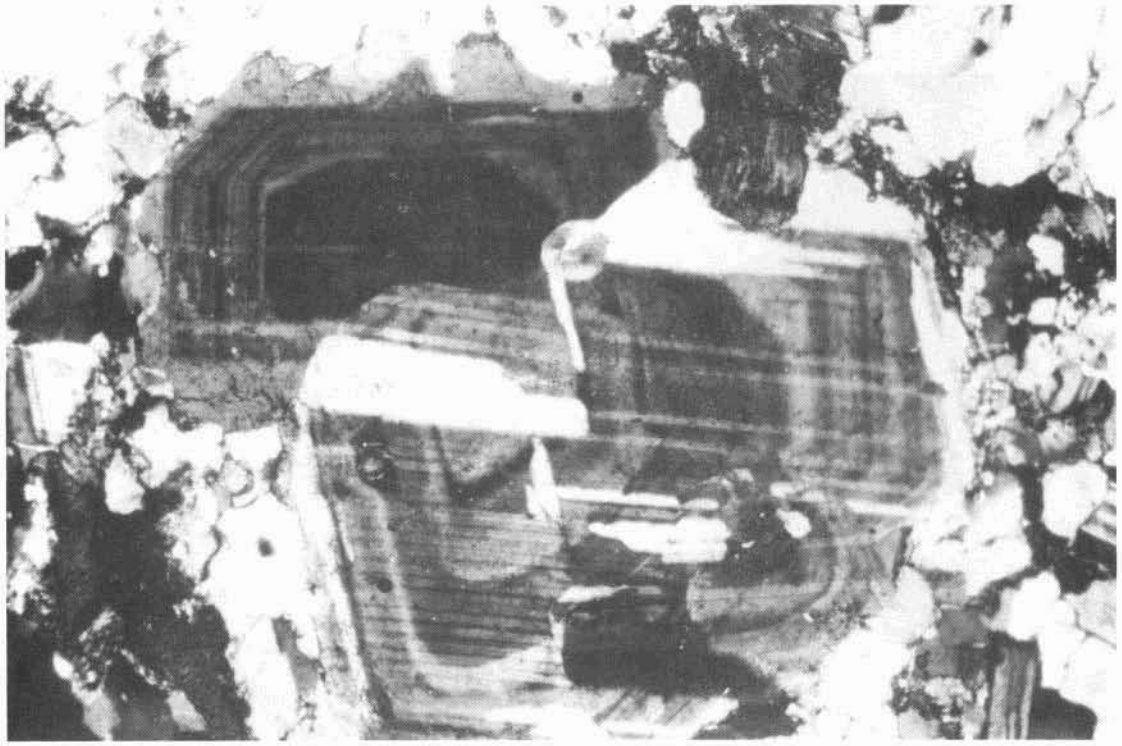

A. CH54, zoned plagioclase feldspars with albite twinning in a Two-bit pluton monzogranite. Photomicrograph taken under crossed nichols, width of field 3400 microns.

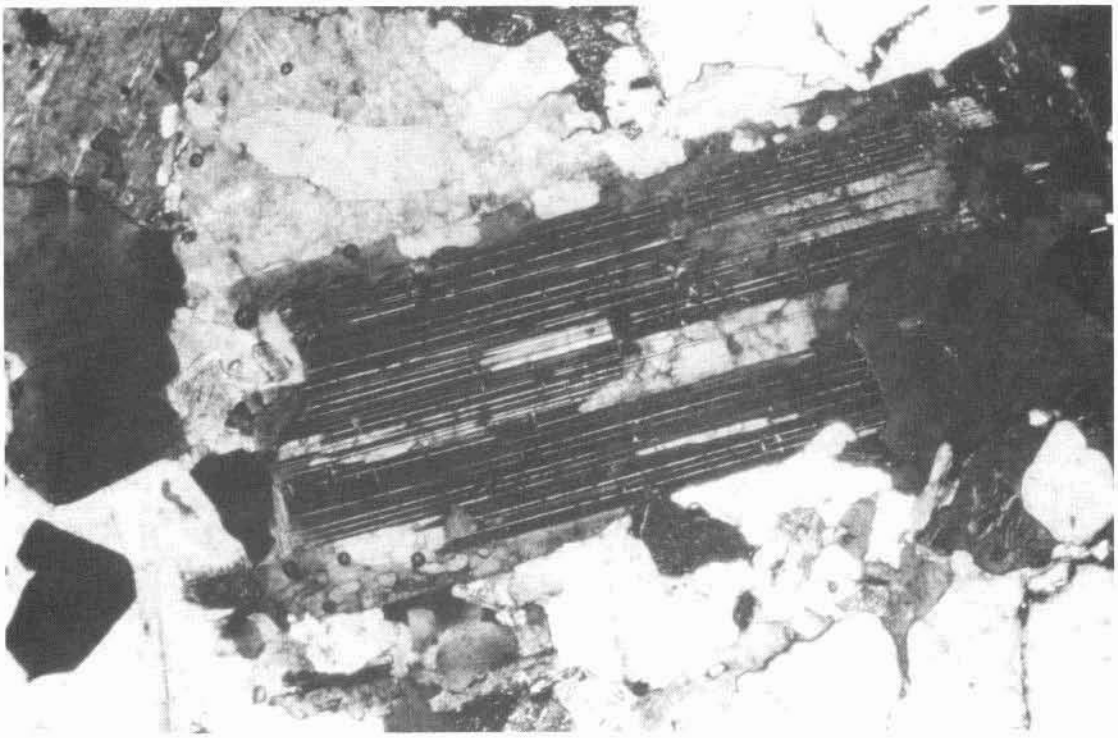

B. PM280, a typical unzoned plagioclase feldspar with albite twinning in a Circle Hot Springs syenogranite. Photomicrograph taken under crossed nichols, width of field 3400 microns.

Plate XXI

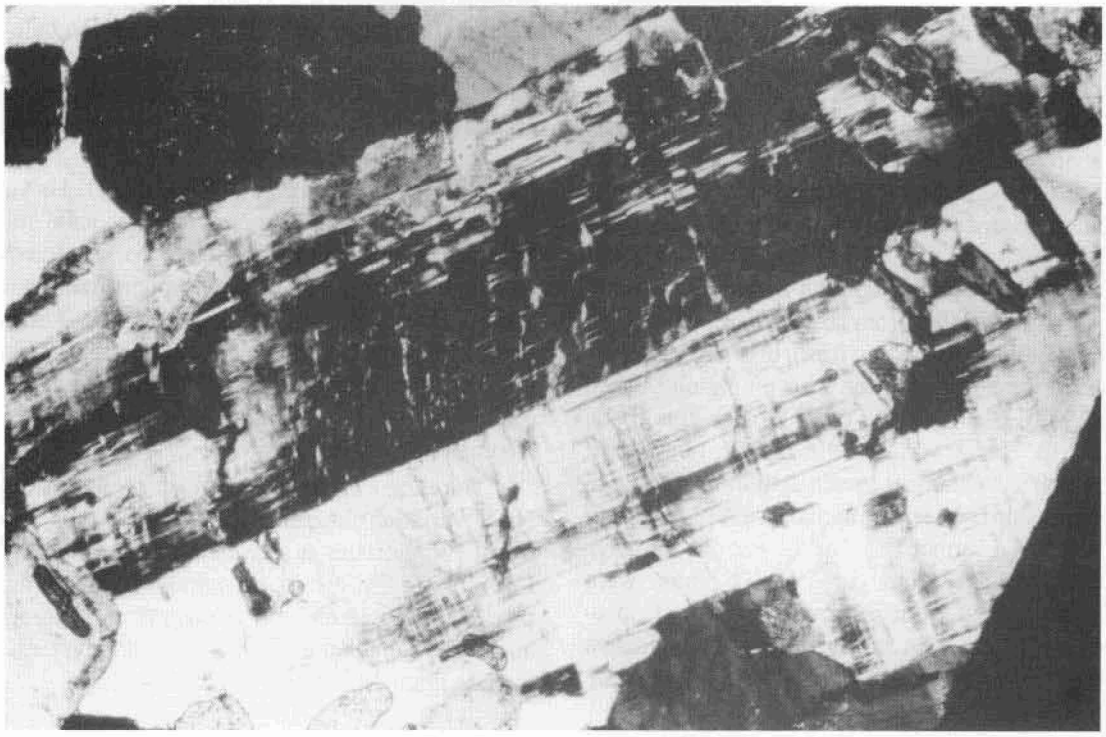

A. CH56A, perthitic microcline with Carlsbad twinning in a Two-bit pluton granodiorite. Photomicrograph taken under crossed nichols, width of field 3400 microns.

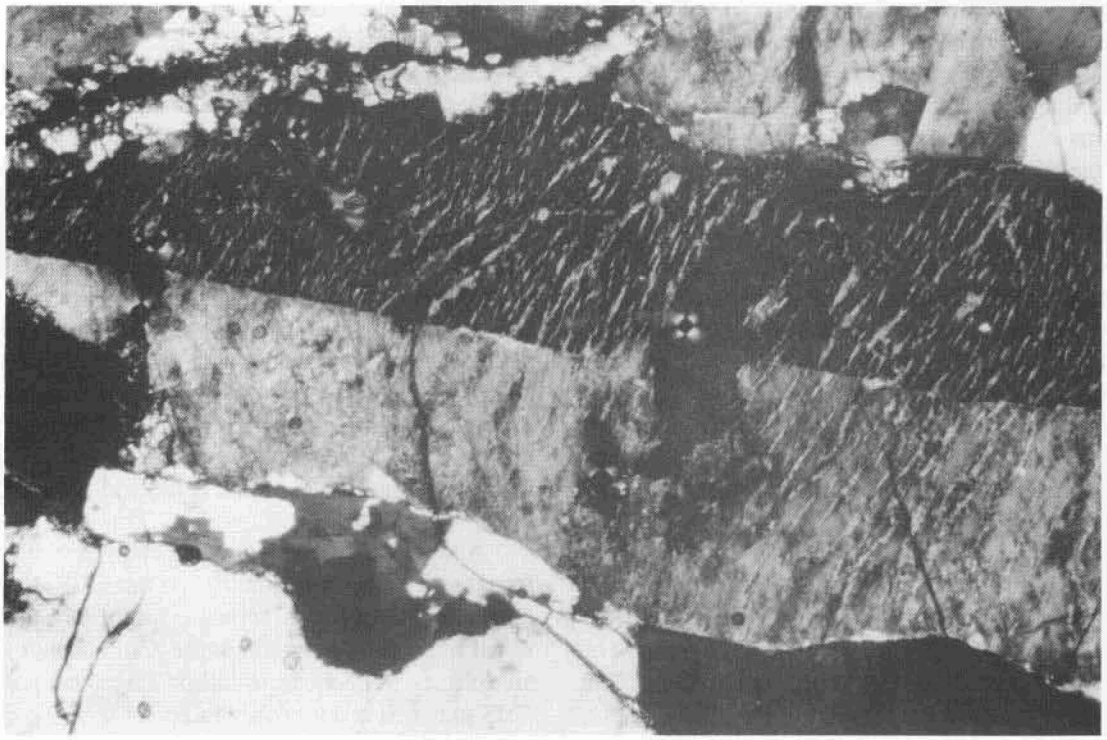

B. CH60, a perthitic orthoclase with Carlsbad twinning in a Circle Hot Springs syenogranite. Photomicrograph taken under crossed nichols, width of field 3400 microns.

interpretations have been determined mathematically by Chayes (1971).

In Figure 23, Harker variation diagrams show the expected decrease in Al_2O_3, FeO_{Total}, CaO, and MgO with increasing SiO_2 and increasing K_2O. The Na_2O plot does not show a pronounced trend. The chemical variation exhibited in the individual rock types basically support the modal variation described in section VII, p. 37.

To describe the chemical variation within each pluton, more samples specifically from each phase should be analyzed. One problem is finding fresh, unaltered samples in the middle to western end of the Two-bit pluton. Based on Barker (1983), Chayes (1971) and D. Hawkins (pers. comm., 1987), the Harker variation diagrams do not support conclusively that the chemical trends exhibited are due to a genetic relationship between the rocks. These plots cannot be reliably used as a further test that the various intrusive phases within the CHS pluton or Two-bit pluton were comagmatic or derived from separate magmas. Consequently, the same is true for using the diagrams as evidence to suggest the CHS and Two-bit plutons were comagmatic or from separate magmas.

AFM and Ca-Na-K Triangular Diagrams

The AFM and Ca-Na-K triangular diagrams are also widely used to show compositional trends. Again, more samples representative of each rock type in each of the plutons is necessary for a better determination of the chemical trends that exist. According to Barker (1983), one point on the AFM diagram represents the bulk composition of a rock in terms of the minerals it contains. The A corner represents the alkali feldspars. In this way, rocks that plot close to the A corner contain minerals composed of Na_2O + K_2O. Mafic rocks will plot along the F-M border if they are composed of minerals that contain little to no alkalis. The Ca-Na-K diagram supplements the AFM diagram by showing the relative proportions of the Ca, Na, and K contained in the bulk composition of each rock. With progressive fractional crystallization, magnesium enters into the ferromagnesium minerals and the melt becomes iron enriched. In the same way, as the early-formed plagioclase crystallizes, the magma becomes enriched in Na and K compared to Ca.

If these variation diagrams are valid for showing genetic relations between kindred rocks of a province, then the chemical trends shown in Figure 24 could be suggestive of fractional crystallization, at least within each pluton. The CHS syenogranites show enrichment in the alkalis with a decrease in alkalis coupled with a slight increase in MgO in the CHS monzogranites. Only one CHS granodiorite is shown and its composition reflects even lesser amounts of alkalis with a slight increase in magnesium.

Only four rocks represent the Two-bit pluton so not enough information is available to conclusively support fractional crystallization as a reason for the bulk composition seen. However, just based on the points plotted, the monzogranites have increased alkalis compared to the granodiorite with no relative enrichment of iron.

According to Chayes (1971) and D. Hawkins (pers. comm., 1987), these diagrams are not valid for showing genetic relations between kindred rocks of province and cannot be conclusively used to support fractional crystallization. However, the compositional trends shown in these plots do support the compositional trends seen in the modal variation diagrams in section VII, p. 35 and 38.

Discussion and Summary

The chemical trends shown with Harker, AFM and Ca-Na-K variation diagrams generally support the compositional variation that is seen in the modal plots (Fig. 18 and Fig. 20). The CHS pluton is composed of two main, intrusive phases (syenogranite and monzogranite) that crystallized about the same time (57 m.y.). Other intrusive phases include granodiorite and quartz monzonite.

The Two-bit pluton is composed of two main intrusive phases (monzogranite and granodiorite). Two K-Ar age dates from a pegmatite dike and a granodiorite (about 70 m.y.) suggest that the Two-bit intrusive phases crystallized at about the same time.

Each pluton has unique petrographic characteristics, chemical similarities between intrusive phases, textural similarities between rock types, and similar age dates between intrusive phases. Therefore, it is reasonable to suggest that for the CHS pluton fractional crystallization from a parent magma could have given rise to the diversity of rocks seen from the granodiorites to the syenogranites. However, the mineralized aplite dated at approximately 54 m.y. suggests that residual, late-stage, melt fractions may or may not have been comagmatic with the main intrusive phases. Additionally, it is reasonable to hypothesize that for the Two-bit pluton, fractional crystallization from a parent magma could have given rise to the diversity of rocks seen from the granodiorites to the aplite and pegmatite dikes.

Although there is a complete compositional gradation from the Two-bit granodiorites to the CHS syenogranites (suggestive of fractional crystallization), there is a compositional overlap in the granodiorite and monzogranite intrusive phases. Without more data on the eastern portion of the CHS pluton it is not possible to determine the importance of the CHS granodiorite phase. The fresh, pristine condition of the granodiorite sample (1933) combined with its age date of 57 m.y. implies that it could represent a viable intrusive phase (as opposed to a single rock limited in area with a

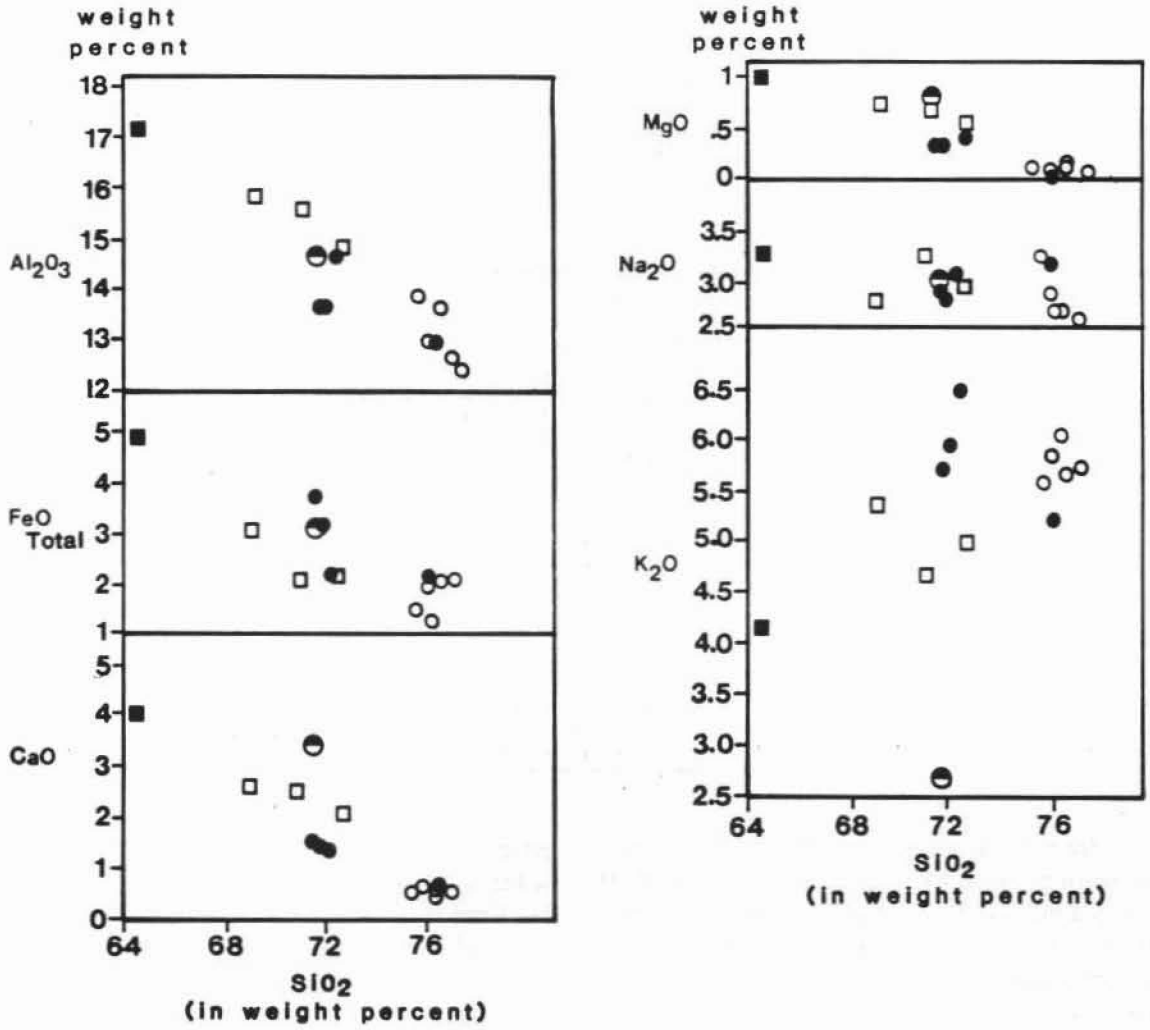

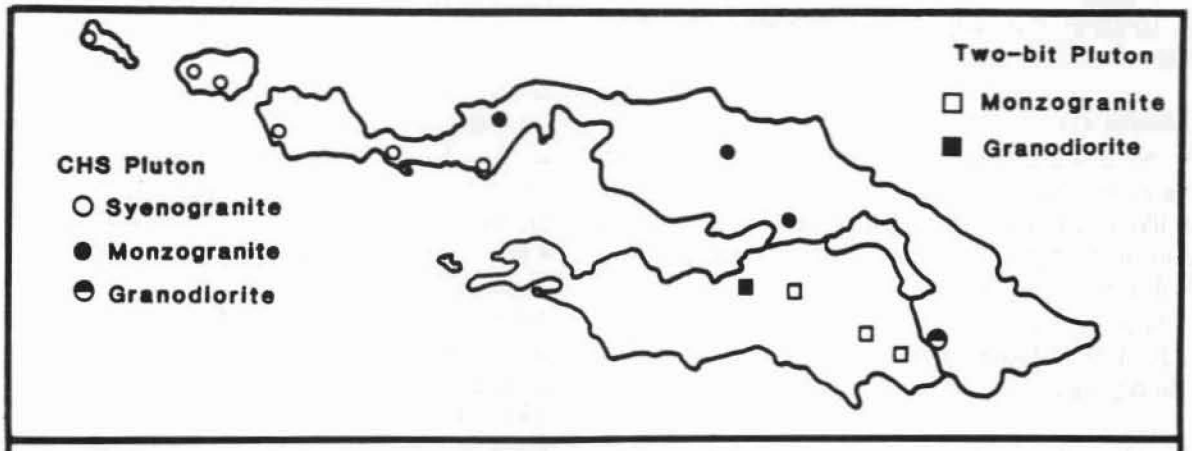

Figure 23. Harker variation diagrams. Map shows location of samples.

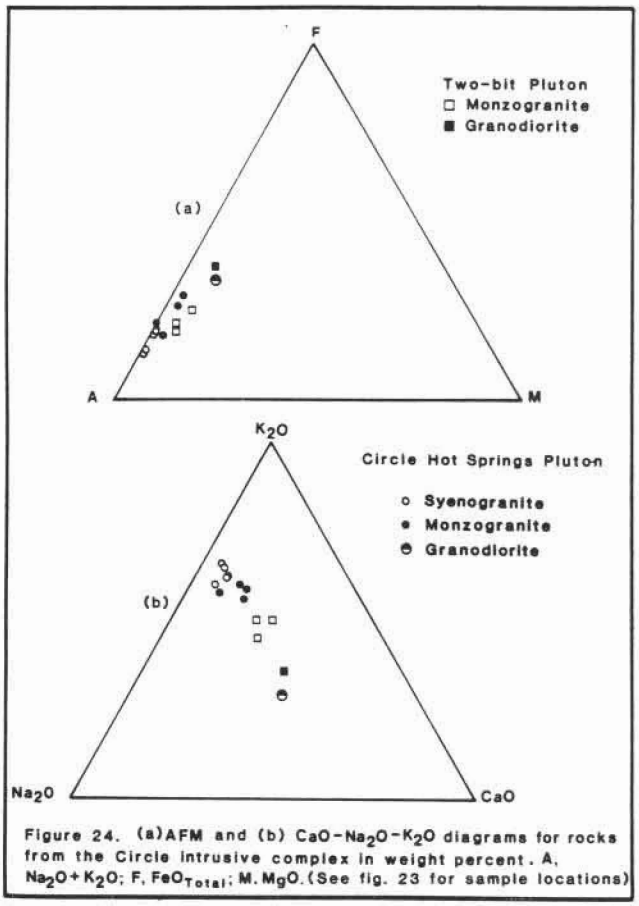

Figure 24. (a)AFM and (b) $CaO-Na_2O-K_2O$ diagrams for rocks from the Circle intrusive complex in weight percent. A, Na_2O+K_2O; F, FeO_{Total}; M, MgO. (See fig. 23 for sample locations)

composition due to wall rock contamination). Differences in texture, chemical analysis, mineralogy and K-Ar dates between the plutons could mean that they were not comagmatic and as likely to have come from two separate parent magmas. Broad similarities between the two plutons and close proximity suggest that the original sources of the individual magmas may have been closely associated. These hypotheses are not supported by conclusive evidence. It is not in the scope of this report to answer all the questions raised. However, this study will provide a solid foundation of reliable data upon which future workers can build.

Trace Elements

If the concentration of an element contained in an igneous rock is less than 0.1 weight percent (or 1,000 parts per million), it is called a trace element (Barker, 1983). Eighteen rocks from the Circle intrusive complex were selected and analyzed for seven trace elements (Appendix E-1). According to R. Taylor (1979), anomalous amounts of Sn, F, Li, B, and Rb may be found in granites associated with tin deposits.

Based on their large, ionic radii or high ionic charge, Li^{+}, Be^{+2}, B^{+3}, F^{-1}, and $Sn^{+2 \text{ or } +4}$ do not enter into the common mineral crystal structures. Instead they become concentrated in residual fluids as fractional crystallization progresses. Consequently, they are often found in late-stage aplite or pegmatite dikes and are called residual elements. For these reasons, aplite-pegmatite dikes and altered intrusive rocks were selected for trace element analysis. One objective of trace element analysis was to narrow down the possible sources of tin mineralization. In the Circle intrusive rocks, limited exposure dictates the availability of samples and therefore interpretations of the results are somewhat speculative.

According to Taylor (1979), major phases that have crystallized from a melt enriched in tin, may contain anomalous amounts of tin and associated elements (i.e. F, B, Li, and Be). Therefore, major phases from the Two-bit and CHS pluton were also analyzed. Rubidium is often found with Sn but for a different reason than that for the residual elements. Rubidium is similar in ionic radius and charge to potassium. Therefore it readily enters into the crystalline structure of potassium-bearing minerals. As a result, as fractional crystallization proceeds, if the melt composition is suitable, it will become enriched in potassium and rubidium. Therefore, the last melt fractions to crystallize will often be composed of minerals containing rubidium and potassium (alkali feldspars), quartz and residual elements.

When the samples were selected for trace element

analysis it was not known that two plutons composed the Circle intrusive bodies. The CHS monzogranites that were selected have both been affected slightly by some form of postmagmatic alteration. CH57 contains tourmaline-rich pods possibly due to crosscutting dikes, and PM278 is slightly altered due to its proximity to greisenized syenogranite. Unaltered monzogranites are not represented nor are unaltered syenogranites of the Ketchem Dome-Ketchem Creek area. In Figure 25, the sample identified as "greisen" contains .13 percent tin. The samples labeled, 'altered intrusive rock' represent rocks that were altered too much to obtain reliable modal analysis data but not as intensely altered as the greisen sample.

Figure 25 and 26 show that rubidium content increases in the more potassic-rich rocks of the CHS pluton. The aplite-pegmatite dikes and altered rocks analyzed from the Two-bit pluton appear to be barren of significant amounts of Sn and associated minerals. The CHS rocks generally contain higher amounts of the residual elements but Sn is only significantly high in the greisen rock. Tungsten is highest in an altered schist found close to the contact near the confluence of Deadwood and Switch Creeks. The samples showing the highest boron values contain visible tourmaline (a boron-bearing mineral).

The trace element data in Fig. 25 and Fig. 26 suggests that the tin potential is greater in the CHS pluton. The highest tin value occurs in the greisen rock (CH58A) with the next highest values (which are considerably lower) occurring in the aplite-pegmatite dikes.

CIPW Norm and the Differentiation Index

Figure 27 shows plots of each trace element versus the corresponding differentiation index determined for each rock. In order to explain what differentiation index is, an explanation of the CIPW norm is necessary. Rock analyses are commonly presented in terms of weight percentages of the major oxides. Comparing rocks based on these percentages can be laborious and somewhat confusing. In 1902, Cross, Iddings, Pirsson, and Washington (C.I.P.W.) developed an igneous rock classification whereby the oxide components were recalculated to form a set of mineralogical equivalents or 'normative minerals'. Their igneous classification is rarely used but the CIPW method of calculating the norm of a rock has been widely adopted (Middlemost, 1985).

According to Barker, (1983):

> "In the calculation of the CIPW norm, oxide components are combined into arbitrary compounds according to a rigidly prescribed order, originally thought to be the order of crystallization of the analogous minerals in most magmas. These arbitrary compounds or normative constituents have the chemical formulas of simple endmembers in the major rock-forming mineral groups, with the important exception that no normative constituent is hydrous. The CIPW norm, expressed in weight percent, thus resembles the mode of an igneous rock composed entirely of anhydrous crystalline phases in which there were no solid solutions."

Appendix D lists the normative mineral values corresponding to the Circle intrusive rocks that were analyzed for the major oxides. Middlemost states (1985), "The differentiation index is a numerical expression of the extent to which a magma has differentiated, and it represents the sum of the weight percentages of normative quartz, orthoclase, albite, nepheline, leucite, and kalsilite (Thornton and Tuttle, 1960)."

The plots in Figure 27 suggest that the two plutons could be chemically distinct, however, not enough data points are plotted to conclusively determine chemical trends within or between the plutons.

Seward Tin Granites Versus the Circle Intrusive Complex

According to Hudson and Arth (1983), seven plutons compose the Seward Peninsula tin-granite belt (Fig. 28). As a means of comparison, normative minerals ratios from six of the Seward tin granites were plotted with Circle intrusive complex normative mineral rations (Fig. 29). The plot supports the findings of this report that the Two-bit pluton is compositionally an unlikely source for tin. The plot also supports the hypothesis that the Circle Hot Springs biotite syenogranite is the most likely host of tin mineralization.

Summary and Conclusions

Given Streckeisen's classification of plutonic rocks, using his granite field without subdivisions of syenogranite and monzogranite, and by using an accepted set of textural terms, most of the intrusive rocks of this study could be described as medium-grained, porphyritic biotite granite. Through a careful study of macrocrystalline igneous textures, based on the size of the large feldspars, two different sets of igneous rock were outlined. Experimental modal plots supported this textural separation of rocks. It became obvious that Streckeisen's granite field covered too broad of a composition range to accurately classify the rocks of the study area. Mineralogy and plots using whole-rock and trace-element data further supported a two-pluton theory. Potassium-argon age dates were the final evidence to suggest that two plutons composed the batholith.

Based on the multiphase character of the plutons, the term "Circle intrusive complex" has been coined in this report. Out of necessity, the two plutons have been named and are called the Circle Hot Springs and Two-bit plutons.

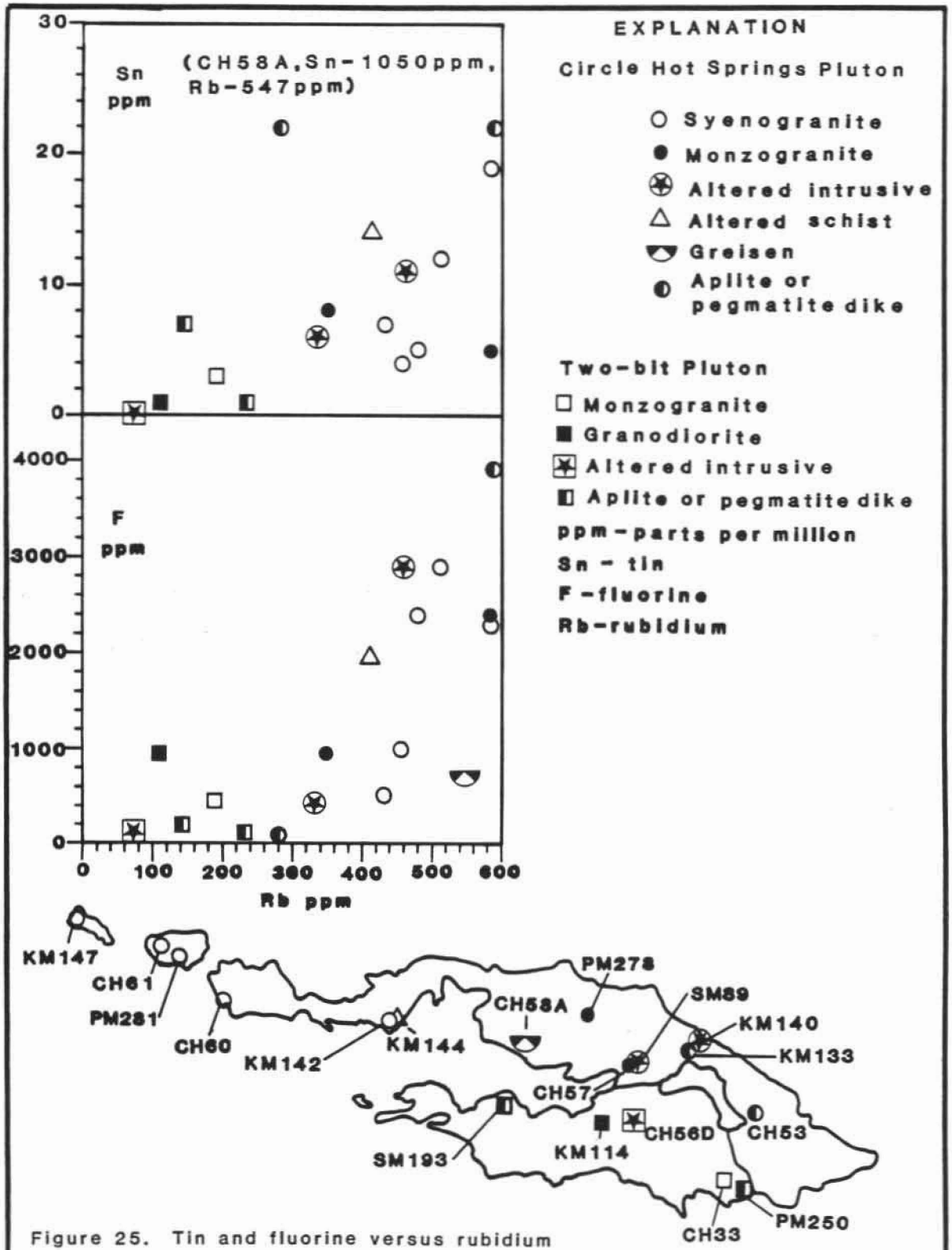

Figure 25. Tin and fluorine versus rubidium plots of 18 samples from the Circle intrusive complex.

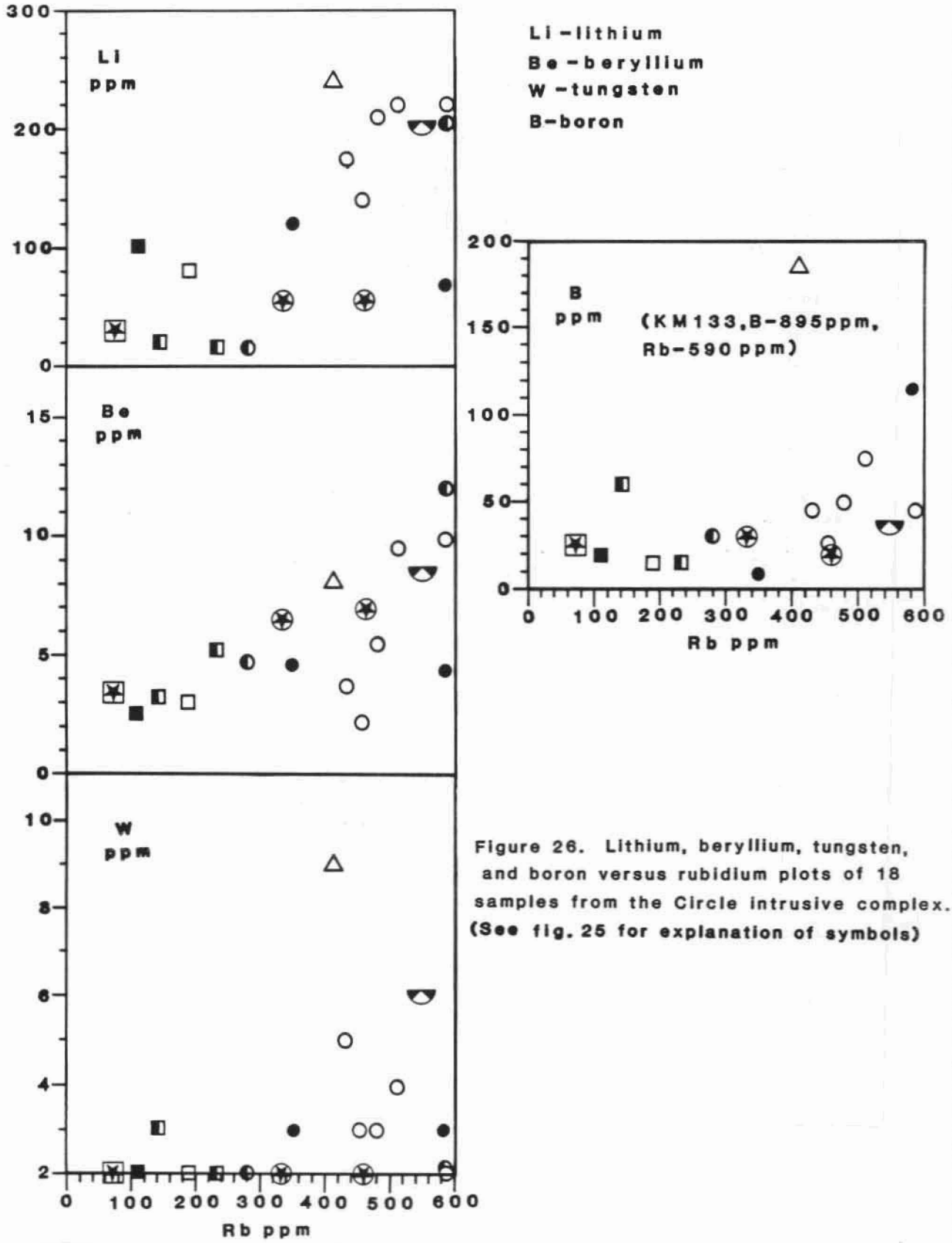

Figure 26. Lithium, beryllium, tungsten, and boron versus rubidium plots of 18 samples from the Circle intrusive complex. (See fig. 25 for explanation of symbols)

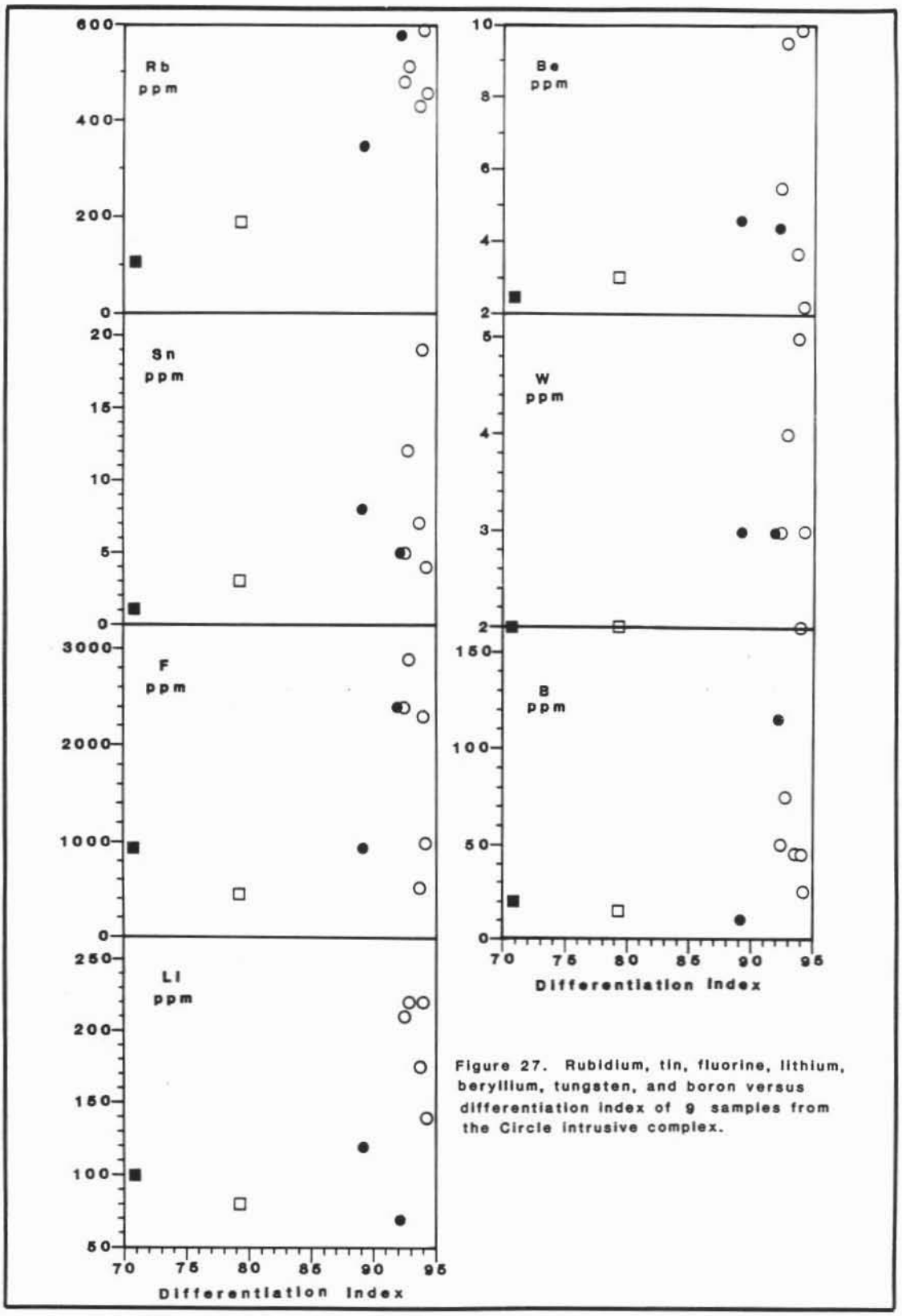

Figure 27. Rubidium, tin, fluorine, lithium, beryllium, tungsten, and boron versus differentiation index of 9 samples from the Circle intrusive complex.

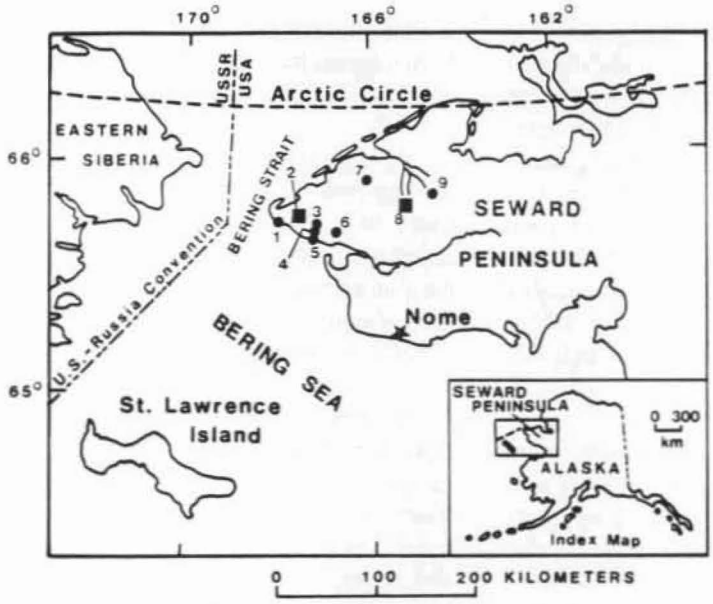

Figure 28. Location of Seward Peninsula and distribution of plutons (circles, exposed; squares, inferred at depth) in the tin-granite belt, northwest Alaska. Plutons include those at Cape Mountain (1), Potato Mountain (2), Brooks Mountain (3), Lost River (4), Tin Creek (5), Black Mountain (6), Ear Mountain (7), Kougarok Mountain (8), and the Oonatut Granite Complex (9). (From Hudson and Arth, 1983).

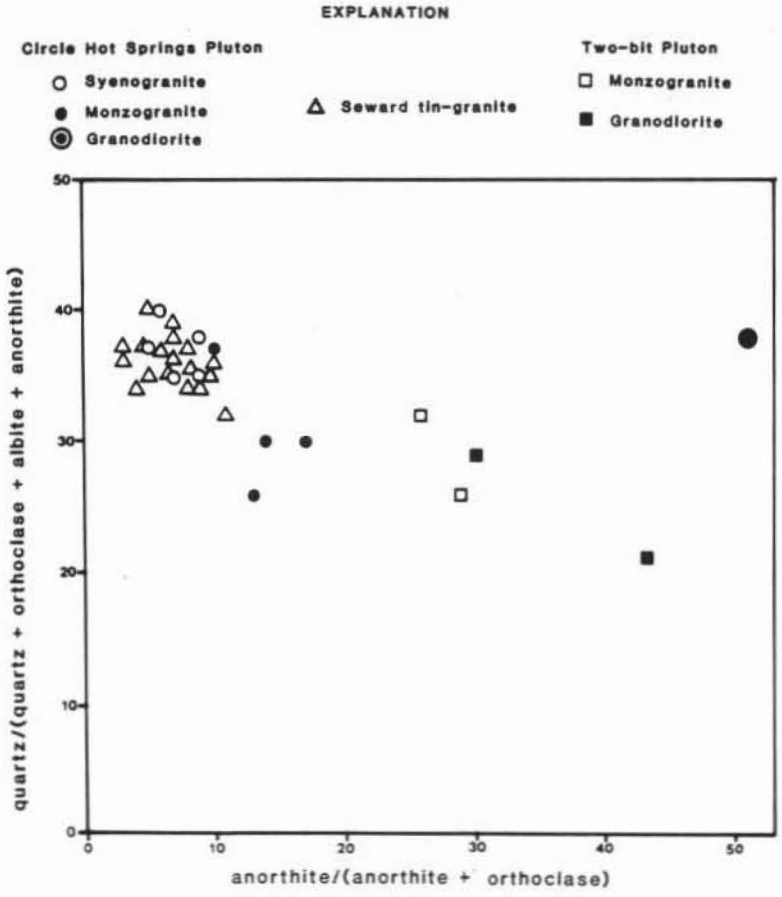

Figure 29. Comparison plot of Seward tin-granite normative mineral ratios versus Circle intrusive complex normative mineral ratios.

The Two-bit pluton is approximately 70 m.y. old. It is composed of two main intrusive phases; granodiorite and monzogranite. Aplite-pegmatite and mafic dikes crosscut these phases. Two age-dates suggest that the granodiorites are about the same age as the crosscutting aplite-pegmatite dikes. This closeness in age between phases, together with the chemical trends shown in modal variation diagrams and similar mineralogies suggests that fractional crystallization of a parent magma could have given rise to the diversity of rocks seen in the Two-bit pluton. At least 13 m.y. lapsed before the emplacement and crystallization of the Circle Hot Springs pluton.

The CHS pluton is composed of granodiorite, monzogranite, quartz monzonite and syenogranite. K-Ar ages indicate that all four phases crystallized about 57 m.y. ago. A K-Ar age of an aplite dike suggests that three million years lapsed before at least some of the aplite dikes crystallized. The closeness in age between intrusive phases combined with chemical trends shown in modal variation diagrams and similar mineralogies, suggest that fractional crystallization from a parent magma could have given rise to the diversity of rocks seen in the CHS pluton.

In contrast, differences in age, composition, textures and mineralogies suggest that the two plutons were not as likely to have originated from the same parent magma. Broad similarities and close proximity support the idea that the plutons could have arisen from two parent magmas from closely associated sources. More detailed work is necessary to better understand these relationships.

Historically, placer tin has been identified in creeks that flow through or adjacent to the batholith. In this report, cassiterite has been identified in greisen on the flank of Ketchem Dome and in altered intrusive alongside Portage Creek. Mineralogy, trace-element data and similar normative mineral ratios to Seward tin-granites, suggest that the biotite syenogranite of the Circle Hot Springs pluton is the most likely to host tin mineralization.

Appendix A-1

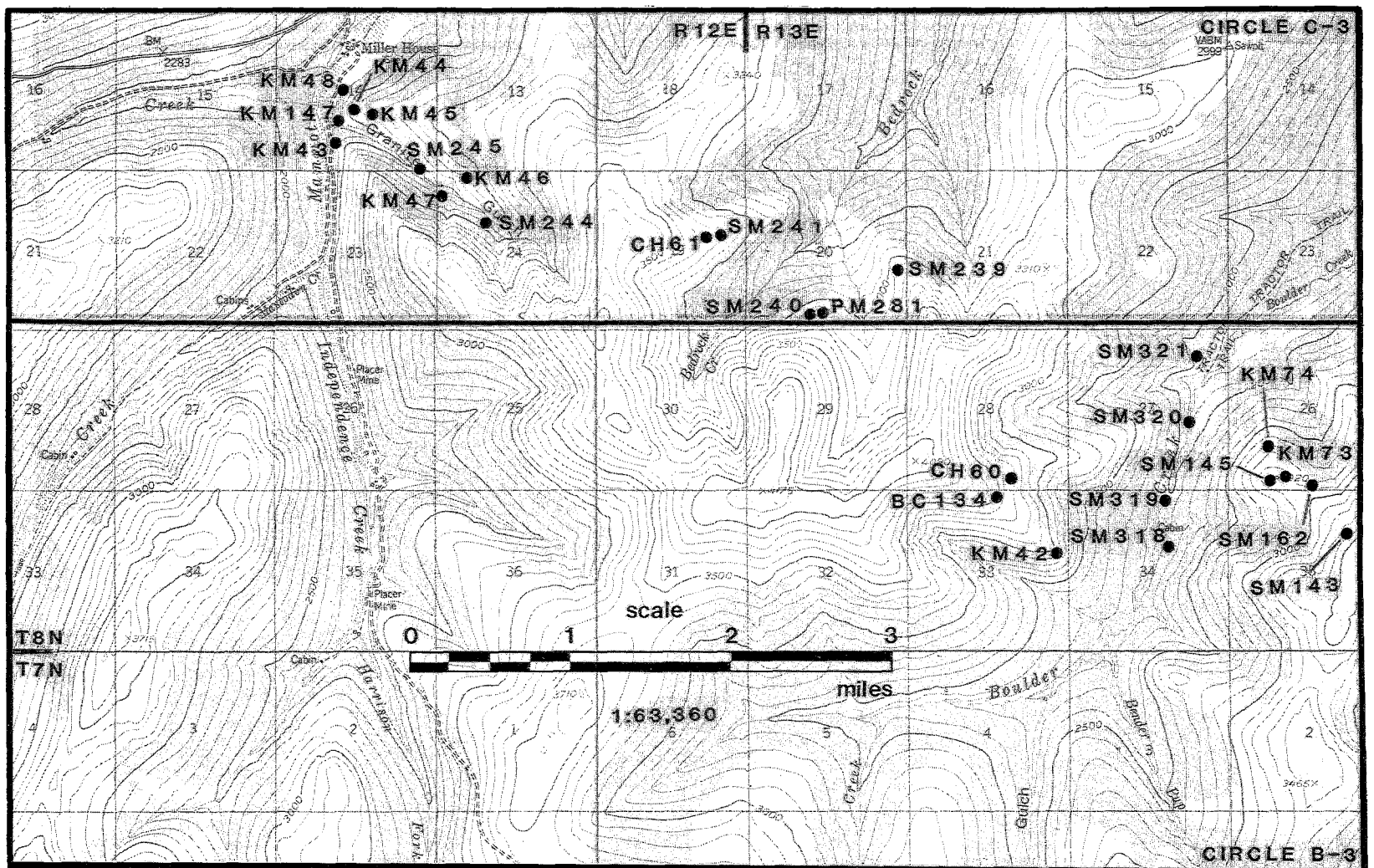

Figure 30. Location of sample sites in the Bedrock Creek area.

Appendix A-2

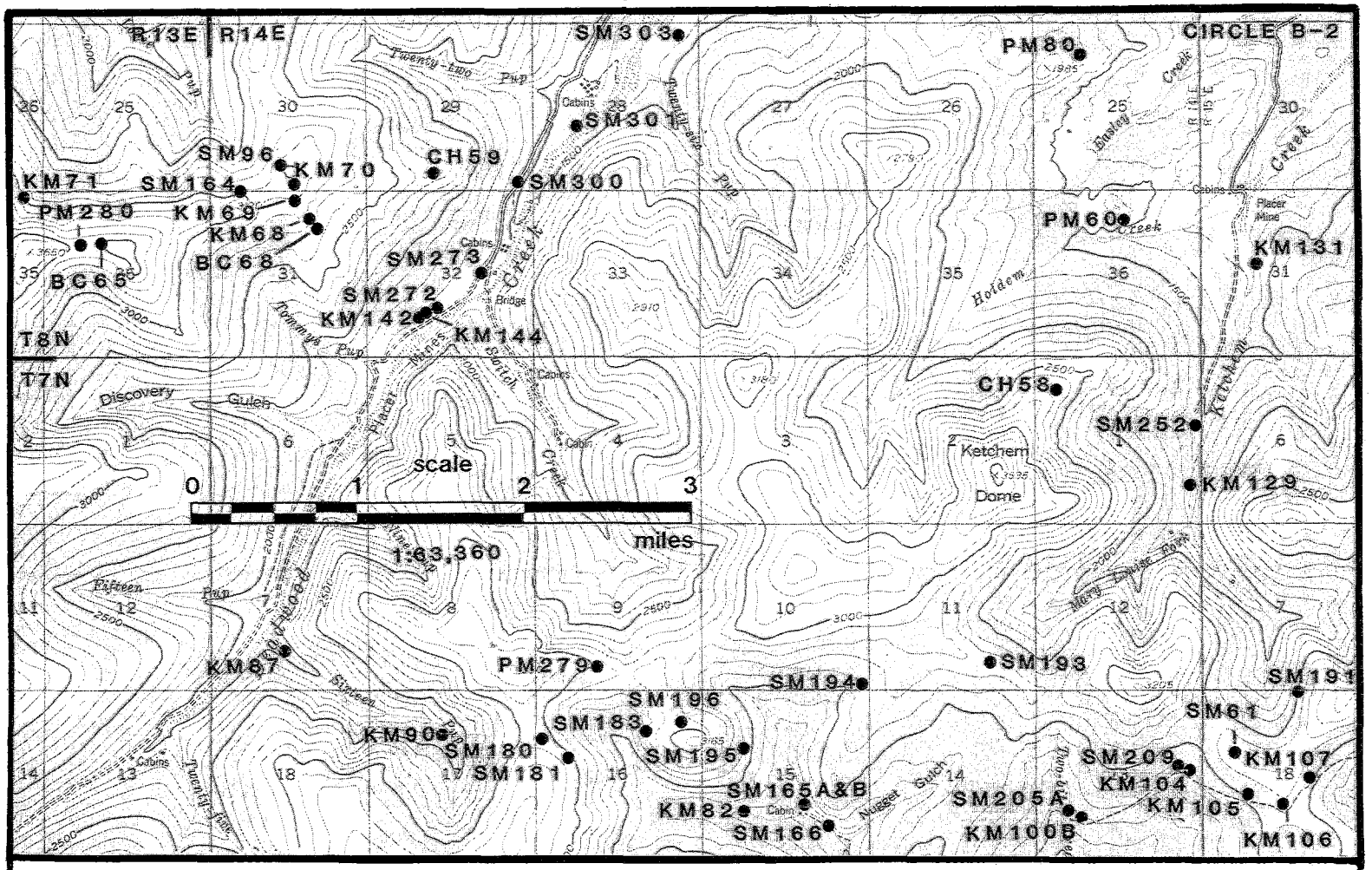

Figure 31. Location of sample sites in the Deadwood Creek area.

Appendix A-3

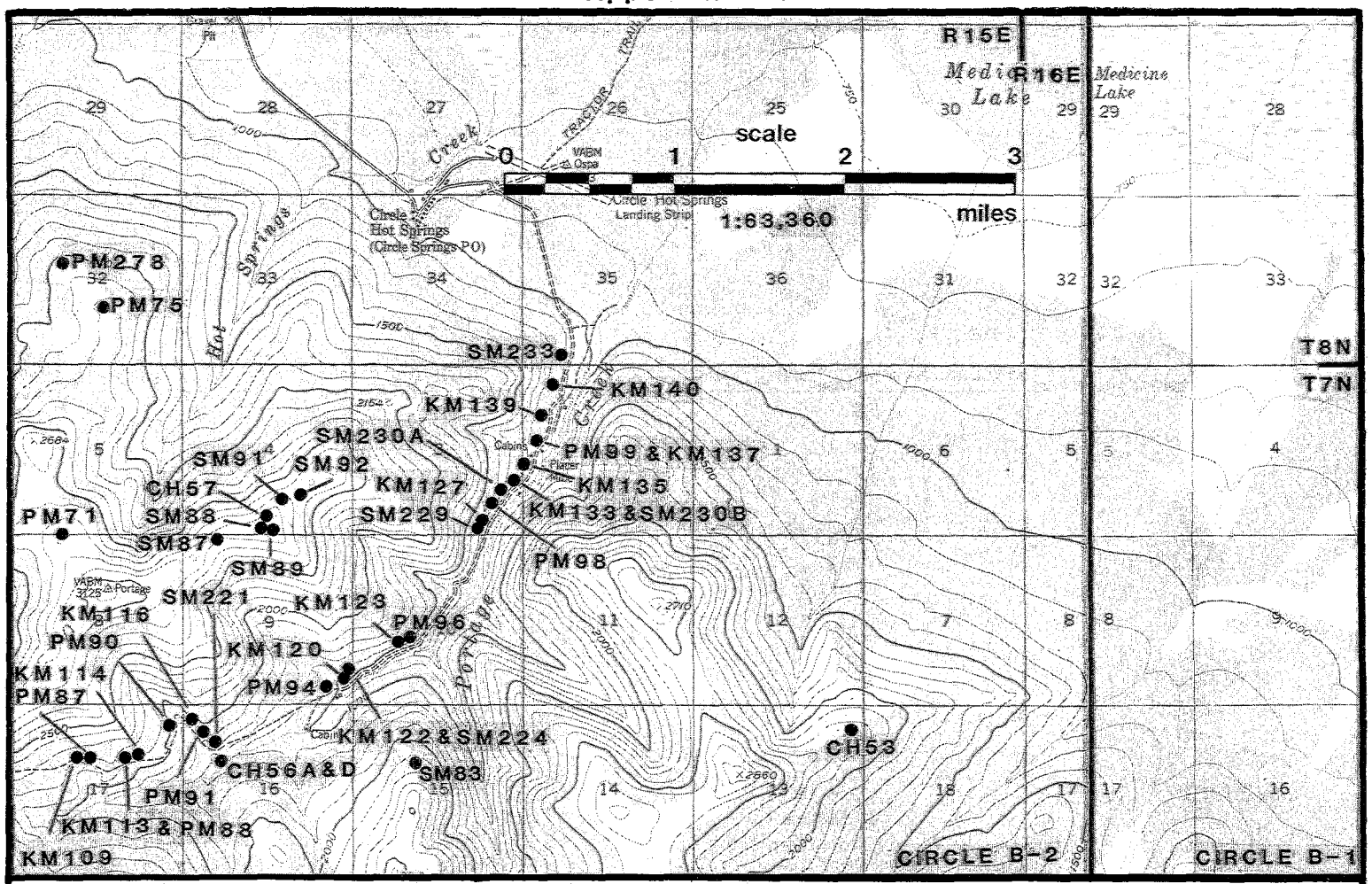

Figure 32. Location of samples in the Portage Creek area.

Appendix A-4

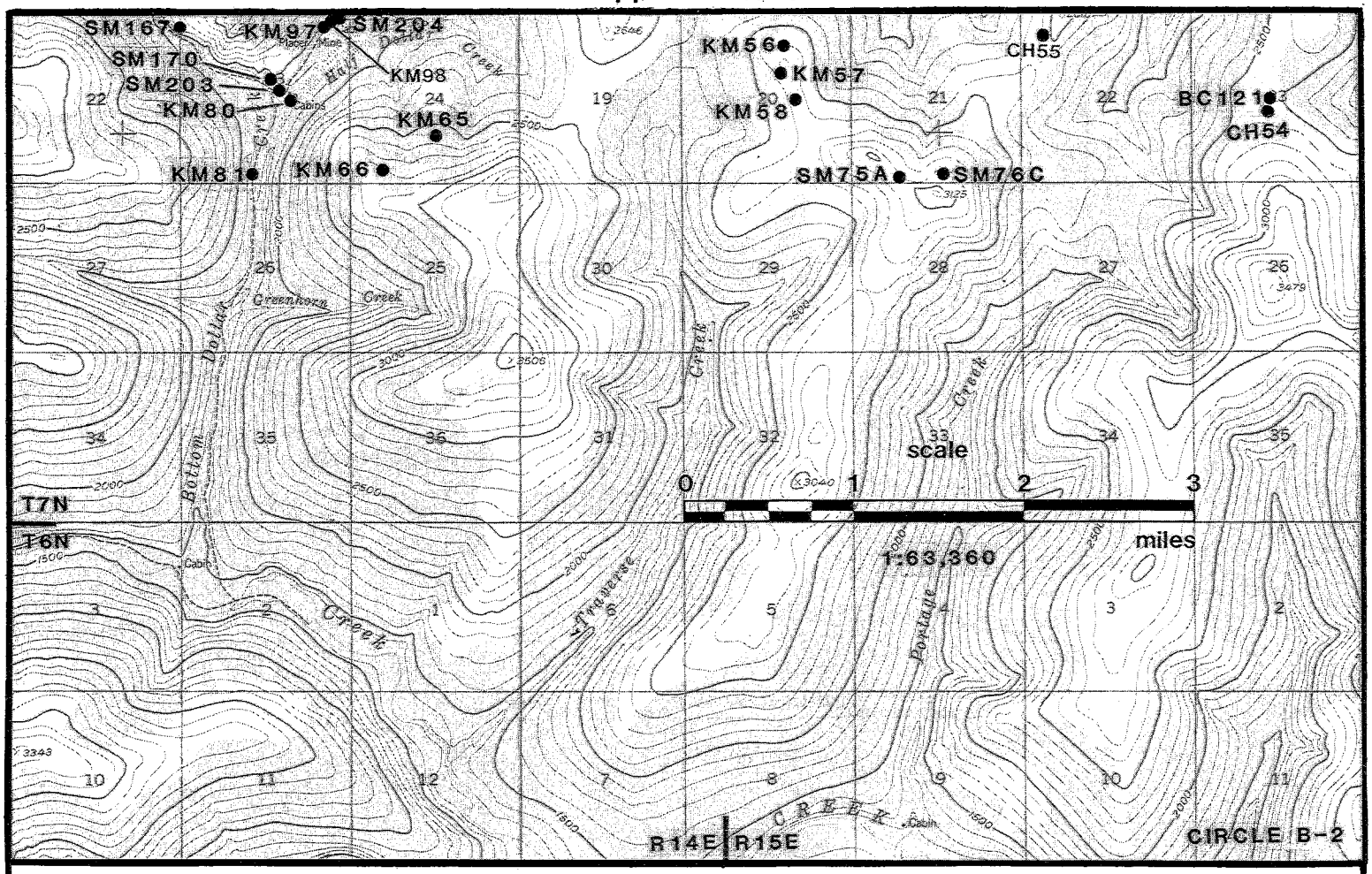

Figure 33. Location of sample sites in the Half Dollar Creek area.

Appendix A-5

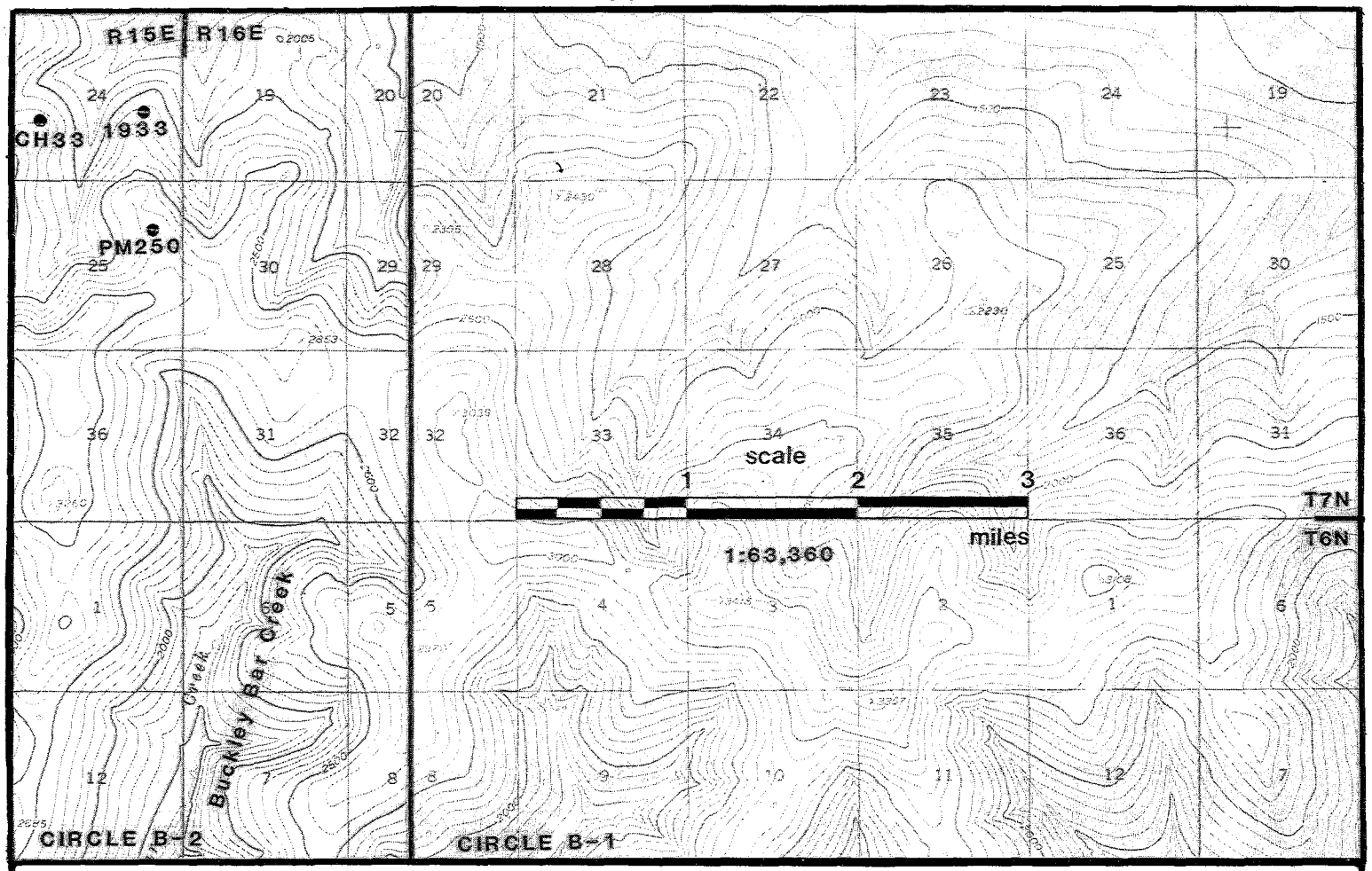

Figure 34. Location of sample sites in the Buckley Bar area.

Appendix B. Grain Size Analysis Of Rocks From The Circle Intrusive Complex

Pluton	Sample No.	Large Quartz (mm)	Large Feldspar (mm)	Groundmass Grains (mm)	% of Large Quartz	% of Large Feldspar	% of Ground-mass
Circle Hot Springs	KM 48	none	none	1 - 3	none	none	100
	KM 147	none	up to 25	1 - 2	none	2	98
	KM 43	none	none	1 - 4	none	none	100
	KM 44	none	up to 10	1 - 4	none	2	98
	KM 45	none	2 - 5	1 - 2	none	58	42
	SM 245	none	up to 12	1 - 2	none	5	95
	KM 46	none	up to 10	1 - 2	none	5	95
	KM 47	none	5 - 7	1 - 4	none	51	49
	SM 244	none	none	1 - 4	none	none	100
	SM 241	none	5 - 10	2 - 5	none	63	37
	PM 281	none	3 - 5	1 - 2	none	58	42
	SM 240	none	up to 10	1 - 5	none	10	90
	SM 239	none	up to 10	1 - 6	none	10	90
	BC 134	none	none	1 - 2	none	none	100
	KM 42	none	none	1 - 2	none	none	100
	SM 318	none	up to 16	1 - 2	none	13	87
	SM 319	up to 4	up to 20	1 - 2	5	28	67
	SM 320	up to 4	up to 20	1 - <1	5	22	73
	SM 321	up to 4	up to 20	1 - 2	5	29	66
	KM 74	none	up to 25	1 - 2	none	5	95
	KM 73	up to 4	up to 10	1 - 2	2	3	95
	SM 145	up to 4	up to 10	1 - 2	2	3	95
	SM 162	up to 4	up to 10	1 - 2	2	3	95
	KM 71	none	up to 10	1 - 3	none	3	97
	SM 143	none	7 - 10	1 - 2	none	3	97
	BC 65	none	up to 10	1 - 2	none	5	95
	SM 164	none	up to 17	1 - 2	*	*	*
	KM 68	none	up to 8	1 - 2	none	52	48
	BC 68	3 - 5	up to 15	1 - 2	5	44	51
	KM 69	1 - 3	up to 5	1 - 3	*	*	*
	KM 70	up to 4	up to 8	1 - 3	1	29	70
	SM 96	none	up to 5	1 - <1	*	*	*
	SM 303	up to 4	none	1	*	*	*
	SM 300	up to 4	up to 15	1 - 3	10	9	81
	SM 301	up to 4	up to 10	1 - 3	10	3	87
	SM 272	up to 3	up to 9	1 - 3	*	*	*

Appendix B. Grain Size Analysis Of Rocks From The Circle Intrusive Complex (Continued)

Pluton	Sample No.	Large Quartz (mm)	Large Feldspar (mm)	Groundmass Grains (mm)	% of Large Quartz	% of Large Feldspar	% of Ground-mass
Circle Hot Springs	SM 273	up to 5	up to 10	1 - 3	*	*	*
	KM 142	up to 5	up to 15	1 - 3	*	*	*
	PM 71	3 - 4	up to 8	1	*	*	*
	KM 129	up to 6	up to 17	4 - 5	10	3	87
	SM 252	up to 6	up to 17	4 - 5	10	3	87
	PM 60	none	up to 15	3 - 5	none	9	91
	SM 87	none	10 - 20	2 - 4	none	27	73
	SM 88	5	12	1 - <1	*	*	*
	SM 91	4	5 - 7	1 - <1	*	*	*
	SM 92	4	5 - 7	1 - <1	*	*	*
	SM 229	5 - 7	up to 20	2 - 5	10	29	61
	PM 98	1 - 4	25	1 - 2	2	3	95
	SM 230B	none	5 - 7	1 - <1	none	10	90
	KM 135	none	15	5 - 6	none	4	96
	PM 99	none	15	5 - 6	none	4	96
	KM 137	none	none	1 - <1	none	none	100
Two-Bit	KM 123	5 - 10	up to 45	2 - 5	34	33	33
	SM 224	5 - 7	up to 20	2 - 3	*	*	*
	PM 94	4 - 6	up to 30	2 - 3	*	*	*
	PM 96	10	up to 40	3 - 5	*	*	*
	KM 120	5 - 7	up to 35	2 - 4	22	21	57
	KM 109	5 - 7	25 - 35	2 - 4	15	31	54
	KM 106	9 - 12	30	2 - 5	9	4	87
	KM 107	up to 10	up to 40	2 - 4	22	33	45
	KM 113	5 - 10	up to 30	1 - 2	5	5	90
	KM 114	5 - 7	15	1 - 2	5	5	90
	KM 116	5 - 7	30	2 - 5	16	5	79
	SM 191	5 - 7	5 - 10	2 - 4	5	5	90
	PM 87	5 - 7	15 - 20	2 - 3	*	*	*
	PM 88	5 - 7	15 - 20	2 - 3	*	*	*
	PM 90	5 - 7	up to 30	2 - 3	*	*	*
	PM 91	5 - 7	20	2 - 3	*	*	*
	SM 205A	5 - 7	up to 40	2 - 4	3	12	85
	KM 100B	5 - 7	up to 25	2 - 3	*	*	*

Appendix B. Grain Size Analysis Of Rocks From The Circle Intrusive Complex (Continued)

Pluton	Sample No.	Large Quartz (mm)	Large Feldspar (mm)	Groundmass Grains (mm)	% of Large Quartz	% of Large Feldspar	% of Ground-mass
Two-Bit	KM 104	5 - 7	40	2 - 4	3	16	81
	KM 105	5 - 7	40	2 - 4	3	16	81
	SM 61	5	up to 10	2 - 4	*	*	*
	SM 170	7	up to 20	3 - 4	*	*	*
	SM 203	5 - 7	up to 33	3 - 5	25	37	38
	KM 80	5 - 7	up to 25	3 - 4	15	31	54
	KM 81	5 - 6	up to 25	3 - 4	*	*	*
	KM 97	5 - 7	25	3 - 4	42	8	50
	SM 204	5 - 10	up to 45	2 - 4	*	*	*
	KM 65	5 - 7	up to 15	2 - 4	33	29	38
	KM 56	up to 5	up to 10	1 - <1	1	7	92
	KM 57	up to 7	up to 20	2 - 4	9	13	78
	KM 58	up to 8	up to 30	2 - 4	13	3	84
	SM 75A	10	15	2 - 4	*	*	*
	SM 76C	up to 10	up to 25	2 - 4	30	21	49
	BC 121	up to 10	25	1 - 3	3	8	89
	SM 80	4	up to 10	1 - 2	*	*	*
	SM 83	5 - 7	25	2 - 4	*	*	*
	KM 82	up to 10	up to 25	2 - 4	12	12	76
	SM 180	none	none	1 - 3	none	none	100
	SM 181	up to 8	none	1 - 3	*	*	*
	SM 183	up to 10	up to 16	2 - 5	*	*	*
	SM 194	2 - 5	up to 30	3	18	25	57
	SM 195	5	up to 20	2 - 6	8	14	78
	SM 196	3 - 6	none	1 - 3	*	*	*
	PM 279	6 - 10	up to 30	3 - 4	28	10	62
	SM 165A	7	15 - 20	3 - 4	8	18	74
	SM 165B	7	15 - 20	3 - 4	8	18	74
	SM 166	7 - 12	up to 35	4 - 5	25	40	35
	SM 167	6	up to 30	2 - 5	*	*	*
	KM 87	up to 9	up to 47	4	20	50	30
	KM 90	up to 9	up to 7	1 - 3	30	12	58

* volumetric percentages were not recorded

Appendix C. A Method of Point-counting Medium-grained, Porphyritic Rocks for Modal Analysis

Step 1. A. Determine what the largest grain in the groundmass is and select a grid size that is larger than the biggest grain.

B. When a point falls on a phenocryst, do not count it.

C. Point-count plagioclase, potassium feldspar, quartz and mafics.

Step 2. A. Normalize to 100% without the mafics as follows:

1. Subtract the number of mafic points counted from the total number of points counted.

2. Divide each mineral's point-count by the new total.

Step 3. A. Determine what the largest phenocryst is and choose a grid size accordingly.

B. Point-count the phenocrysts and count anything other than a phenocryst as groundmass.

C. Determine what percentage of the sample is phenocrysts versus groundmass as follows:

1. Divide each of the phenocryst point-counts by the total number of points counted.

Step 4. A. At this point it is necessary to multiply the total percentage of groundmass (found with the coarse-grain grid) by the percentage of each mineral found in the groundmass (found with the medium-grain grid). Do this as follows:

1. Multiply the coarse-grained grid groundmass percentage by each of the medium-grained grid groundmass mineral percentages.

These values now represent the total percentages of plagioclase, potassium feldspar and quartz found in the groundmass.

Step 5. A. In order to get the modal composition of the entire sample, it is necessary to add the percentages of the phenocrysts to the groundmass percentages. As a check, the total percentage of plagioclase, potassium feldspar and quartz should add up to 100 percent.

Throughout the calculations it is easier to round to three places and keep the decimal form as opposed to percentages until the final calculation.

MODAL POINT-COUNT DATA WORKSHEET

Groundmass (m.g. grid)(3mm)

sample no	plag.	k-spar	quartz	mafics	total no. of points
SM301	no. of points	no. of points	no. of points	no. of points	301
	55	134	93	19	

Normalize to 100% without mafics

plag.	k-spar	quartz
20%	47%	33%

total points

w/out mafics
282

Phenocrysts (c.g. grid)(15mm)

plag.	k-spar	quartz	ground-mass	total no. of points
no. of points	no. of points	no. of points	no. of points	33
	1		32	
%	%	%	%	
	3		97	

Multiply the coarse-grained grid groundmass percentage by each of the medium-grained grid groundmass mineral percentages.

Total mineral percentages found in the groundmass

plag.	k-spar	quartz
19%	46%	32%

Add the percentages of the phenocrysts to the groundmass percentages.

Total percentages of plag., k-spar and quartz (phenocrysts and groundmass)

plag.	k-spar	quartz
19%	49%	32%

OBSERVATIONS

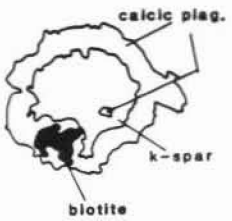

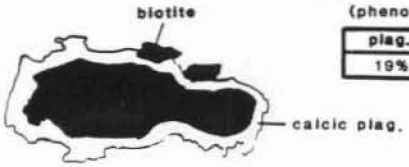

m.g. - medium-grained
c.g. - coarse-grained

Appendix D
Whole-rock Analytical Data of Fourteen Samples from the Circle Intrusive Complex

Sample Number	KM 147	CH 61	PM 281	PM 280	CH 60	CH 59	KM 142	CH 57	1933	PM 278	KM 114	CH 56A	CH 33	CH 54
*Rock Type	Granite	Granite	Alkali Granite	Quartz Monzonite	Alkali Granite	Granite	Alkali Granite	Granite	Grano-diorite	Granite	Grano-diorite	Quartz Monzonite	Quartz Monzonite	Quartz Monzonite
Pluton	CHS	CHS	CHS	CHS	CHS	CHS	CHS	CHS	CHS	CHS	Two-Bit	Two-Bit	Two-Bit	Two-Bit
Major Oxides														
SiO_2	76.03	76.62	75.64	71.77	77.33	71.91	76.34	76.00	71.62	72.30	64.78	71.13	69.19	72.71
Al_2O_3	12.96	12.63	13.82	13.62	12.34	13.69	13.59	12.99	14.60	14.69	17.14	15.51	15.83	14.75
Fe_2O_3	0.15	0.24	0.49	0.56	0.40	0.21	0.24	0.41	0.52	0.09	1.71	0.10	0.59	0.34
FeO	1.83	1.81	1.01	3.14	1.68	2.96	1.08	1.80	2.69	2.01	3.31	1.95	2.49	1.86
MgO	0.09	0.11	0.11	0.39	0.06	0.34	0.09	0.04	0.81	0.42	1.00	0.65	0.77	0.52
CaO	0.74	0.74	0.58	1.54	0.51	1.45	0.48	0.76	3.44	1.35	4.05	2.50	2.69	2.14
Na_2O	2.85	2.66	3.22	2.88	2.53	2.79	2.63	3.11	2.93	3.04	3.24	3.19	2.77	2.89
K_2O	5.88	5.64	5.58	5.72	5.72	5.96	6.09	5.20	2.62	6.48	4.14	4.65	5.37	4.95
TiO_2	0.17	0.19	0.12	0.52	0.17	0.47	0.10	0.14	0.35	0.32	0.73	0.27	0.32	0.22
P_2O_5	0.04	0.04	0.08	0.13	0.04	0.20	0.08	0.04	0.10	0.11	0.22	0.10	0.09	0.06
MnO	0.05	0.05	0.05	0.08	0.06	0.07	0.03	0.07	0.09	0.07	0.09	0.07	0.12	0.07
FeO Total	1.96	2.03	1.45	3.64	2.04	3.15	1.30	2.17	3.16	2.09	4.85	2.04	3.02	2.17
Sum of Oxides	100.79	100.73	100.70	100.35	100.84	99.95	100.85	100.56	99.77	100.88	100.41	100.12	100.23	100.51

* (After Streckeisen, 1976) - Rock names are based on chemical analysis.
CHS - Circle Hot Springs

CIPW Norms of Fourteen Samples from the Circle Intrusive Complex

Sample Number	KM 147	CH 61	PM 281	PM 280	CH 60	CH 59	KM 142	CH 57	1933	PM 278	KM 114	CH 56A	CH 33	CH 54
*Rock Type	Granite	Granite	Alkali Granite	Quartz Monzonite	Alkali Granite	Granite	Alkali Granite	Granite	Grano-diorite	Granite	Grano-diorite	Quartz Monzonite	Quartz Monzonite	Quartz Monzonite
Pluton	CHS	CHS	CHS	CHS	CHS	CHS	CHS	CHS	CHS	CHS	Two-Bit	Two-Bit	Two-Bit	Two-Bit
Normative Minerals	CIPW Values													
Quartz	33.96	36.61	33.76	27.52	38.48	27.72	36.04	35.13	34.39	25.15	18.89	27.29	24.15	30.45
Corundum	0.66	0.90	1.62	0.20	1.16	0.39	2.09	0.96	0.93	0.48	0.49	0.92	0.78	0.89
Orthoclase	34.75	33.33	32.97	33.80	33.80	35.22	35.99	30.73	15.48	38.29	24.46	27.48	31.73	29.25
Albite	24.11	22.51	27.24	24.37	21.41	23.61	22.25	26.31	24.79	25.72	27.41	26.99	23.44	24.45
Anorthite	3.41	3.41	2.36	6.79	2.27	5.89	1.86	3.51	16.41	5.98	18.66	11.75	12.76	10.22
Hypersthene	3.27	3.18	1.62	5.56	2.74	5.46	1.90	2.96	6.12	4.26	6.12	4.80	5.70	4.20
Magnetite	0.22	0.35	0.71	0.81	0.58	0.30	0.35	0.59	0.75	0.13	2.48	0.14	0.86	0.49
Ilmenite	0.32	0.36	0.23	0.99	0.32	0.89	0.19	0.27	0.66	0.61	1.39	0.51	0.61	0.42
Apatite	0.09	0.09	0.18	0.30	0.09	0.46	0.18	0.09	0.23	0.26	0.51	0.23	0.21	0.14
Sum	100.79	100.73	100.70	100.35	100.84	99.95	100.85	100.56	99.77	100.88	100.41	100.12	100.23	100.51

* (After Streckeisen, 1976) - Rock names are based on chemical analysis.
CHS - Circle Hot Springs

Appendix E-1.
Trace-element Analyses of 18 Samples from the Circle Intrusive Complex

Sample No.	Rock Type	Pluton	Be ppm	Li ppm	F ppm	W ppm	Sn ppm	Rb ppm	B ppm
CH 53	Pegmatite pod in intrusive (composition unknown)	CHS	4.7	15	45	2	22	281	30
CH 57	Tourmaline-rich pod in monzogranite	CHS	4.4	70	2400	3	5	581	115
CH 58A	Greisen	CHS	8.4	200	700	6	1050	547	35
KM 133	Aplite dike with cross-cutting tourmaline veinlet	CHS	12.0	205	3900	2	22	590	895
KM 140	Altered intrusive	CHS	6.5	55	425	2	6	331	30
KM 144	Felsic vein-dike in altered schist	CHS	8.1	240	1950	9	14	412	185
CH 60	Syenogranite	CHS	3.7	175	525	5	7	432	45
CH 61	Syenogranite	CHS	5.5	210	2400	3	5	480	50
KM 142	Syenogranite	CHS	2.2	140	1000	3	4	456	25
KM 147	Syenogranite	CHS	9.5	220	2900	4	12	512	75
PM 278	Monzogranite	CHS	4.6	120	950	3	8	349	10
SM 89	Fluorite in altered intrusive	CHS	6.9	55	2900	2	11	459	20
PM 281	Syenogranite	CHS	9.9	220	2300	2	19	590	45
CH 56D	Altered intrusive	2-Bit	3.4	30	100	2	<1	71	25
PM 250	Pegmatite	2-Bit	3.2	20	190	3	7	143	60
SM 193	Aplite	2-Bit	5.2	15	100	2	1	233	15
CH 33	Monzogranite	2-Bit	3.0	80	450	2	3	189	15
KM 114	Granodiorite	2-Bit	2.5	100	950	2	1	108	20

Appendix E-2
Trace-element Analyses of 14 Samples from the Circle Intrusive Complex

Sample No.	Rock Type	Pluton	Zn ppm	Cu ppm	Co ppm	Ni ppm	Fe ppm	Mn ppm	Cr ppm	Pb ppm	Au ppm	Ag ppm	Mo ppm	Sb ppm	As ppm
KM 147	Syenogranite	CHS	24	8	2	4	13,000	316	197	11	<.1	0.2	4	<5	20
CH 61	Syenogranite	CHS	38	4	1	4	14,000	348	157	11	<.1	0.2	2	<5	24
PM 281	Syenogranite	CHS	21	8	2	4	9,000	278	88	25	<.1	0.3	2	<5	12
PM 280	Monzogranite	CHS	67	7	3	4	24,000	483	119	7	<.1	0.2	1	<5	22
CH 60	Syenogranite	CHS	31	6	2	5	14,000	399	226	10	<.1	0.2	2	<5	<10
CH 59	Monzogranite	CHS	65	4	3	5	23,000	406	236	7	<.1	0.2	2	<5	<10
KM 142	Syenogranite	CHS	27	10	2	4	9,000	163	161	9	<.1	0.1	1	<5	<10
CH 57	Monzogranite	CHS	31	3	1	2	14,000	406	138	11	<.1	0.1	2	<5	<10
1933	Granodiorite	CHS	47	7	4	5	21,000	589	185	14	<.1	0.1	1	<5	<10
PM 278	Monzogranite	CHS	61	5	3	4	15,000	465	144	10	<.1	0.1	1	<5	<10
KM 114	Granodiorite	2-Bit	87	16	4	4	26,000	555	133	20	<.1	0.1	1	<5	<10
CH 56A	Granodiorite	2-Bit	44	2	3	3	14,000	430	132	17	<.1	0.1	1	<5	<10
CH 33	Monzogranite	2-Bit	54	5	4	4	19,000	753	137	9	<.1	0.1	1	<5	<10
CH 54	Monzogranite	2-Bit	34	6	3	4	14,000	474	172	55	<.1	0.2	<1	<5	<10

Detection Limits Used in the Trace-element Analysis of 14 Samples from the Circle Intrusive Complex

*ICP/ AES	Detection Limits	*AAS (flame)	Detection Limits
Zn	0.003 ppm ± 0.65% SD	Pb	1 ppm
Cu	0.012 ppm ± 1.53% SD	Au	0.1 ppm
Co	0.0003 ppm ± 0.63% SD	Ag	0.1 ppm
Ni	0.002 ppm ± 0.51% SD	Mo	1 ppm
Fe	12.6 ppm ± 7.99% SD	Sb	1 ppm
Mn	0.031 ppm ± 5.45% SD	As	10 ppm
Cr	0.016 ppm ± 0.49% SD		

* Analyzed by an inductively coupled plasma atomic emission spectrometer

* Analyzed by an atomic absorption spectrometer

SD - standard deviation

REFERENCES

Aleinikoff, J.N., Dusel-Bacon, Cynthia, Foster, H.L., and Kiyoto, Futa, 1981, Proterozoic zircon from augen gneiss, Yukon-Tanana Upland, east-central Alaska: Geology, v. 9, p. 469-473.

Barker, D. S., 1983, Igneous rocks: New Jersey, Prentice-Hall, 417 p.

Barker, J.C., 1979, A trace-element study of the Circle mining district, Alaska: United Stated Department of the Interior Open-file Report No. 57-79, 32 p.

Bates, R. L. and Jackson, J. A., 1980, Glossary of geology: Falls Church, Virginia, American Geological Institute, 749 p.

Berg, H.C. and Cobb, E.H., 1967, Metalliferous lode deposits of Alaska: U.S. Geological Survey Bulletin 1247, 254 p.

Bowen, N.L., 1956, The evolution of the igneous rocks, New York, Dover Publications, 322 p.

Brooks, A.H., 1909, The mining industry in 1908: U.S. Geological Survey Bulletin 379, p. 21-62.

Brooks, A.H., 1910, The mining industry in 1909: U.S. Geological Survey Bulletin 442, p. 20-46.

Chayes, F., 1971, Ratio correlation: A manual for students of petrology and geochemistry: Chicago, University Chicago Press, 99 p.

Clarke, D.B., Barr, S.M. and Donohoe, H.V., 1980, Granitoid and other plutonic rocks of Nova Scotia, in Proceedings: The Caledonides in the U.S.A., I.G.C.P. project 27: Caledonide Orogen, Department of Geological Science, Virginia Polytechnic Institute and State University, Memoir 2, p. 107-116.

Cobb, E.H., 1973, Placer deposits of Alaska: U.S. Geological Survey Bulletin 1374, 213 p.

Cobb, E.H., 1976, Summary of references to mineral occurrences (other than mineral fuels and construction materials) in the Circle quadrangle, Alaska: U.S. Geological Survey Open-file Report 76-633, 72 p.

Cox, K.G., Bell, J.D., and Pankhurst, R.J., 1979, The interpretation of igneous rocks: London, George Allen and Unwin, 450 p.

Craig, J.R. and Vaughan, D.J., 1981, Ore microscopy and ore petrography, New York, John Wiley, 406 p.

Dixon, W.J., Brown, M.B., Engleman, L., Frane, J.W., Hill, M.A., Jennrich, R.I. and Toporek, J.D., 1983, BMDP statistical software - 1983, printing with additions, Los Angeles, University of California Press, 733 p.

Foster, H.L., Laird, Jo, Keith, T.E.C., Cushing, G.W., and Menzie, W.D., 1983, Preliminary geologic map of the Circle quadrangle, Alaska: U.S. Geological Survey Open-file Report 83-170-A, 30 p.

Foster, H.L., Weber, F.R., Forbes, R.B. and Brabb, E.E., 1973, Regional geology of the Yukon-Tanana Upland, Alaska, in Arctic geology: American Association of Petroleum Geologists, Memoir 19, p. 388-395.

Harker, A., 1909, The natural history of igneous rocks: New York, MacMillan, 384 p.

Heinrich, E. W., 1965, Microscopic identification of minerals: New York, McGraw-Hill, 414 p.

Hess, F.L., 1912, Tin resources of Alaska: U.S. Geological Survey Bulletin 520, p. 89-92.

Hudson, Travis and Arth, J.G., 1983, Tin granites of the Seward Peninsula, Alaska: Geological Society of America Bulletin, v. 94, p. 768-790.

Hyndman, D. W., 1972, Petrology of igneous and metamorphic rocks: New York, McGraw-Hill, 533 p.

Joesting, H.R., 1942, Strategic mineral occurrences in interior Alaska: Alaska Department of Mines Pamphlet 1, 46 p.

Johnson, B.L., 1910, Occurrence of wolframite and cassiterite in the gold placers of Deadwood Creek, Birch Creek district: U.S. Geological Survey Bulletin 442, p. 246-250.

Johnson, M.J. and Maxwell, J.A., 1981, Rock and mineral analysis: New York, John Wiley, 489 p.

MacKenzie, W.S., Donaldson, C.H. and Guilford, C., 1982, Atlas of igneous rocks and their textures: New York, John Wiley, 148 p.

MacKenzie, W.S. and Guilford, C., 1980, Atlas of rock-forming minerals in thin section: New York, John Wiley, 98 p.

Menzie, W.D., Foster, H.L., Tripp, R.B., and Yeend, W.E., 1983, Mineral resource assessment of the Circle quadrangle, Alaska: U.S. Geological Survey Open-file Report 83-170B, 57 p.

Mertie, J.B., 1930, Geology of the Eagle-Circle district, Alaska: U.S. Geological Survey Bulletin 815, 168 p.

Mertie, J.B., 1937, The Yukon-Tanana region, Alaska: U.S. Geological Survey Bulletin 872, 276 p.

Mertie, J.B., 1938, Gold placers of the Fortymile, Eagle, and Circle districts, Alaska: U.S. Geological Survey Bulletin 897-C, p. 133-261.

Middlemost, Eric, 1985, Magmas and magmatic rocks: New York, Longman Group, 266 p.

Nelson, A.E., West, W.S., and Matzko, J.J., 1954, Reconnaissance for radioactive deposits in eastern Alaska, 1952: U.S. Geological Survey Circular 348, 21 p.

Norman, Meade, 1974, Improved techniques for selective staining of feldspar and other minerals using amaranth: Jour. Research U.S. Geological Survey, V. 2, no. 1, p. 73-79.

Phillips, W.R. and Griffen, D.T., 1981, Optical mineralogy - The nonopaque minerals: San Francisco, W.H. Freeman, 677 p.

Prindle, L.M., 1913, A geologic reconnaissance of the Circle quadrangle, Alaska: U.S. Geological Survey Bulletin 538, 82 p.

Putnam, W.C., 1971, Geology: New York, Oxford University Press, 586 p.

Raguin, E. and Wegmann, C.E., 1965, Geology of granite: London, Interscience.

Ransome, A.L. and Kerns, W.H., 1954, Names and definitions of regions, districts, and subdistricts in Alaska: United Stated Department of the Interior Information Circular 7679, 91 p.

Streckeisen, A., 1973, Classification and nomenclature recommended by the International Union of Geological Science Subcommission on the Systematics of Igneous Rocks: Geotimes, Oct. issue, p. 26-30.

Streckeisen, A., 1976, To each plutonic rock its proper name: New York, Earth Science Review, v. 12, p. 1-33.

Taylor, R.G., 1979, Geology of tin depostis: New York, Elsevier.

Thornton, C.P. and Tuttle, O.F., 1960, Chemistry of igneous rocks: Pt. I, Differentiation Index:, American Journal of Science, v. 258, p. 664-684.

Van Der Plas, L. and Tobi, A.C., 1965, A chart for judging the reliability of point counting results: American Journal of Science, v. 265, p. 87-90.

Wahrhaftig, C., 1965, Physiographic divisions of Alaska: United States Geological Professional Paper 482, 52p.

Wedow, H., Jr., White, M.G. and Moxham, R.M., 1952 Interim report on an appraisal of the uranium possibilities of Alaska: U.S. Geological Survey Open-file report 51, 123 p.

Wedow, Helmuth, Jr., White, M.G. and others, 1954, Reconnaissance for radioactive deposits in east-central Alaska, 1949: U.S. Geological Survey Circular 335, 22 p.

Williams, Howel, Turner, F.J., and Gilbert, C.M., 1982, Petrography, An introduction to the study of rocks in thin sections: San Francisco, W.H. Freeman, 406 p.

Wilson, F.H., Smith, J.G. and Shen, N., 1985, Review of radiometric data from the Yukon Crystalline Terrane, Alaska and Yukon Territory; Canadian Journal of Earth Sciences, v. 22, no. 4, p. 525-537.

ABOUT THE AUTHOR

Katy Wilkinson has held a lifelong interest in earth processes and her jobs and recreational activities have always focused on outdoor activities. At 15 years of age she was standing on Mount Rainier's summit, marveling at the distant peaks shrouded in clouds. Following four years of climbing experience with the Spokane Mountaineering Club, she found herself looking for gold in the wilds of Montana, in the stifling heat of Hells Canyon, Idaho and in southwestern Oregon. She has dug fireline in the Siskiyou National Forest and climbed telephone poles as a lineman in eastern Washington. She explored for uranium in the Nevada desert and northeastern Washington. While exploring for gold in southwestern Alaska she would often find the mighty Alaskan brown bear searching for parka squirrels or feeding on salmon.

In 1982 she graduated summa cum laude with a Bachelor of Science degree in Geology from Eastern Washington University. She had a dream to complete a geologic study in a relatively unresearched area in Alaska. This report represents the realization of that dream.

She and her husband, Richard Wilkinson, own and operate K.T. and R. Consultants. For two years she has worked on a consulting basis for a local precious metals refinery, buying gold from Alaskan miners. In the summers, Richard mines gold from Alaskan creeks. Together they plan to reside in Fairbanks, Alaska. They are currently investigating mining ventures to occupy the winter months.